COMPUTATIONAL INVESTIGATION ON STRUCTURE AND SOME APPLICATIONS OF SELECTED FLAVANONES

Thesis submitted to the University of Calicut in partial fulfilment of the requirements for the award of the degree of

DOCTOR OF PHILOSOPHY IN CHEMISTRY

under the Faculty of Science

by

AJMALA SHIREEN P.

Supervising Teacher

Prof. V.M. Abdul Mujeeb

DEPARTMENT OF CHEMISTRY
UNIVERSITY OF CALICUT
KERALA 673635
INDIA

2018

COMPUTATIONAL INVESTIGATION ON STRUCTURE AND SOME APPLICATIONS OF SELECTED FLAVANONES

Thesis submitted to the
University of Calicut in partial fulfilment of
the requirements for the award of the degree of

DOCTOR OF PHILOSOPHY IN CHEMISTRY
under the Faculty of Science

by

AJMALA SHIREEN P.

Supervising Teacher

Prof. V.M Abdul Mujeeb

DEPARTMENT OF CHEMISTRY
UNIVERSITY OF CALICUT
KERALA 673635
INDIA

2018

DECLARATION

I hereby declare that the research work embodied in this thesis entitled "**Computational investigation on structure and some applications of selected flavanones"**, is based on the original research work carried out by me under the guidance of Dr. V. M. Abdul Mujeeb, Professor , Department of Chemistry, University of Calicut, Kerala and the same has not been submitted elsewhere previously for the award of any other degree or diploma.

Calicut University **Ajmala Shireen P.**
Date:

Dr.V.M.Abdul Mujeeb
Professor
Department of Chemistry
University of Calicut

CERTIFICATE

This is to certify that the dissertation entitled "**Computational investigation on structure and some applications of selected flavanones**" bound herewith is a bonafide work done by **Mrs. Ajmala Shireen P.** under my supervision in the Department of Chemistry, University of Calicut, Kerala in partial fulfilment of the requirements for the award of degree of Doctor of Philosophy in Chemistry of the University of Calicut, and the results embodied in this thesis, have not been included in any other thesis previously for the award of any other degree.

Calicut University **Dr.V.M Abdul Mujeeb**

Dr.V.M.Abdul Mujeeb
Professor
Department of Chemistry
University of Calicut

CERTIFICATE

This is to certify that the dissertation entitled "**Computational investigation on structure and some applications of selected flavanones**" bound herewith is a bonafide work done by **Mrs. Ajmala Shireen P.** under my supervision in the Department of Chemistry, University of Calicut, Kerala in partial fulfilment of the requirements for the award of degree of Doctor of Philosophy in Chemistry of the University of Calicut, and the results embodied in this thesis, have not been included in any other thesis previously for the award of any other degree. I also hereby certify that the corrections/suggestions from the adjudicators have been incorporated in the revised thesis. Content of the CD submitted and the hardcopy of the thesis is one and the same.

Calicut University **Dr.V.M Abdul Mujeeb**

ACKNOWLEDGEMENT

It is my proud privilege to express my deep sense of gratitude, whole hearted sincerity and respect to my esteemed supervisor Dr. V. M. Abdul Mujeeb, Professor, Department of Chemistry, University of Calicut, for giving me an opportunity to join his research team. His constant encouragement, support and valuable suggestions throughout the period of research enabled me to complete this study.

I am extremely grateful to Dr. P.Raveendran, Head of the Department of Chemistry and also to the former HOD Dr. K. Muraleedharan for providing research facilities in the department. I would like specially than Dr. K. Muraleedharan for his valuable, positive suggestions that helped in the improvement of the research problem. I also take this opportunity to express my sincere gratitude to Dr. Abraham Joseph, Dr. N. K. Renuka, Dr. A. I. Yahia, Dr. Pradeepan Periyatt, Dr.D..Bahulayan, Dr. K. Aravindakshan and Dr. Ramesan , for their timely intervention, encouragement and motivation. I would like to acknowledge non teaching staff in the department for the help and support rendered by them.

I express my sincere thanks to Dr.Shahin, Department of Physics, University of Calicut and his students for extending their Gaussian 09 version in the initial days of research.

It gives me immense pleasure to put on record my deepest gratitude to my research group members Dr. Basila Hassan, Dr. Kavitha A.P., Dr. Mujeeb Rahman, Dr. Alykutty, Nadira, and Julia for their help, support, suggestions and discussion throughout the research. I express my special thanks to Vijisha K. Rajan, Shameera

Ahamed and Sabira of computational lab for their sincere friendship, help and support.

I would like to express my gratefulness and thanks to University Grant Commission (UGC) for providing me the research financial assistant during full time registration. I am also obliged to Principals Dr. Anita Nair, Sri. M. B. Sasidharan and Manager Dr. Junaid Rahman of Al-Ameen College, Edathala, Aluva for allowing me to continue research in part time mode. I am also indebted to my collegues, Mrs. Indu G, Dr. Leji Latheef and Mrs. Shibini Mol P.A. at Department of Chemistry, Al-Ameen College for their support, encouraging approach, motivation and finely continuous cooperation wherever needed.

I am deeply indebted to my parents Mr. Zainuddeen P. and Mrs. P. M. Nadia and brother, Mr. Nabeel Sabique P., for their prayers and their care was a source of strength and support to my effort. I ran short of words to express my immense gratitude to my husband Mr. Ashiq N.K. and daughter Ms. Niya Ashiq for their support, help, motivation, encouragement, prayers and patience all along the research programme. They have to adjust a lot during my research tenure and had to forego many things in life for helping me complete my research on time. I am obliged to my grandmother and in laws for their concern and support.

Above all, I bow to the God Almighty (Allah), the most merciful and beneficent for all the blessings. By the grace of Him I could reach upto this level.

Ajmala Shireen P.

Dedicated To

My Family

ABBREVIATIONS

MM	-	Molecular Mechanics
SE	-	Semi-empirical
DFT	-	Density functional theory
HF	-	Hartree Fock
MPn	-	Moller-Plesset approximation
CI	-	Configuration interaction
CIS	-	Configuration interaction first-excitation
CISD	-	Configuration interaction single and double excitation
CISDT	-	Configuration interaction single, double and triple excitation
CISDTQ	-	Configuration interaction single, double, triple and quadruple-excitation
CASSCF	-	Complete active space self-consistent field
GVB	-	Generalized valence bond
MRCI	-	Multi-reference configuration interaction
CC	-	Coupled Cluster method
PPP	-	Pariser-Parr-Pople method
CNDO	-	Complete neglect of differential overlap method
INDO	-	Intermediate neglect of differential overlap method
NDDO	-	Neglect of diatomic differential overlap method
KS	-	Kohn-Sham approach
LDA	-	The local density approximation
LSDA	-	The local spin density approximation
GGA	-	The generalized gradient approximation
LYP	-	Lee-Yang-Parr
MGGA	-	Meta Generalized Gradient Approximation functionals
HGGA	-	Hybrid GGA Functionals
ACM	-	Adiabatic connection method
HMGGA	-	Hybrid meta GGA functionals
DZ	-	Double zeta
SV	-	Split valence
GTOs	-	Gaussian type orbitals
CGTOs	-	Contracted GTOs

PGTOs	-	Primitive GTOs
DPPH	-	2,2-diphenyl--picrylhydrazyl
FRAP	-	Ferric reducing/antioxidant power
PES	-	Potential energy surface
NMR	-	Nuclear magnetic resonance
GIAO	-	Gauge independent or invariant or including atomic orbital
TMS	-	Tetra methyl silane
CPCM	-	Conductor-like polarizable continuum model
IEFPCM	-	Integral equation formalism polarizable continuum model
TDDFT	-	Time-Dependent Density Functional Theory
NLMO	-	Natural Localized Molecular Orbital
NBO	-	Natural bond orbital
B3LYP	-	Becke, three-parameter, Lee-Yang-Parr
DMSO	-	Dimethyl sulphoxide
HOMO	-	Highest occupied molecular orbital
LUMO	-	Lowest unoccupied molecular orbital
MEP	-	Molecular electrostatic potential
IP	-	Ionization potential
EA	-	Electron affinity
χ	-	Electronegativity
ω	-	Electrophilicity
S	-	Softness
η	-	Hardness
μ	-	Chemical potential
HAT	-	Hydrogen atom transfer
SET-PT	-	Single-electron transfer followed by proton transfer
SPLET	-	Sequential proton loss electron transfer
BDE	-	Bond dissociation energy
IP	-	Adiabatic Ionization potential
NPA	-	Natural population analysis
ZPE	-	zero point energy
PDE	-	Proton dissociation enthalpy
PA	-	Proton affinity
ETE	-	Electron transfer enthalpy
PDTD	-	Potential drug target database

CDK6	-	Human cyclin dependent kinase 6
TGase 3	-	Transglutaminase 3
RTK	-	Receptor tyrosine kinases
AKR1C3	-	Aldo-keto reductase family
CBR1	-	Carbonyl reductase 1
Hsp90	-	Heat shock protein 90

CONTENTS

PREFACE

Flavonoids are plant polyphenols which find tremendous applications in therapeutics. There are several subclasses of flavonoids based on their structure.

The present research work focuses on flavanones which is a subclass of flavonoids. The thesis titled as "Computational investigation on structure and some applications of selected flavanones" is divided into nine chapters. The first chapter is dedicated to discuss the different computational methods. It then provides a brief description of the different flavonoid classes and in particular flavanones. Different applications of flavanones are discussed based on literature survey. A brief overview of the theoretical works carried out in flavonoids is also provided. Chapter two decribes the various computational methodologies and strategies adopted in this research work. It also introduces the several softwares used and the computer power. Third chapter introduces the flavanone molecules studied in this thesis namely pinocembrin, pinostrobin and alpinetin. Structure of these molecules are optimized and ^{13}C NMR and ^{1}H NMR spectra are discussed along with frontier molecular orbital analysis and molecular electrostatic potential analysis. Chapter four discusses the antioxidant potentiality of the title molecules based on the computed global reactive descriptors and also provides a detailed study of antioxidant mechanism operating in these molecules in different media from a thermodynamic point of view. Druggability and toxicity studies carried out on these molecules were also discussed. Chapter five is an attempt

to improve the existing antioxidant potentialities of the molecules via derivatization using electron withdrawing and releasing substituents. Druggability and toxicity studies on the substituted molecules were also discussed. Sixth chapter is the study of absorption characteristics and UV filtering potentialities of the title molecules based on TDFDT and NLMO formalisms. Seventh chapter describes the ability of pinocembrin and pinostrobin molecules to chelate heavy metals like Zinc, Cadmium, Mercury, Palladium and Lead. Optical characteristics of the metal-ligand complexes were also studied. Chapter eight is an inverse molecular docking study followed by conventional docking to identify the multiple target proteins the title molecules can interact with. Chapter nine summarizes the results of investigations done and suggests lists of possible areas of future work.

Chapter 1

Introduction

Chemistry began entirely as an empirical science which deals with classification and properties of substances and their transformation in various chemical reactions. As this large body of information developed into a science, it becomes necessary to focus on the nature of atoms and their constituents, especially electrons. These extremely small particles called electrons fail to obey laws of classical physics.

The great puzzle of the late 19^{th} century was Black body radiation. Classical Physics, then at its zenith, could not find a satisfactory explanation to address this phenomenon. In 1900, Max Planck proposed his theory of quantized radiation, which could explain black body radiation [1]. Later in 1905, Einstein proposed that not only absorption and emission of light are quantized; quantization is inherent to light [2]. These packets of energy were called 'photons'. Using these theories, Einstein could explain the photoelectric effect, which was again a phenomenon which classical physics failed to explain. These contributions by Max Planck and Einstein indicated that flow of

energy takes place not continuously but as discrete packets of energy called quantum. These theories marked the beginning of quantum theory and a transition from classical to modern physics.

In 1913, Neil's Bohr developed the modern theory of atom [3]. Bohr model could be applied successfully for hydrogen and hydrogen-like atoms but suffered when coming to other atoms. Limitations of Bohr theory is mainly due to the failure to incorporate wave nature of particles. Years later, in 1924, de-Broglie deduced the 'wave-particle duality' [4]. According to his hypothesis, just like light, electrons can also possess wave and particle nature. By that time, in 1925, Heisenberg published his matrix mechanics [5] for solving molecular properties and in 1926 Schrödinger [6] devised a version of quantum mechanics based on waves called wave mechanics and also deduced his famous equation called Schrödinger wave equation. This matrix mechanics and wave mechanics are believed to mark the beginning of quantum mechanics [7].

According to Schrödinger wave equation, the total energy of the electron is regarded as the sum of potential and kinetic energy. This equation may be represented as:

$$\frac{\partial^2\psi}{\partial x^2}+\frac{\partial^2\psi}{\partial y^2}+\frac{\partial^2\psi}{\partial z^2}+\frac{8\pi^2 m}{h^2}(E-V)\psi=0 \qquad (1.1)$$

where m is the mass of the electron, h is the Planck's constant, E is the total energy of the electron, V is the potential energy and x, y, z are Cartesian co-ordinates and ψ is called wave function. Schrödinger wave equation could overcome the shortcomings of Bohr model.

Quantum numbers follow as a consequence of Schrödinger wave equation. These equations are exactly solvable only for hydrogen and hydrogen-like systems. The Schrödinger equation that we have been talking about is time independent Schrödinger wave equation, which is largely used in computational chemistry. But more general form is the time dependent Schrödinger wave equation which is used in some applications like studying the interaction of molecules with light, calculating UV spectra etc. This opens up a vast field of mathematical formulation of chemistry.

Theoretical chemistry was born when physicists tried to apply the principles of quantum mechanics to molecular systems. To have an accurate description of the entities of the sub-atomic world we have to resort to quantum chemistry or so to say to theoretical chemistry [8]. Theoretical chemistry is the mathematical description of chemistry. That is, mathematical equations are used to solve chemical problems.

1.1 Computational Chemistry

The term computational chemistry is used when mathematical methods can be automated on a computer. It refers to the application of chemical, mathematical and computing skills to solve interesting chemical problems. Only very few aspects of chemistry can be computed exactly but a qualitative or approximate quantitative description can be made of almost every aspect of chemistry. Computational techniques can be broadly classified into different categories:

1. Molecular mechanics (MM)

2. Semiempirical (SE) methods

3. Ab –initio methods

4. Density functional theory (DFT) methods

1.1.1 Molecular Mechanics

According to this theory [9,10], molecules are considered as balls connected by springs which depict the bonds between atoms. Different geometries can be brought about by stretching and bending of springs but is limited to certain lengths and angles. Thus, the natural geometry is restored in this model. Resistance towards bond stretching, bond bending, and atom crowding is used to calculate the energy of a molecule. The energy expression contains simple classical equations like harmonic oscillator equation in order to calculate the energy associated with bond stretching, bending, rotation and intermolecular forces, such as Van der Waals interactions and hydrogen bonding [11].

This method is also called force field method as the mathematical expression for energy and the parameters in it constitute a force field. In this method, a molecule is defined by the atoms and the bonds, and thus we must specify each bond as single, double, etc. to do an MM calculation. A serious drawback of this method is it completely ignores electrons.

Potential energy expression according to molecular mechanics is given by the sum of energies of bond stretching, angle bending, torsional motion and non-bonded interactions.

$$E = \sum_{bonds} E_{stretch} + \sum_{angles} E_{bend} + \sum_{dihedrals} E_{torsion} + \sum_{pairs} E_{nonbond} \quad (1.2)$$

Bond stretching is found to be proportional to the square of change in the bond length which can be expressed as:

$$E_{stretch} = k_{stretch}(l - l_{eq})^2 \quad (1.3)$$

Where $k_{stretch}$ is the proportionality constant which is one-half the force constant of the spring or bond, l is the length of the bond when stretched, l_{eq} is the equilibrium length of the bond or natural length.

Angle of bending energy is proportional to the square of the difference in angle and hence the expression is given by:

$$E_{bend} = k_{bend}(a - a_{eq})^2 \quad (1.4)$$

Torsional energy is expressed as

$$E_{torsion} = k_0 + \sum_{r=1}^{n} k_r[1 + \cos(r\theta)] \quad (1.5)$$

Non-bonding interactions are given by Lennard - Jones 12 - 6 potential [12,13]

$$E_{nonbond} = k_{nb}[(\tfrac{\sigma}{r})^{12} - (\tfrac{\sigma}{r})^{6}] \quad (1.6)$$

Where ‘r’ is the distance between the centers and ‘σ’ is calculated from Vander Waal’s radii. The values of $k_{stretch}$, l_{eq}, k_{bend}, etc., can be

obtained by ab initio calculations or by experimental methods. This is known as parameterization.

Main applications are:

1. Geometries and energies of small to medium sized molecules can be calculated by this method. The resulting structure can be used as starting geometry for other methods like ab initio, Semi-Empirical method, Density Functional Theory method etc.

2. It can be used to calculate the geometries and energies of polymers mainly proteins and nucleic acids.

3. Geometries and energies of transition states can be found out. But it is not so frequently used.

4. The potential energy function can be generated under which molecules move, for molecular dynamics calculations.

Drawbacks of MM methods [14]:

1. Force fields have to be parameterized for each class of compounds separately.

2. Solvent effects are not taken care off and thus polar geometries and energies may not be correct.

3. This method is insufficient to distinguish between molecules with small differences like isomeric molecules.

1.1.2 Ab - initio method

The Latin term *ab initio* means “from the beginning”. These are computations that are derived only from theoretical calculations without including experimental information [15,16]. There are different types of ab-initio calculation

a) Hartree - Fock Approximation

b) Correlation Methods

a) Hartree - Fock approximation

Hartree Fock (HF) approximation [17,18] is one of the most common ab-initio methods used. This method is based on two important approximations. The primary approximation is that coulombic electron-electron repulsion is taken by integrating the repulsion term. This can give only an average effect of repulsion but cannot consider explicit repulsion interaction. This is called central field approximation. This is a variational calculation, and the approximate energies calculated are always equal to or greater than the exact energy. One of the main advantages is that it could break the complex Schrödinger equation into simpler, one electron equation. The secondary approximation is that HF calculations demand a wave function that must be described by a mathematical equation which is known exactly only for a few one electron systems.

Hartree Fock method begins with an initial guess for orbital coefficients. Using this function, energy and a new set of orbital coefficients are calculated. The coefficients so obtained are used to

calculate a new set, and so on. This process is continued until the energies and orbital coefficients remain constant from one iteration to the other. This is called calculation convergence. This procedure is called self-consistent field procedure (SCF).

Hartree method has several limitations like it does not consider indistinguishability and spin of electrons. Antisymmetric nature of electronic wave functions was also not taken into account by Hartree. Limitations of Hartree were corrected by Fock and then by Slater. Unlike Hartree wave function, Slater wave functions are a product of spatial and spin orbitals

Limitations of Hartree - Fock method

HF method does not take into account electron correlation. According to this theory, probability of finding an electron at a point is determined by the distance from the nucleus and is not influenced by the distance from the other electron. This is a consequence of central field approximation and physically is not true.

Roothan-Hall equations

Hartree - Fock equations are not used to do molecular calculations as it does not provide a mathematically viable procedure to calculate the initial guess for molecular orbital wave functions and these wave functions are so complicated and contribute nothing to the understanding of electron distribution. In 1951, Roothan [19] and Hall [20] pointed that molecular orbitals can be represented as linear combination of basis functions.

$$\psi_i = \sum_{s=1}^{m} c_{si}\phi_s \qquad (1.7)$$

The set of basis functions used for a particular calculation is called basis set.

b) Correlation methods

Many of the calculations begin with HF calculation and then include correlation. These are called correlated calculations which include Moller-Plesset approximation (MPn), Configuration interaction (CI), Multi-configurational self-consistent field (MCSCF), Generalized valence bond (GVB) method, Multi-reference configuration interaction (MRCI) and Coupled cluster theory (CC).

a) Møller-Plesset approximation (MPn)

Correlation can be added to HF calculations as a perturbation. This is called Møller-Plesset perturbation theory. This theory is developed by Møller and Plesset in 1934 [21] and is developed into a practical molecular computational method by Binkley and Pople in 1975 [22]. The basic idea behind this theory is to treat a complex system as a mathematically altered or perturbed version of the simple system if they are not very different. MP energy levels are designated as MP0, MP1, MP2 etc. successive versions account more thoroughly for interelectronic repulsion.

b) Configuration interaction (CI)

Configuration interaction [23] wave function is a multiple-determinant wave function that is constructed starting from an HF wave function and promoting electrons from occupied orbitals to unoccupied orbitals. Configuration interaction calculations generally require more CPU time. Depending on the number of excitations used to make determinants, CI is classified into many. Configuration interaction first-excitation (CIS) calculation moves only one electron to make each determinant. CIS calculations can give approximate energies for the excited state but cannot alter ground state energy. If single and double excitation (CISD) calculations are carried out, ground state energy which is corrected for correlation could be obtained. Highly accurate results are obtained by performing triple excitation (CISDT) and quadruple-excitation (CISDTQ) calculations. Configuration interaction calculation with all possible excitations is called a full CI. These are rarely done as it requires immense computer power.

c) Multi - configurational self-consistent field (MCSCF)

This is again a multiple-determinant wave function but uses optimized orbitals. These calculations can give accurate results with limited CPU time. MCSCF [24] can give correlation energy with fewer configurations. This method is recommended particularly when HF wave function poorly describes the system. But this method requires high technical sophistication from the user. The user is required to choose the molecular orbitals and ensure that the bonding and anti-

bonding orbitals chosen are correlated. Thus, accuracy depends on the choice made by the user.

If all combinations of active space orbitals are included in an MCSCF calculation, it is called a complete active space self-consistent field (CASSCF) calculation. These calculations give maximum correlation in valence region. The generalized valence bond (GVB) method is an MCSCF calculation which includes a pair of orbitals for each molecular bond.

d) Multi-reference configuration interaction (MRCI)

If a CI wave function is made starting from an MCSCF calculation rather than an HF wave function, it is called Multi-reference configuration interaction (MRCI) calculation [25,26]. There will be more CI determinants in this calculation than in conventional CI. These calculations are very costly in terms of computing resources. Some examples for MRCI calculations are: MCSCF+1+2, CASSCF+1+2 and GVB+1+2.

e) Coupled Cluster (CC) method

The wave functions used in couple cluster calculations are also a linear combination of many determinants just like CI calculations. But the method of choosing determinants in CC is more complex than in CI method. There are various orders of CC calculations like CCSD, CCSDT, etc. Coupled cluster calculations give variational energies if excitations are included successively [27]. The accuracy of both these methods are similar but the advantage of CC method is that it is a size

extensive method. If all possible configurations are included, a full coupled-cluster calculation is same as full CI calculation.

1.1.3 Semi-empirical (SE) method

Semi-empirical method is not as empirical as molecular mechanics nor is as theoretical as ab-initio calculations. It stands in between the two. In this method, a Fock matrix is constructed and is diagonalized to get MOs and their corresponding energy levels. Fock matrix element is calculated from a core integral H_{rs}^{core}, density matrix elements P_{tu} and electron repulsion integrals $(rs \mid tu), (ru \mid ts)$ in the expression:

$$F_{rs} = H_{rs}^{core}(1) + \sum_{t=1}^{m}\sum_{u=1}^{m} P_{tu}\left[(rs \mid tu) - \frac{1}{2}(ru \mid ts)\right] \qquad (1.8)$$

An initial guess of coefficients is needed to initiate the process by calculating density matrix values P_{tu}. This guess can be obtained from simple Huckel calculation or an extended Huckel calculation. The Fock matrix element F_{rs} is subjected to repeated diagonalization to refine the energy levels and coefficients [28–30].

The difference between semi-empirical and ab-initio methods are [7]:

1. Treating only valence or π electrons: Semi-empirical calculations take care of at most the valence electrons. Thus, the core becomes atomic nucleus plus the core electrons. In an ab initio calculation, on the other hand, H_{rs}^{core} is the kinetic

energy of an electron moving under the influence of atomic nuclei plus the potential energy of attraction of electron to atomic nuclei. Thus, unlike in ab initio calculation where we have a cloud of all electron moving in the framework of nuclei, in SE calculations we have a cloud of valence electrons moving in the framework of atomic cores. E_{SE} is the valence electron energy and V_{CC} is the core- core repulsion. Thus total energy is given by,

$$E_{SE}^{total} = E_{SE} + V_{CC} = \sum_{i=1}^{n} \varepsilon_i + \frac{1}{2} \sum_{r=1}^{m} \sum_{s=1}^{m} P_{rs} H_{rs}^{core} + V_{CC} \qquad (1.9)$$

2. Basis set functions: In the semi-empirical method, Slater functions are used as basis functions instead of approximating slater orbitals as the sum of Gaussian functions. Slater functions are more accurate compared to Gaussian functions. The only reason ab initio method uses Gaussian functions than Slater functions is that calculations of the electron-electron repulsion two-electron integrals are faster using Gaussian functions. These integrals are parameterized in SE calculations. But to calculate overlap integral, $< \Phi_r | \Phi_s >$, mathematical forms of basis functions are needed.

3. Integrals: In SE calculations, core integrals and the two-electron repulsion integrals are not calculated from first principles. Many integrals are set to zero and those that are used are evaluated in an empirical way from the types of atoms involved and their bond distances. On the other hand, in ab-

initio method, much of the time is dedicated to calculating two-electron integrals mainly those involving three and four centers.

4. Overlap matrix: In SE method, overlap integral is taken as a unit matrix; $S=1$. Thus S vanishes from Roothan - Hall equations, $FC = SC\varepsilon$. Thus the equation takes the standard eigen form, $FC = C\varepsilon$ without the necessity of using an orthogonalizing matrix.

The different types of SCF-type semi-empirical methods are:

a) Pariser-Parr-Pople (PPP) method:

The first semi-empirical SCF-type method to gain popularity was Pariser-Parr-Pople (PPP) [31,32] method. Only π electrons are considered and other electrons are part of a σ framework to hold atomic *p* orbitals in place. This method is especially used to predict the UV spectra of conjugated compounds and the accuracy can be further improved by incorporating electron correlation using configuration interaction (CI) method. Fixed geometry is mainly used though bond length optimization is permitted. Classical PPP method is not much used nowadays, giving way to other neglect of differential overlap methods like INDO/S and ZINDO/S.

b) Complete neglect of differential overlap (CNDO) method

The first semi-empirical SCF method which goes beyond π electrons is CNDO [33]. CNDO calculations use minimal valence basis set of Slater type orbitals. Fock matrix elements

for a CNDO calculation H_{rs}^{core} represents nuclei and core electrons, P_{tu} is calculated based on the coefficients of valence atomic orbitals (AOs).

c) Intermediate neglect of differential overlap (INDO) method

INDO [34,35] is superior to CNDO. In INDO, zero differential overlap (ZDO) is not applied to one center two electron integral $(rs|tu)$ with Φ_r, Φ_s, Φ_t and Φ_u all on the same atom. These repulsion integrals should be the most important. INDO is mostly used for calculating UV spectra, in special parameterized versions INDO/s and ZINDO/S.

d) Neglect of diatomic differential overlap (NDDO) method

NDDO [33] is even superior to INDO in that it applies ZDO is not applied to orbitals on the same atom that means ZDO is used only on atomic orbitals on different atoms. NDDO methods are the gold standards in general purpose semi-empirical methods. Some examples are modified NDDO (MNDO), Austin method 1 (AM1) and parametric method (PM3).

1.1.4 Density functional theory (DFT) method

Density functional theory depends not on wave function but on electron density function. It is designated as ρ (x, y, z). In this theory, electron density is expressed as a linear combination of basis functions. A determinant is formed of these functions, which is called Kohn-

Sham orbitals [36]. Electron density of this determinant of orbitals is used to calculate energy. From this electron density, a density functional is used to formulate energy. A functional is a function of a function, which is electron density here.

The advantage of using electron density is that it is a function of position only and hence can be denoted by three variables (x, y, z). On the other hand wave function of 'n' electron system is a function of 4n variables, three spatial coordinates and one spin coordinate. Thus, as the complexity of molecule increases, complexity of wave function increases whereas electron density remains a function of three electrons. Electron density is thus measurable, intuitively comprehensible and mathematically tractable.

The relationship between wave function and electron density is given as:

$$\rho = \sum_{i=1}^{n} n_i \mid \psi_i \mid^2 \qquad (1.10)$$

All properties are calculated from this electron density which will be more complicated for a multi electron system.

Hohenberg-Kohn Theorems

Current DFT theorems are based on Kohn-Sham equations; these are based primarily on two Hohenberg- Kohn theorems. The first Hohenberg-Kohn theorem [37] states that all properties of the ground electronic state are determined by ground state electron density function $\rho_0(x, y, z)$.

$$\rho_0(x,y,z) \rightarrow E_0 \tag{1.11}$$

First Hohenberg - Kohn theorem may be restated as any ground state property of a molecule is a functional of ground state electron density.

$$E_0 = F(\rho_0) = E(\rho_0) \tag{1.12}$$

The second Hohenberg - Kohn theorem [37] states that energy calculated using any trial electron density function will give an energy higher than or equal to true ground state energy. Mathematically it is given by:

$$E_v[\rho_t] \geq E_0[\rho_0] \tag{1.13}$$

where ρ_t is the trial electron density, ρ_0 is the true electron density and $E_0[\rho_0]$ is the true ground state energy. The conditions that trial electron density must satisfy are, $\int \rho_t(r)dr = n$ where n is the number of electrons in the molecule and $\rho_t(r) \geq 0$ for all values of r.

Kohn-Sham (KS) approach

Kohn Sham approach is based on the two Hohenberg- Kohn theorems discussed above. The two basic ideas put forward by Kohn-Sham approach [36],[38] may be summarized as:

1) Molecular energy is expressed as a sum of terms in which a relatively small term involves the unknown functional, so that errors in this term will not introduce significant errors in total energy.

2) An initial guess of electron density is used in KS equations to calculate KS orbitals and energy analogous to HF equations. This initial function is iteratively refined to get final KS orbital which is used to calculate electron density and thereby energy.

Summation of electron kinetic energies, nucleus-electron attraction potential energies and electron-electron repulsion potential energies [7] gives the ground state electronic energy, E_0.

$$E_0 = \langle T[\rho_0]\rangle + \langle V_{Ne}[\rho_0]\rangle + \langle V_{ee}[\rho_0]\rangle \tag{1.14}$$

Nucleus-electron potential energy is the sum over all 2n electrons of the potential corresponding to the attraction of electron to nucleus A, which can be given by:

$$\langle V_{Ne}\rangle = \int \rho_0(r)v(r)dr \tag{1.15}$$

To address the kinetic energy, we define a term $\Delta\langle T[\rho_0]\rangle$ which gives the deviation of electronic kinetic energy from the reference system. This is given by:

$$\Delta\langle T[\rho_0]\rangle \equiv \langle T[\rho_0]\rangle_{rea} - \langle T[\rho_0]\rangle_{ref} \tag{1.16}$$

To address the electronic potential energy, a term $\Delta\langle V_{ee}\rangle$ is defined which gives the difference of real electron-electron repulsion energy from the classical charge cloud repulsion energy. This is expressed as:

$$\Delta\langle V_{ee}[\rho_0]\rangle = \langle V_{ee}[\rho_0]\rangle_{rea} - \frac{1}{2\iint \frac{\rho_0(r_1)\rho_0(r_2)}{r_{12}} dr_1 dr_2} \quad (1.17)$$

Incorporating all these, KS equations can be expressed as:

$$E_0 = \int \rho_0(r)v(r)dr + \langle T[\rho_0]\rangle_{ref} + \frac{1}{2}\iint \frac{\rho_0(r_1)\rho_0(r_2)}{r_{12}} dr_1 dr_2 + \Delta\langle T[\rho_0]\rangle + \Delta\langle V_{ee}[\rho_0]\rangle \quad (1.18)$$

The sum of the last two terms, namely deviation of kinetic energy from a reference system and deviation of electron-electron repulsion energy from the classical system is together called exchange-correlation energy. Exchange-correlation energy, E_{XC} is given by:

$$E_{XC}[\rho_0] \equiv \Delta\langle T[\rho_0]\rangle + \Delta\langle V_{ee}[\rho_0]\rangle \quad (1.19)$$

Devising good exchange-correlation functionals for calculating energy from electron density becomes the main concern of DFT research. Several methods employed include: The local density approximation (LDA), The local spin density approximation (LSDA), The generalized gradient approximation (GGA), meta GGA (MGGA), hybrid GGA, etc.

a) The local density approximation (LDA)

This method is based on the assumption that at every point in the molecule, energy density has a value equal to that of homogeneous electron gas of same electron density at that point [36].

b) The local spin density approximation (LSDA)

Spin means that electron of opposite spins α and β are placed in separate Kohn Sham orbitals ψ_{α}^{KS} and ψ_{β}^{KS}. LSDA has an advantage that it can handle systems with one or more unpaired electrons like radicals. LSDA and LDA are equal for systems with paired electrons [39,40].

c) The generalized gradient approximation (GGA)

Most DFT calculations now use functionals that use energy density and its gradient in exchange-correlation energy functional, and is called Generalized gradient approximation (GGA). Exchange-correlation energy functional can be written as the sum of exchange - energy functional and correlation - energy functional as; $E_{XC} = E_X + E_C$. Both these values are negative, $|E_X|$ being greater than $|E_C|$. Thus gradient corrections are more effective when used for exchange energy functionals. B88 functionals (Becke 1988) [41] is one of the greatly improved functional for exchange energy. Gradient-corrected correlation energy functionals known are LYP (Lee-Yang-Parr) and the P86 (Perdew 1986). All these functionals are used in Gaussian functions to represent KS orbitals.

d) Meta Generalized Gradient Approximation functionals (MGGA)

GGA functionals use first derivative of electron density. Those functionals which use the second derivative of energy density, that is the Laplacian of electron density function is called meta- GGA

(MGGA) [42]. Though they offer some improvement, there are some problems associated with functionals that depend on Laplacian. Some examples are τHCTH (Hamprecht, Cohen, Tozer, Handy) and B98 (Becke 1998).

e) Hybrid GGA Functionals (HGGA)

These functionals have Hartree-Fock exchange being added. According to this method which is also called adiabatic connection method (ACM) [43], exchange-correlation energy can be taken as the weighted sum of DFT exchange-correlation energy and HF exchange energy. Exchange energy functional developed by Becke in 1993 is one of the popular hybrid functional. B3LYP [44] which includes LYP correlation energy functional is one of the common functionals used in DFT.

f) Hybrid meta GGA (HMGGA) functionals

This is analogous to hybrid GGA but in this method, HF exchange is added to meta GGA and not to GGA functionals. These are the highest level functional in use [45].

g) Fully Nonlocal Theory

Non-local functionals have been under development for years [46]. Fully non-local theories are those in which all properties are treated non-locally.

1.2 Basis sets

A basis set is a set of mathematical functions which determine the shape of the orbitals in an atom. Linear combination of these basis functions and angular functions together yield molecular orbitals. Semi-empirical calculations use predefined basis sets whereas ab initio and DFT calculations require basis set specification. Accuracy of results depends on the choice of the basis set made [47,48].

Mathematical expression for atomic orbitals is given by the expression

$$\psi_i = \Sigma_i C_{\mu i} \phi_\mu \qquad (1.20)$$

Where ψ_i is the i^{th} molecular orbital, $C_{\mu i}$ the coefficients of linear combination and ϕ_μ is the μ^{th} atomic orbital.

Electron distribution can be expressed by hydrogen-like functions, slater type orbitals and Gaussian type orbitals. Hydrogen-like functions are generally represented by

$$Y_{nlm} = R_{nl}(r) Y_l^m \qquad (1.21)$$

These functions being complicated and time consuming are not generally used. Semi-empirical calculations use slater type orbitals and ab initio calculations use Gaussian type orbitals.

The main difference between hydrogen-like orbital and slater type orbital (STO) is that it has no node.

$$S^{\zeta}_{nlm}(r,\theta,\phi) = Nr^{n-1}e^{-\zeta r}Y_l^m(\theta,\phi) \quad (1.22)$$

STO can represent electron density in valence region and beyond almost well but is not good for core electron density. There are different types of STOs. A minimal basis set consists of one STO for every inner and outer atomic orbitals. Number of basis functions will be equal to number of atomic orbitals. In double zeta (DZ) basis set, single STO of minimal basis set will be replaced by two STOs having different exponents. Another type of basis set is split valence (SV) basis set, in which each valence AO consist of two STOs. It could thus be treated as having minimal basis set for inner atomic orbitals and DZ basis set for valence atomic orbitals. These STOs form complex integrals and is thus not used nowadays.

Instead of STOs, nowadays Gaussian type orbitals (GTOs) are popularly used. It is represented as:

$$G_{nlm}(r,\theta,\phi) = N_n r^{n-1}e^{-\alpha r^2}Y_l^m(\theta,\phi) \quad (1.23)$$

GTO has the advantage that the term $e^{-\alpha r^2}$ is easy to compute but it has the disadvantage that it cannot represent electron density as good as that of STOs. This problem is overcome by using combinations of GTOs to approximate an STO function. This combined function is called contracted GTOs (CGTOs) and individual GTOs in the combination is called primitive GTOs (PGTOs).

Usually, linear combination of Gaussian functions is used. Basis sets most commonly used are those described by Pople and co-workers [48]. If one Gaussian function is used, it is denoted by STO-1G, if combination of three Gaussians are used it is denoted as STO-

3G and so on. Based on the number and type of GTOs used, basis sets are named 3-21G, 6-31G*, 6-31+G**, 6-311G*etc. Here * denotes addition of polarization functions and + denoted addition of diffuse functions [49]. Polarization function means to include orbitals of higher angular momentum to increase the flexibility of basis sets i.e., to consider asymmetry of molecular orbitals. Diffuse functions use larger versions of s- and p- type functions. These functions improve the accuracy of calculations.

In recent years, Density functional theory is finding increasing applications in the field of natural products. Advancements in DFT have reached to such an extent that these can be used to complement experimental results and in some cases to predict experimentally unexplored territory. DFT appears to be quite reliable for geometry and is quite successful in predicting a number of molecular properties and spectroscopic properties [50].

1.3 Flavonoids

As early as in 1936, flavonoids were discovered by Albert Szent-Györgyi [51]. Flavonoids are a group of polyphenols which are characterized by the presence of several hydroxyl groups over aromatic rings. These flavonoids are mostly concentrated over fruit skin, bark, seeds, flowers, etc. Over 4000 different flavonoids are known making them one of the largest plant chemicals known [52].

Flavonoids have notable health benefits, that a considerable number of plant medicines include flavonoids. Flavonoids are known to possess anti-allergic, anti-bacterial, anti-mutagenic, anti-inflammatory, anti-neoplastic, anti-viral, anti-thrombotic, and

vasodilatory actions [53–56]. Excess production of free radicals can damage biomolecules and are implicated in the etiology of several diseases [57]. Most of the pharmacological effects of flavonoids are related to the radical scavenging activity. There are quite a lot of studies on flavonoids as antioxidants [58–60]. The catch phrase, 'French paradox' (lack of direct relation between consumption of fat and coronary heart diseases) can be related at least partly to consumption of red wine which is rich in flavonoids [61].

Flavonoids have a C-15 skeleton containing two aromatic rings A and B which are connected by a three carbon bridge. A benzo-γ-pyrone (chromone ring) is linked to a phenyl ring. Flavonoids are classified into several subgroups depending on the carbon of C ring to which B ring is attached. Flavonoids are those in which B ring is attached to C-2 of C-ring, those in which B ring is attached to 3-Carbon of C-ring is called isoflavones and those in which B ring is attached to 4-carbon of C-ring is called neoflavonoids.

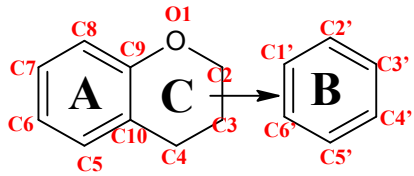

Fig.1.1: Basic skeletal framework of flavonoids

Flavonoids are further classified into several subgroups based on the structural features of C-ring, these are: flavones, flavonols, flavanones, flavanonols or catechins and isoflavones [62]. Flavones are those in which there is a double bond between C2 and C3 and a keto group in 4th carbon. Flavones with an additional hydroxyl group at C-3 are called flavonols. There are two subgroups flavan-3, 4-diol, flavan-

3-ol. Dihydroflavones are called flavanones in which the double bond between C2 and C3 is saturated. Dihydroflavonols are called flavanonols or catechins.

Anthocyanins are a related class of flavonoids glycosylated and have a positive charge on oxygen atom of the C-ring. This ring is called 2-phenylchromenylium (flavylium) ion. They also lack keto group at the 4th carbon. Anthocyanidins are aglycones of anthocyanins [63]. Chalcones are characterized by the absence of C- ring and are called open chain flavonoids [64]. Some literature considers anthocyanidins and chalcones as subgroups of flavonoids [65] whereas others do not [66].

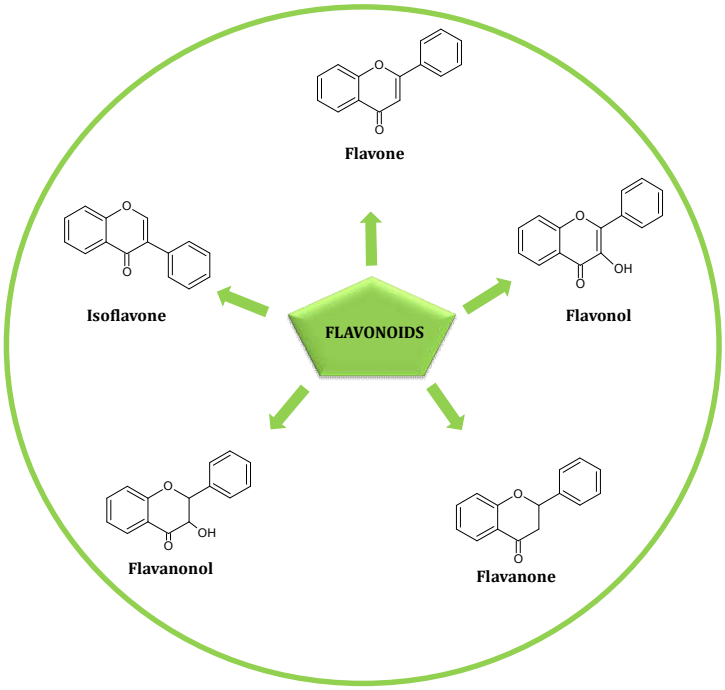

Fig.1.2: Classification of flavonoids

1.3.1 Flavanones

Flavanones encompass a wide range of compounds with O- or C- substitutions done at the A or B ring, like hydroxyl, methoxy, etc. [67]. A few decades ago, flavanones were considered as minor flavonoids [68] but during the last 15 years, total number of flavanones have increased tremendously that it is now considered as a major flavonoid [67]. About 350 flavanone aglycones and about 100 glycones are known till date [69]. Absence of C2-C3 double bond, presence chiral carbon at C2 and absence of C3-OH are the characteristic features of flavanones. Flavanones can exist as aglycones or in glycosylated form [70]. Flavanones are known to have several therapeutic effects. Flavanones exhibit antioxidant, radical scavenging activities, apart from these they also exhibit anti-bacterial, antiviral, antimicrobial, anti-inflammatory, anti-ulcer, anti-allergenic effects and are effective against several kinds of cancer [70–72].

There are several flavanones known in the literature like naringenin, hesperetin, isosakuranetin, eriodictyol, liquirtigenin, homoeriodictyol, pinocembrin, pinostrobin, alpinetin etc [70][72]. One of the main sources of flavanones is citrus fruits [70]. Apart from this some *Piperaceae* family and some genera of gingers etc. are also known to possess flavanones [71]. Honey and propolis are also important sources of flavanones [73].

1.3.2 Biological Activity of flavanones

a) Anti-oxidant activity

Reactive free radicals are produced in our body as a byproduct of several physiological metabolisms. Increase in these free radicals leads to oxidative stress which may lead to several diseases. Flavanones play an important role in scavenging these free radicals. Their scavenging ability depends on several factors like number of OH groups, glycosylation, etc. Hesperidin and their aglycone, hesperitin play an important role in preventing diseases associated with oxidative stress like cancer and cardiovascular diseases [70]. Pinocembrin and pinostrobin are found to have antioxidant activity *in vitro* 2,2-diphenyl--picrylhydrazyl (DPPH) scavenging assay [74,75]. The ferric reducing/antioxidant power (FRAP) value of pinostrobin was found to be 116.11 ± 0.004 [76]. Radical scavenging effects of alpinetin were studied by DPPH radical scavenging assay and the IC50 value is found to be 0.727 mg/mL [77].

b) Anti-inflammatory activity

Anti-inflammatory activities exhibited by flavanones are partly due to antioxidant activity and partly due to their ability to inhibit key enzymes involved in inflammatory response of the body like cyclooxygenase, phosphodiesterase, protein kinase, lipoxygenase, and phospholipase [70]. Hesperetin, naringenin and their glycosylated forms are studied for their anti-inflammatory action. Naringenin is known to inhibit neuronal inflammation and CCl_4 induced hepatic inflammation [78–80]. Hesperidin and Hesperitin are also known to

have ability to down regulate the production of pro-inflammatory cytokines and NFkB [81]. Pinocembrin is used as an anti-inflammatory agent against sheep red blood cell - induced mouse paw oedema. Pinocembrin is recommended for modulating inflammatory response [82,83]. Pinostrobin is shown to inhibit TNF-α (IC50 < 22 μM) and IL-1β (IC50 < 40 μM) in murine macrophages and Sprague Dawley rats [84]. Alpinetin is known to attenuate inflammatory response in dextran sulfate sodium (DSS)-induced colitis in mice [85].

c) Cardioprotective activity

Several studies have been conducted which illustrates the cardioprotective effects of flavanones. The major flavanones studied being naringenin, hesperetin and their glycosides. Kakadiya et. al. [86] established the protective effects of hesperetin against myocardial infarction in diabetic rats. They could effectively control systolic and diastolic blood pressures, serum total cholesterol, blood glucose etc. Chio et. al. [87] and Liu et. al. [88] have shown that hesperetin increases endothelium-derived relaxing factors, NO in human umbilical vein endothelial cells (HUVEC). Cardioprotective effects of naringenin against ischemia/reperfusion (I/R) injury in rats were studied by L.Testai et.al. [89] recently. Pinocembrin is shown to inhibit angiotensin II-induced vasoconstriction [90] and is also prescribed for combination therapy with other drugs to treat atherosclerosis [91,92]. Though cardioprotective effects of flavanones are promising more clinical data are required in this field.

d) Anti-cancer activity

Flavanones are found to be very effective in inhibiting proliferation in different types of cancers. These molecules could exhibit anti-cancer activity by inhibiting tumor growth, inducing cancer cell apoptosis through cell cycle arrest, death receptors, and the involvement of caspase-dependent and mitochondrial pathways. 2' hydroxyl flavanone have been tested in human breast, colon and lung cancer cells [93]. Alshatwi et al. [94] have demonstrated the antiproliferative activity of hesperetin in human cervical cancer cells in vitro. There are also studies which demonstrate the effect of hesperetin against multiple cancer cells like human colon cancer cells [95]. Pinocembrin shows cytotoxicity against human colon cancer cell line (HCT116). Pinocembrin can also have a protective effect against chemical induced hepatocarcinogenesis. Alpinetin can affect human lung cancer cells possibly by influencing mitochondria and the PI3K/Akt signaling pathway [96]. Alpinetin is also known to inhibit pancreatic cancer cells and is suggested to be a potential agent in pancreatic cancer therapy [97].Pinostrobin is shown to have potent activity against glioblastoma and breast tumor cell lines [98]. These indicate the potentiality of flavanones to prevent deadly diseases like cancer.

e) Anti-microbial activity

According to the studies of Moon et. al. [99] anti-microbial activities of flavanones namely hesperetin and naringenin stood out among other flavonoids in his study against Helicobacter pylori strains.

Derivatives of these flavanones which are more potent than them are also identified. Pinostrobin is found to have anti-bacterial effect against *Staphylococcus aureus,* reduces the mycelia growth of fungus *Cytospora persoonii.* Antibacterial effects of pinocembrin and alpinetin were also studied using different bacterial strains [100,101]. Different flavanones are found to be effective against gram +ve and gram –ve bacterial strains. Though several mechanisms like disruption of bacterial cell wall, interference with bacterial DNA synthesis, etc., are proposed, actual mechanism of action remains unclear [70].

f) Metal Chelation ability

Flavonoids including some flavanones are involved in metal complexation. Naringenin is shown to attenuate Cd induced and cisplatin induced nephrotoxicity. Hesperetin also seems to ameliorate damaging effects of Cd on liver. Cu complexes of naringenin and hesperetin were evaluated for their cytotoxic activities and DNA binding properties [102]. Hesperedin complex of aluminium is expected to have anticoagulant activity. Heavy metal chelates of flavonoids can have good therapeutic implications.

These are only some of the applications of flavanones. There are quite a lot of diseases against which flavanones are being used. The flavonoid structural framework is indeed a potential lead for pharmaceutical industry.

1.3.3 Theoretical studies on flavonoids

There is a huge volume of literature focusing on the structure and properties of different types of flavonoids. Quercetin is one of the most commonly studied flavonoids. Mendoza-Wilson et. al have studied the structure of quercetin using CHIH-DFT model chemistry and elucidated that quercetin is a good electron donor and is capable of acting as antioxidant molecule [103]. Several flavone molecules are systematically analyzed using B3LYP/6-311++G** basis set by Aparicio [104]. They have commented on the planarity of the flavone ring as enforced due to the presence of 3-OH and also have compared the strength of different hydrogen bonds present in the molecule. A detailed study of anti-oxidant, anti-radical and pro-oxidant activities of quercetin was studied by Fiorucci et. al. [105].

Another set of literature focuses on illustrating the antioxidant mechanism adopted by different flavonoids in different media. Reactivity of different OH groups in quercetin and taxifolin are compared by Trouillas et. al. , it shed light on the importance of B ring and 3-OH group on the antioxidant mechanism [106]. Antioxidant capability of quercetin was compared to that of the sugar containing analogues of rutin and hyperin by W.Cai et.al. [107], who demonstrated that sugar moieties decrease the antioxidant activity. Experimental and gas phase acidities of different classes of flavonoids were examined by Martins et. al., which included the flavanone naringenin [108].

An elaborate study of UV-Visible spectra of different flavonoid types including flavanones is carried out by Anouar E. H. et. al. [109]. Some flavonoid families are known to provide strong colours to different plant parts like fruits, leaves, flowers and vegetables. On the other hand, some flavonoids which are colourless are known to protect plants against UV radiation and protect DNA damage produced by UV A and UV B light [110,111].

Flavonoids could also be used to form complexes with metal ions especially transition metal ions. Ren et. al [112] have studied the complexes of iron with quercetin, luteolin, galangin, kaempferol and chrysin. Leopolidini et. al.[113] conducted an extensive study of Fe with neutral and anionic quercetin which may be bare or hydrated. Structural, electronic and optical properties of Cu-flavonoid complexes were studied by Lekka et. al.[114]. A bathochromic shift in the UV spectra was observed. Similar results were also found in Al-apigenin [115] complexes.

Molecular modeling studies involving docking studies using flavonoids as potential ligands against multiple protein targets are available in the literature. Different classes of flavonoids were docked against cyclooxygenase (COX) namely COX-2 which is involved in inflammatory response. Flavones and Flavonols containing 2-3 double bond were more potent as anti-inflammatory agents [116]. Flavonoids have been proposed as potential targets against different types of cancers [117,118] including breast cancer [119], prostate cancer [120], etc.

1.4 Scope of the present study

Theoretical works on flavanone molecules are scarce compared to other flavonoids. There are several applications of flavonoids and other polyphenols which could be possibly extended to the family of flavanones. In the present study, we have selected three flavanone molecules which are common in ancient medicine namely pinocembrin, pinostrobin and alpinetin. We have attempted a theoretical study on structure and many plausible applications of these molecules.

1.5 Objectives of the present study

Pinocembrin, Pinostrobin and Alpinetin are some of the important flavonones found in the plant kingdom. Pinocembrin is traditionally used in medicine and is known to have pharmacological activities like antioxidant, anti-inflammatory, anti-microbial, anti-apoptotic, vasorelaxant and anti-proliferative properties [121]. It is proved recently that pinocembrin can prevent rat brain from ischemic injury and it is now in phase I clinical trials to develop as a drug for ischemic stroke [122]. Pinostrobin is known to act as an antispasmodic agent, reduce estrogen induced cell proliferation, mediates anti-inflammatory activities etc. [76][123]. Alpinetin is also quite significant in ancient medicine and is known to possess anti-bacterial, anti-tumor, anti-inflammatory and many other biological properties [124,125]. To the best of our knowledge, theoretical knowledge about these molecules are very limited in the literature. In this context, we attempt:

- Theoretical investigation of the structure of pinocembrin, pinostrobin and alpinetin.
- Theoretical study of antioxidant potential and antioxidant mechanism operating in these flavanones.
- Elucidation of druggability and toxicity studies on the title molecules.
- To improve the antioxidant potentialities of these compounds by derivatization.
- Theoretical study of UV absorbance of these molecules and their potential application as UV filters.
- To check the potential metal chelation ability pinocembrin and pinostrobin for heavy metals.
- To study the multiple targets for these flavanones using inverse docking followed by conventional docking protocol.

References

[1] M. Planck, Ann. Phys. 4 (1901) 553.

[2] A. Einstein, Ann Phys 17 (1905) 132.

[3] N. Bohr, Phil. Mag. 26 (1913) 1.

[4] L. de Broglie, Recherche Sur La Theorie Des Quanta., University of Paris, 1924.

[5] W. Heisenberg, Z. Phys. 33 (1925) 879–893.

[6] E. Schrödinger, Ann. Phys. 79 (1926) 361.

[7] E. Lewars, Computational Chemistry; Introduction to the Theory and Applications of Molecular and Quantum Mechanics, Springer Dordrecht Heidelberg London New York, 2011.

[8] M.J. Nye, Chemical Philosophy to Theoretical Chemistry: Dynamics of Matter and Dynamics of Disciplines, University of California Press, 1994.

[9] N. Allinger, Calculation of Molecular Structures and Energy by Force Methods in Advances in Physical Organic Chemistry, Academic, New York, 1976.

[10] E. Engler, J. Andose, P. Schleyer, J. Am. Chem. Soc. 95 (1973) 8005.

[11] J. Williams, P. Stang, P. Schleyer, Ann. Rev. Phys. Chem. 19 (1968) 531.

[12] P.W. Atkins, Physical Chemistry, 5th Edn, Freeman New York, 1994.

[13] W. Moore, Physical Chemistry, 4th edn., Prentice-Hall, New Jersey, 1972.

[14] K. Lipkowitz, J. Chem. Ed 72 (1995) 1070.

[15] P.W. Atkins, R.S. Friedman, Molecular Quantum Mechanics, Oxford, 1997.

[16] I.N. Levine, Quantum Chemistry, Prentice Hall, Upper Saddle River, NJ, 2000.

[17] D.A. McQuarrie, Quantum Chemistry, 1983.

[18] F. Jensen, Introduction to Computational Chemistry, New York, 1999.

[19] C. Roothaan, Rev Mod Phys 23 (1951) 69–89.

[20] G. Hall, Proc R Soc 205 (1951) 541–52.

[21] C. Møller, M. Plesset, Phys Rev (1934) 46:618.

[22] J. Binkley, J. Pople, Int J Quant Chem (1975) 9:229.

[23] I. Shavitt, Mol. Phys. 94 (1998) 3.

[24] G. Das, J .Chem. Phys . 58 (1973) 5104.

[25] H.-. J. Werner, Adv. Chem. Phys. 69 (1987) 1.

[26] H.-J. Werner, P.J. Knowles, J. Chem. Phys. 89 (1988) 5803.

[27] A. Szabo, N. Ostlund, in:, Mod. Quantum Chem., McGraw-Hill, New York, 1989.

[28] M.J.S. Dewar, in:, Mol. Orbital Theory Org. Chem., McGraw-Hill, New York, 1969.

[29] T. Clark, J Mol Struct 530 (2000) 1.

[30] J.A. Pople, D.L. Beveridge, Approximate Molecular Orbital Theory, McGraw-Hill, New York, 1970.

[31] R. Pariser, R. Parr, J Chem Phys 21 (1953) 466.

[32] J. Pople, Trans. Faraday Soc. 49 (1953) 1475.

[33] J.A. Pople, G.A. Segal, J .Chem. Phys . 44 (1966) 3289.

[34] J. Pople, D. Beveridge, P. Dobosh, J. Chem. Phys. 47 (1967) 2026.

[35] R. Dixon, Mol. Phys. Phys 12 (1967) 83.

[36] W. Kohn, L. Sham, Phys. Rev. 140 (1965) A1133.

[37] P. Hohenberg, W. Kohn, Phys .Rev. B 136 (1964) 864.

[38] W. Kohn, a D. Becke, R.G. Parr, J. Phys Chem (1996) 12974–12980.

[39] J.P. Perdew, K. Burke, M. Ernzerhof, Phys. Rev. Lett. 77 (1996) 3865.

[40] J.P. Perdew, K. Burke, M. Ernzerhof, 78 (1997) 1396(E).

[41] A.D. Becke, Phys. Rev. A 38 (1988) 3098.

[42] S. Kurth, J. Perdew, P. Blaha, Int. J. Quant. Chem. 75 (1999) 889.

[43] C. Cramer, Essentials of Computational Chemistry, 2004.

[44] P.J. Stephens, F.J. Devlin, C.F. Chabalowski, M.J. Frisch, J.Phys.Chem. 98 (1994) 11623–11627.

[45] S. Sousa, O. Fernandes, M. Ramos, J. Phys. Chem. A 111 (2007) 10439.

[46] J. Perdew, A. Ruzsinszky, J. Tao, V. Staroverov, G. Scuseria, G. Csonka, J. Chem. Phys. 123 (2005) 62201.

[47] W.J. Hehre, Practical Strategies for Electronic Structure Calculations. Wavefunction, Inc., Irvine, CA, 1995.

[48] W. Hehre, L. Radom, P. Schleyer, J. Pople, Ab Initio Molecular Orbital Theory., Wiley, New York., 1986.

[49] P. Warner, J .Org. Chem. (1996) 7192.

[50] M. Orio, D.A. Pantazis, F. Neese, Photosynth. Res. 102 (2009) 443–453.

[51] S. Rusznyak, A. Szent–Györgyi, Nature 138 (1936) 798.

[52] D. Malesev, V. Kunti, J. Serb. Chem. Soc. 72 (2007) 921–939.

[53] M.L. Neuhouser, Nutr. Cancer 50 (2004) 1.

[54] M. Katan, Am. J. Clin. Nutr. 65 (1997) 1542.

[55] R.R. Huxley, H.A. Neil, Eur. J. Clin. Nutr. 57 (2003) 904.

[56] W. Ren, Z. Qiao, H. Wang, L. Zhu, L. Zhang, Med. Res. Rev. 23 (2003) 519.

[57] B.N. Ames, M.K. Shigenaga, T.M. Hagen, Proc. Natl. Acad. Sci. 90 (1993) 7915.

[58] C.A. Rice–Evans, N.J. Miller, G. Paganga, Free Rad. Biol. Med. 20 (1996) 933.

[59] S.R. Husain, J. Cillard, P. Cillard, Phytochemistry 26 (1987) 9.

[60] M.M. Silva, M.R. Santos, G. Caroco, R. Rocha, G. Justino, L. Mira, Free Rad. Res. 36 (2002) 1219.

[61] S. Renaud, M. DeLorgeli, Lancet 339 (1992) 1523.

[62] E. Middleton, C. Kandaswami, The Flavonoids: Advances in Research Since 1986, Chapman & Hall, London, 1994.

[63] H.E. Khoo, A. Azlan, S.T. Tang, S.M. Lim, Food Nutr. Res. 61 (2017) 1361779.

[64] C. Zhuang, W. Zhang, C. Sheng, W. Zhang, C. Xing, Z. Miao, Chem. Rev. 117 (2017) 7762–7810.

[65] A.N. Panche, A.D. Diwan, S.R. Chandra, J. Nutr. Sci. 5 (2016).

[66] S. Kumar, A.K. Pandey, Sci. World J. 2013 (2013) 1–16.

[67] R.J. Veitch, N. C., & Grayer, Chalcones, Dihydrochalcones, and Aurones in Flavonoids: Chemistry, Biochemistry and Applications, CRC Press, Taylor & Francis Group, Boca Raton, FL, 2006.

[68] B.A. Bohm, The Minor Flavonoids. in The Flavonoids: Advances in Research since 1986, Chapman & Hall, London, UK., 1994.

[69] T. Iwashina, J. Plant Res. 113 (2000) 287–299.

[70] D. Barreca, G. Gattuso, E. Bellocco, A. Calderaro, D. Trombetta, A. Smeriglio, G. Laganà, M. Daglia, S. Meneghini, S.M. Nabavi, BioFactors. 43 (2017) 495–506.

[71] A. Rasul, F.M. Millimouno, W.A. Eltayb, M. Ali, J. Li, X. Li, BioMed Res. Int. 2013 (2013).

[72] Y. Murti, P. Mishra, Int. J. ChemTech Res. 6 (2014) 3160–3178.

[73] J.W. Fahey, K.K. Stephenson, J. Agric. Food Chem. 50 (2002) 7472–7476.

[74] Wahyuni, M.H. Malaka, N.A. Yanti, R. Hartati, Sukrasno, I. Sahidin, Indian J Pharm Sci 80 (2018) 143–149.

[75] R. Christov, B. Trusheva, M. Popova, V. Bankova, M. Bertrand, Nat Prod Res. 20 (2006) 531–536.

[76] S.I. Abdelwahab, S. Mohan, M.A. Abdulla, M. Aspollah, A.B.A. Sukari, M.M.E. Taha, S. Syam, S. Ahmad, J. Ethnopharmacol. 137 (2011) 963–970.

[77] Z.T. Lü, Y.L. Zou, R. Deng, H. Shan, Asian J. Chem. 25 (2013) 9503–9507.

[78] K. Vafeiadou, D. Vauzour, H.Y. Lee, A. Rodriguez-Mateos, R.J. Williams, J.P.E. Spencer, Arch. Biochem. Biophys. 484 (2009) 100–109.

[79] M.A. Esmaeili, M. Alilou, Clin. Exp. Pharmacol. Physiol. 41 (2014) 416–422.

[80] C.L. Chao, C.S. Weng, N.C. Chang, J.S. Lin, S. Te Kao, F.M. Ho, Nutr. Res. 30 (2010) 858–864.

[81] A.S.A. Abuelsaad, G. Allam, A.A.A. Al-Solumani, Mediat. Inflamm. 2014 (2014) 1–11.

[82] A. Sala, M. Recio, G. Schinella, S. Máñez, R. Giner, M. Cerdá-Nicolás, J. Rosí, Eur J Pharmacol. 461 (2003) 53–61.

[83] L. Soromou, X. Chu, L. Jiang, M. Wei, M. Huo, N. Chen, S. Guan, X. Yang, C. Chen, H. Feng, D. X., Int Immunopharmacol. 14 (2012) 66–74.

[84] N. Patel, K. Bhutani, Phytomedicine. 21 (2014) 946–53.

[85] X. He, Z. Wei, J. Wang, J. Kou, W. Liu, Y. Fu, Z. Yang, Sci. Rep. 6 (2016) 1–11.

[86] J. Kakadiya, H. Mulani, N. Shah, J. Basic Clin. Pharm. 1 (2010) 85–91.

[87] C.S. Chiou, J.W. Lin, P.F. Kao, J.C. Liu, T.H. Cheng, P. Chan, Clin. Exp. Pharmacol. Physiol. 35 (2008) 938–943.

[88] L. Liu, D.-M. Xu, Y.-Y. Cheng, J. Agric. Food Chem. 56 (2008) 824–9.

[89] L. Testai, E. Da Pozzo, I. Piano, L. Pistelli, C. Gargini, M.C. Breschi, A. Braca, C. Martini, A. Martelli, V. Calderone, Front Pharmacol. 8 (2017) 1–11.

[90] L. Li, H. Yang, T. Yuan, Y. Zhao, G. Du, Chin J Nat Med. 11 (2013) 258–263.

[91] H. Sang, N. Yuan, S. Yao, F. Li, J. Wang, Y. Fang, S. Qin, Lipids Heal. Dis. 11 (2012) 166.

[92] X. Lan, W. Wang, Q. Li, W. Jian, Mol Neurobiol. 53 (2016) 1794–1801.

[93] S.Y. Shin, J.H. Kim, J.H. Lee, Y. Lim, Y.H. Lee, (2012) 761–774.

[94] A.A. Alshatwi, E. Ramesh, V.S. Periasamy, 27 (2013) 581–592.

[95] S. Aranganathan, J.P. Selvam, N. Nalini, (2008) 1385–1392.

[96] L. Wu, W. Yang, S.N. Zhang, J. Bin Lu, Drug Des Devel Ther. 9 (2015) 6119–6127.

[97] J. Du, B. Tang, J. Wang, H. Sui, X. Jin, L. Wang, Z. Wang, Int. J. Mol. Med. 29 (2012) 607–621.

[98] W.A. Roman Junior, D.B. Gomes, B. Zanchet, A.P. Schönell, K.A.P. Diel, T.P. Banzato, A.L.T.G. Ruiz, J.E. Carvalho, A. Neppel, A. Barison, C.A.M. Santos, Brazilian J. Pharmacogn. 27 (2017) 592–598.

[99] S.H. Moon, J.H. Lee, K. Kim, Y. Park, S. Nah, Int. J. Environ. Res. Public Heal. (2013) 5459–5469.

[100] P.S. Ruddock, M. Charland, S. Ramirez, L. A, N.T. GH, A. JT, L. M, D. JA, Sex Transm Dis. 38 (2011) 82–88.

[101] W.-Z. Huang, X.-J. Dai, Y.-Q. Liu, C.-F. Zhang, M. Zhang, Z.-T. Wang, J. Plant Resour. Environ. 15 (2006) 37–40.

[102] M. Tan, J. Zhu, Y. Pan, Z. Chen, H. Liang, H. Liu, H. Wang, Bioinorg. Chem. Appl. 2009 (2009) 1–9.

[103] A.M. Mendoza-Wilson, D. Glossman-Mitnik, J. Mol. Struct. Theo-Chem 716 (2005) 67–72.

[104] S. Aparicio, Int. J. Mol. Sci. 11 (2010) 2017–2038.

[105] S. Fiorucci, J. Golebiowski, D. Cabrol-Bass, S. Antonczak, Food Chem. (2007) 903–911.

[106] P. Trouillas, P. Marsal, D. Siri, R. Lazzaroni, J.-L. Duroux, Food Chem. 97 (2006) 679–688.

[107] W. Cai, Y. Chen, L. Xie, H. Zhang, C. Hou, Eur. Food Res. Technol. 238 (2013) 121–128.

[108] H.F.P. Martins, J.P. Leal, M.T. Fernandez, V.H.C. Lopes, M.N.D.S. Cordeiro, J. Am. Soc. Mass Spectrom. 15 (2004) 848–861.

[109] E.H. Anouar, J. Gierschner, J.L. Duroux, P. Trouillas, Food Chem. 131 (2012) 79–89.

[110] C.S. Cockell, J. Knowland, Biol. Rev. 74 (1999) 311–345.

[111] A. Kootstra, Plant Mol. Biol. 26 (1994) 771–774.

[112] J. Ren, S. Meng, C.E. Lekka, E. Kaxiras, J. Phys. Chem. B 112 (2008) 1845–1850.

[113] M. Leopoldini, N. Russo, S. Chiodo, M. Toscano, J. Agric. Food Chem. 54 (2006) 6343–6351.

[114] C.E. Lekka, J. Ren, S. Meng, E. Kaxiras, J. Phys. Chem. B 113 (2009) 6478–6483.

[115] A. Amat, C. Clementi, C. Miliani, A. Romani, A. Sgamellotti, S. Fantacci, Phys. Chem. Chem. Phys. 12 (2010) 6672– 6684.

[116] P.D. Mello, M.K. Gadhwal, U. Joshi, P. Shetgiri, Int. J. Pharm. Pharm. Sci. 3 (2011).

[117] D. Ravishankar, A.K. Rajora, F. Greco, H.M.I. Osborn, Int. J. Biochem. Cell Biol. 45 (2013) 2821–2831.

[118] L. Scotti, F. Jaime Bezerra Mendonca Junior, D. Rodrigo Magalhaes Moreira, M. Sobral da Silva, I. R. Pitta, M. Tullius Scotti, Curr. Top. Med. Chem. 12 (2013) 2785–2809.

[119] J. Suganya, M. Radha, D.L. Naorem, M. Nishandhini, Asian Pacific J. Cancer Prev. 15 (2014) 8155–8159.

[120] S. Shukla, R. Kanwal, E. Shankar, M. Datt, M.R. Chance, P. Fu, G.T. MacLennan, S. Gupta, Oncotarget 6 (2015) 31216–31232.

[121] S.-Y. Zhou, S.-X. Ma, H.-L. Cheng, L.-J. Yang, W. Chen, Y.-Q. Yin, Y.-M. Shi, X.-D. Yang, J. Mol. Struct. 1058 (2014) 181–188.

[122] Q. Yang, Y. Tong, F. Chen, Y. Qi, W. Li, S. Wu, Chin. J. Chem. 30 (2012) 1315.

[123] J.-C. Le Bail, L. Aubourg, G. Habrioux, Cancer Lett. 156 (2000) 37–44.

[124] W. He, Y. Li, C. Xue, Z. Hu, X. Chen, F. Sheng, Bioorg. Med. Chem. 13 (2005) 1837–1845.

[125] M. Huo, N. Chen, G. Chi, X. Yuan, S. Guan, H. Li, W. Zhong, W. Guo, L.W. Soromou, R. Gao, H. Ouyang, X. Deng, H. Feng, Int. Immunopharmacol. 12 (2012) 241–8.

Chapter 2

Theoretical and Methodological Overview

In the process of computational investigation of flavanone molecules attempted in this thesis, we have adopted several methodologies. These methodologies and the different softwares employed to carry out different works are briefly outlined in this chapter.

2.1 Potential Energy Surface

The concept of Potential energy surface (PES) is important in computational chemistry as it helps us in understanding the relationship between potential energy and molecular geometry. For a system with N atoms, the energy of such a system is a function of 3N-6 internal or 3N Cartesian co-ordinates. Gradient is a vector constituted by 3N-6 first partial derivatives of energy with respect to the variables on which energy is dependent. Points on the PES where the gradient is

zero is called a stationary point. There are three types of stationary points on a potential energy surface namely saddle point, local minima and global minima.

Saddle point is a stationary point which is a maxima in one direction and minima in all other directions. Local minima are stationary points which are minima compared to only nearby surfaces whereas global minima is the lowest energy minima on the whole potential energy surface.

During potential energy scan, the process starts with an initial structure at a given level of theory and proceeds through structures created by altering the specified variables. A 2D or 3D plot of potential energy v/s the variable (dihedral angle) is drawn. From the graph, the structure corresponding to global minima can be nominated for further geometrical optimization [1, 2].

2.2 Geometry optimization

Characterization of a stationary point on the PES is termed as geometry optimization [1]. The geometry considered may be a saddle point, a local minima or a global minima. The process of characterizing a global minima on the PES surface is called energy minimization. Energy minimization is done by supplying a plausible geometry which is closer to the global minima to the computer algorithm which then systematically changes the geometry to achieve the best minimized geometry [3].

Energy minimization can be mathematically stated as minimizing the first derivative of a function *f* which depends on independent variable x_1, x_2, x_3 …….. x_i with respect to each of the variable to zero and second derivative to a positive value.

$$\frac{\partial f}{\partial x_i} = 0 \text{ and } \frac{\partial^2 f}{\partial x_i} > 0 \qquad (2.1)$$

2.3 Frequency Calculations-Normal- Mode vibrations

Once the stationary point of choice is optimized, it is mandatory to check whether the resulting geometry is a minima or a saddle point [1]. This is done by calculating the normal mode of vibrations which are the simplest vibrations that a molecule can display. These are the vibrations where all atoms move in phase with frequency. All other vibrations are combinations of normal modes of vibration. This is in fact the calculation of theoretical Infrared spectrum.

A structure which is a real minima should have all the normal mode force constants to be positive. Since frequency calculations involve taking square root of force constant, all the frequencies for a minima will be real. On the other hand, for a transition state, all vibrations except one will be periodic vibration. For this vibration force, constant will be negative and vibrational frequency (square root of force constant) will be imaginary. An *n*-th order saddle point will have 'n' negative force constant or imaginary frequencies.

2.4 Nuclear magnetic resonance (NMR) spectra:

NMR spectroscopy is an exceptional tool for elucidating the structure and conformation of molecules. Evaluating derivatives of energy with respect to the magnetic field, nuclear magnetic moments and electric field helps to predict the position and splitting pattern of NMR. There are several methods to calculate chemical shifts like IGLO (individual gauge localized orbital)[4], LORG (localized or Loacaorbital origin) and GIAO (gauge independent or invariant or including atomic orbital) [5–7]. GIAO method of Ditchfield [7] was combined with DFT by Friedrich et al. [8]. DFT/GIAO is known to satisfactorily calculate the NMR spectra of organic molecules [9–11].

Both ^{13}C and ^{1}H NMR spectra were recorded using DFT/GIAO formalism. The shielding tensors obtained are compared to the shielding tensors of tetra methyl silane (TMS) (which is used as the reference) using the same level of theory. These shielding tensors are then converted to chemical shifts using the equation:

$$\delta_i = \sigma_{TMS} - \sigma_i \qquad (2.2)$$

NMR spectra can also be recorded in the solvent phase by combining it with solvation models which are discussed below. In such cases, TMS should also be optimized in the solvent phase and then NMR spectra of the reference compound should be recorded in the solvent phase.

2.5. Frontier Molecular Analysis

Frontier Molecular Orbital (FMO) theory developed in 1950s by Kenichi Fukui [12] describes chemical reactivities of molecules by focusing on frontier molecular orbitals namely highest occupied molecular orbital (HOMO) and lowest unoccupied molecular orbital (LUMO). Using this theory one can identify probable electrophilic and nucleophilic centers within a molecule.

For example, in molecules like naphthalene, frontier molecular theory describes electron density to be higher in α positions. Thus we can infer that electrophiles will prefer to attack α position of naphthalene.

2.6 Solvation model

Most of the theoretical calculations are done in gas phase. Solvation is one prime factor that perturbs the properties of a system. Solvent interactions could be added to these by employing solvation models. These interactions can be short range interactions or long range interactions. Currently, several implicit or solvation models are available to incorporate the effect of solvents. Well established continuum solvation models which account for long-range interactions are available in computational chemistry. Polarizable continuum model (PCM) is one of the commonly used solvation models [13]. This model places the solute in an appropriately shaped cavity and the apparent surface charge is distributed on the surface of the cavity. With variation in this apparent surface charge, several solvation models are available such as CPCM, IEFPCM etc. Two PCM models are

employed in the current study namely conductor-like polarizable continuum model (CPCM) and Integral equation formalism polarizable continuum model (IEFPCM) solvation models.

2.7 UV - Visible spectra – Time - Dependent Density Functional Theory (TDDFT)

DFT is a ground-state theory and it could not be used to study the properties of excited states. Time-Dependent Density Functional Theory (TDDFT)[14][15], which is a modified DFT incorporating time-dependent external potentials, can be used to study the excited states as the processes describing photon-electron interactions are time dependent. TDDFT is based on Runge-Gross (RG) theorem[14], which is the time dependent analogue of Hohenberg-Kohn theorem. Applying an external potential by virtue of this theorem on a system of non-interacting electrons, a time dependent Kohn-Sham scheme is created which obeys time dependent Schrödinger equation.

$$i\,\frac{\partial}{\partial t}\phi_j\,(r,\,t)\;=\;\hat{H}_{KS}(r,\,t)\phi_j\,(r,\,t) \qquad (2.3)$$

The main success of TDDFT is that it enables the calculation of the electronic excitations and the optical spectra. Applying Linear response theory and Casida equations to TDDFT, it can be enabled to capture the dynamical nature of the excitations processes by including the many-body effects, mixing of the Kohn-Sham states and the charge fluctuations during the transition to an excited state.

2.8 Natural Localized Molecular Orbital (NLMO)

The natural bond orbital (NBO) analysis involves transforming the input orbital basis into localized basis sets, which proceeds via natural atomic orbitals (NAOs), hybrid orbitals (NHOs), bond orbitals (NBOs) and localized molecular orbitals (NLMOs) The sequence involved in the is as follows: Input basis $\rightarrow$ NAOs $\rightarrow$ NHOs $\rightarrow$ NBOs $\rightarrow$ NLMOs. An orthogonalization procedure is applied to the input orbitals to construct the NAOs. To avoid the unphysical non-Hermitian terms in the Hamiltonian, NAOs are required to be orthogonal. The orthonormal NAOs are used in natural population analysis (NPA) to calculate the charges on the atoms [16].

Depending on the Energetic and spatial separation, parent NBOs were classified into different groups. Depending on these NLMOs were grouped into different "NLMO clusters". Those clusters having highest energy among the bonding NLMOs were called HOMO cluster and the lower ones as HOMO-1, HOMO-2 etc. Similarly, those clusters having the lowest energy among the vacant orbitals are designated as LUMO clusters and the higher ones as LUMO+1, LUMO+2, etc.

2.9 Thermochemistry

Most of the reactions happening around us are governed by the thermodynamic parameters like internal energy ΔE, formation enthalpy ΔH, Gibbs free energy ΔG, specific heat capacity at constant volume CV, entropy ΔS, etc. The values of all these parameters may be computed from Gaussian software assuming non-interacting particles.

Errors due to assumption of classical behavior for rotation and explicit consideration of lower vibrational frequencies are not corrected for in the thermochemistry data included in this thesis.

Internal thermal energy, E_{tot} is given by:

$$E_{tot} = E_t + E_r + E_v + E_e \quad (2.4)$$

here E_t is the translational contribution to internal energy, E_r is rotational contribution to internal energy and E_v is the vibrational contribution to internal energy and E_e is the electronic contribution to internal energy.

Enthalpy of formation, H can be calculated as:

$$H = E_{tot} + k_B T \quad (2.5)$$

Gibb's free energy, G is given by:

$$G = H - TS_{tot} \quad (2.6)$$

where S_{tot} is given by $S_{tot} = S_t + S_r + S_v + S_e$.

2.9.1 Enthalpy change of a reaction

For a reaction of reactant giving products, the enthalpy change of the reaction may be found out using the equation:

$$\Delta_r H^o = \sum_{products} \Delta_f H^o_{prod} - \sum_{react} \Delta_f H^o_{react} \quad (2.7)$$

2.10 Molecular Docking

Molecular docking is a well-established computational protocol to study the interaction between two molecules. Usually, the interaction between small molecules called ligands with the active site of proteins is studied using this methodology [17]. It helps to find out the best orientation of the ligand in the active site of the protein which gives overall minimum energy. It has wide applications in the field of drug design as it helps to study drug-protein/receptor interactions. In conventional docking methodology, different ligand molecules are screened against a given protein active site. Recently, inverse docking strategies are utilized wherein a given ligand is screened against a database of pharmacophores to identify multiple targets possible for a given ligand.

2.11 Softwares

2.11.1 Computational softwares

a) Gaussian

Gaussian is a computational chemistry software package developed by John Pople and his research group at Carnegie Mellon University as early as in 1970s in the name Gaussian 70 [18]. This name arose from the use of Pople's Gaussian type orbitals used instead of Slater type orbitals to speed up molecular calculations. This software has been updated continuously since then.

Different methods of calculations available are simple molecular mechanics (such as Amber force field), semi-empirical

methods (such as CNDO), Hartree-Fock (restricted and unrestricted), MPn (Mollar-Plesset perturbation theory of order n=2, 3, 4), CI (Configuration-Interaction), CC (Coupled-Cluster), Multi-configurational SCF (such as CAS-SCF) and various DFT (Density-Functional Theory) methods.

Gaussian software helps to do electronic- structure calculations and quantum chemical calculations. Several spectral data can be reproduced like NMR chemical shifts, Infra Red spectra, Raman spectra Ultraviolet spectra and the like. A wide range of molecular properties that can be computed includes nonlinear optical properties, thermochemistry etc. Reaction mechanisms can be elucidated in details including transition state structures and intrinsic reaction coordinates. Gaussian is one of the very popularly used computational softwares among the scientists of different fields of study like physics, chemistry and biology. In the current study, the version of Gaussian software used is Gaussian 09 [19].

b) NBO software

NBO is a mutually consistent and comprehensive analysis tool, ensuring harmonious chemical interpretations. NBOs are intrinsic realizations of orbital-type bonding concepts. It helps to understand various electronic effects like hyperconjugation, delocalization of charge etc. It also helps to visualize various orbitals. In the current work NBO 3.1 [20] inbuilt in Gaussian 09 is used for NLMO analysis.

c) Autodock Vina

Autodock-Vina is an open source platform developed by Molecular Graphics Lab at The Scripps Research Institute [21]. It offers multi-core capability, high performance, enhanced accuracy software for drug discovery, molecular docking and virtual screening. Autodock Vina presents results in a user friendly way.

Autodock Vina does not provide the user with a choice of search algorithm. It uses Iterated Local search global optimizer. Partial charges, solvation parameters are not required for Autodock Vina. Preparation of receptor and ligands were performed using AutoDock Tools which is an interactive graphics software distributed with AutoDock.

d) Open Babel

Open babel [22] is a chemical toolbox which allows to search, analyze or convert data for research. Open Babel is an open software which helps to file type convertion. This software has been put use throughout this work for file type conversion.

e) SwissPDB Viewer

It is a user friendly application which helps to analyze proteins. It helps to visualize, edit, compare the structure alignments, active sites etc. In this thesis, swissPDB viewer [23,24] is used to add missing residues of proteins prior to docking using Autodock Vina.

2.11.2 Visualization softwares

a) Gauss View

Gauss View is a graphical user interface designed to prepare input structures for submission to Gaussian software. Gauss View allows to rapidly sketch even very large molecules. It also allows to rotate, translate and zoom in on these molecules. Gauss View makes it easy to set up many complex Gaussian calculations like, STQN (The Synchronous Transit-Guided Quasi-Newton), transition structure optimizations, our own n-layered integrated molecular orbital and molecular mechanics (ONIOM), CASSCF calculations, periodic boundary conditions (PBC) calculations, and many more. Gauss View also helps to examine the results of Gaussian calculations using a variety of graphical techniques. The current work has a heavy dependence on Gauss View for creating inputs to analyzing output structures.

b) Chemcraft

Chemcraft [25] is also a graphical program for working with quantum chemistry computations. It acts as a convenient tool for visualizing computed results and preparing new jobs for a calculation. It helps to render 3-dimensional pictures of molecules, visualization of molecular orbitals in form of isosurfaces or colored planes and many more. In the current work, I have used Chemcraft mainly to create some publication-ready images of molecules in customizable display modes and to construct NLMOs and NLMO clusters which are discussed in successive chapters.

c) Chemissian

Chemissian [26] is a visualization tool for analyzing molecules electronic structure and spectra. It helps to visualize molecular orbital energy-level diagrams (Hartree - Fock and Kohn - Sham orbitals), Natural transition orbitals, calculated and experimental UV-VIS electronic spectra, electronic/spin density maps and prepare them for publication. Chemissian has a user-friendly graphical interface and helps to visualize the output of Gaussian quantum chemical program package. In this work, Chemissian have been used for analyzing molecular orbital energy level diagram.

d) Chemsketch

Chemsketch [27] is a freeware drawing platform for organic molecules. It helps to calculate molecular properties like molecular weight, density, etc. In this thesis, chemsketch is used to draw line diagram of molecules.

2.11.3 Online softwares

a) Molinspiration

Molinspiration [28] is an online cheminformatics tool supporting molecule manipulation and processing. It helps in the calculation of various molecular properties needed in QSAR, molecular modeling and drug design. It also supports fragment-based virtual screening, bioactivity prediction and data visualization.

b) Osiris Property Explorer

The OSIRIS Property Explorer [29] helps to calculate various drug-relevant properties on a valid structural input. Different properties significant for drug action are computed and are summed up as a drug-likeness score and a drug score. Besides this, the toxicity risk of the given molecule is also analyzed. But now this software is replaced by a similar analog named DataWarrior [30].

c) PharmMapper

PharmMapper [31–33] is a freely accessed web server which helps to identify potential target candidates for given small molecules. It is highly efficient and robust mapping method. It is backed by a huge in-house repository of pharmacophore database. The uploaded molecules are compared against these pharmacophore models and molecule's aligned poses and fit scores are given as output.

2.12 Computer Power

All the calculations included in this thesis are performed using Lenovo Thinkstation with processor Intel®Xeon®CPU E5-2660 v3 @2.60 GHz and 32.0 GB RAM.

References

[1] E. Lewars, Computational Chemistry; Introduction to the Theory and Applications of Molecular and Quantum Mechanics, Springer Dordrecht Heidelberg London New York, 2011.

[2] D. Young, Computational Chemistry, Wiley/Interscience, New York, 2001.

[3] C. Cramer, Essentials of Computational Chemistry, 2004.

[4] V.G. Malkin, O.L. Malkina, D.R. Salahub, Chem. Phys. Lett. 204 (1993) 87.

[5] F. London, J. Phys. Radium 8 (1937) 397–409.

[6] R. McWeeny, Phys. Rev. 126 (1962) 1028.

[7] R. Ditchfield, Mol. Phys. 27 (1974) 789–807.

[8] K. Friedrich, G. Seifert, G. Grossmann, Z. Phys. D 17 (1990) 45.

[9] S.K. Wolff, T. Ziegler, J .Chem. Phys . 109 (1998) 895.

[10] M. Siskos, M. Choudhary, I. Gerothanassis, Molecules. 22 (2017) 415.

[11] L.A. De Souza, W.M.G. Tavares, A.P.M. Lopes, M.M. Soeiro, W.B. De Almeida, Chem. Phys. Lett. 676 (2017) 46–52.

[12] K. Fukui, T. Yonezawa, H. Shingu, J .Chem. Phys . 20 (1952) 722.

[13] J. Tomasi, B. Mennucci, R. Cammi, Chem.Rev. 105 (2005) 2999–3094.

[14] E. Runge, E.K.U. Gross, Phys. Rev. Lett. 52 (1984) 997–1000.

[15] M.E. Casida, Recent Advances in Density Functional Methods, World Scientific, Singapore, 1995.

[16] J. Tošović, S. Markovic, Chem. Pap. 74 (2017) 543–552.

[17] X.-Y.M. Meng, H.-X. Zhang, M. Mezei, M. Cui, Curr Comput Aided Drug Des. 7 (2011) 146–157.

[18] W.J. Hehre, W.A. Lathan, R. Ditchfield, M.D. Newton, J.A. Pople, Gaussian 70 (Quantum Chem. Progr. Exch. Progr. No.237) (1970).

[19] M.J. Frisch, G.W. Trucks, H.B. Schlegel, G.E. Scuseria, M.A. Robb, J.R. Cheeseman, G. Scalmani, V. Barone, B. Mennucci, G.A. Petersson, H. Nakatsuji, M. Caricato, X. Li, H.P. Hratchian, A.F.

Izmaylov, J. Bloino, G. Zheng, J.L. Sonnenberg, M. Hada, M. Eha, D.J. Fox, (2009).

[20] E.D. Glendening, A.E. Reed, J.E. Carpenter, F. Weinhold., NBO Version 3.1.

[21] O. Trott, A.J. Olson, J. Comput. Chem. 31 (2010) 455–461.

[22] N.M. O'Boyle, M. Banck, C.A. James, C. Morley, T. Vandermeersch, And, G.R. Hutchison, J. Cheminf. 3 (2011) 33.

[23] N. Guex, M.C. Peitsch, Electrophoresis 18 (1997) 2714–2723.

[24] http://www.expasy.org/spdbv/.

[25] G.A. Zhurko, D.A. Zhurko, Chemcraft 1.6, Chemcraft Graphical Program for Working with Quantum Chemistry Results, 2009.

[26] L.V. Skripnikov, Chemissian Version 4.43 Visualization Computer Program.

[27] ACD/Chemsketch,Advanced Chemistry Development, Inc., www.acdlabs.com, Toronto, ON, Canada, 2015.

[28] http://www.molinspiration.com/.

[29] http://www.organic-Chemistry.org/prog/peo.

[30] http://www.openmolecules.org/datawarrior/download.html .

[31] X. Liu, S. Ouyang, B. Yu, K. Huang, Y. Liu, J. Gong, S. Zheng, Z. Li, H. Li, H. Jiang, Nucleic Acids Res. 38 (2010) W609–W614.

[32] X. Wang, C. Pan, J. Gong, X. Liu, H. Li, J. Chem. Inf. Model. 56 (2016) 1175–1183.

[33] X. Wang, Y. Shen, S. Wang, S. Li, W. Zhang, X. Liu, L. Lai, J. Pei, H. Li, Nucleic Acids Res. 45 (2017) W356–W360.

Chapter 3

Structural elucidation and spectral characterization

3.1. Introduction

Flavanones are flavonoids which do not have C2-C3 double bond and C3-OH. These molecules have a chiral centre at C2 carbon. Several flavanones known include naringenin, hespertin, naringin, hesperidin, pinocembrin, pinostrobin, alpinetin etc. [1–5]. As already discussed, flavanones are known to possess several therapeutic effects and some of them are in clinical trials [6].

The flavanones selected for current study were pinocembrin, pinostrobin and alpinetin. These are structurally related, pinocembrin is 5, 7-dihydroxyflavanone whereas pinostrobin and alpinetin are respectively 7-Omethyl and 5-Omethyl derivatives of pinocembrin. These molecules are experimentally known to have many pharmacological functions like antioxidant, anti-bacterial, anti-inflammatory and even anti-cancer effects [3,4,7]. Most of these activities can be traced back to the radical scavenging effects of these molecules and some are due to interaction with proteins/receptors. Computational and molecular modeling studies can shed light into the mechanism of action of these molecules.

As a pre-requisite for detailed computational study, we attempt a detailed structural characterization of the title molecules along with a thorough description of their spectral characteristics. Frontier Molecular orbital analysis is also carried out in the selected molecules. We also predicted the reactivity of different sites through molecular electrostatic potential (MEP) studies [8]. Theoretical studies with the use of computational tools always help us in understanding the properties and reactivity of the molecules which will equip us with different strategies for fine tuning and exploiting their properties.

3.2. Computational Methodology

B3LYP and M06 functionals were tried for simple molecules. Thermodynamic parameters calculated using both these functionals showed only slight difference and was similar in trend, so considering computational cost and time we opted to continue with B3LYP functional.

Flavanone molecules namely pinocembrin, pinostrobin and alpinetin were initially subjected to potential energy scans using B3LYP functional at 6-31G (d,p) level of theory. B3LYP functional is a combination of Becke's exchange functional [9] and Lee-Yang-Parr correlation functional [10]. For pinocembrin, the dihedral angle C6'-C1'-C2-C3 which decides the planarity between chromone ring and phenyl ring was initially scanned from 0° to 360°. The lowest conformer resulting from this scan was then scanned for dihedral C8-C7-O7-H7 to decide the orientation of 7-OH. The lowest energy conformer so obtained was then scanned for C10-C5-O5-H5 which decides the orientation of 5-OH group. This is crucial in deciding feasibility of intramolecular H-bond. Based on the huge volume of

literature [11-13] available on flavonoids some commonly used functionals and basis sets were chosen for the present study. Structure of pinocembrin was then subjected to geometry optimization using B3LYP/6-31+G (d,p), B3LYP/6-311+G (d,p) and B3LYP/6-311++G (d,p) functional. The structural parameters were analyzed and were compared with the available experimental data. The optimal basis set was selected for further study.

Pinostrobin and Alpinetin which are 7-Omethyl and 5-Omethyl derivatives of pinocembrin respectively were then constructed from the optimized geometry of pinocembrin after resorting to potential energy scans for the dihedrals connecting the substituents. Harmonic frequency calculations were then performed on the optimized structures to confirm that the structures are real. Nuclear Magnetic resonance spectra (NMR) are recorded for the molecules studied. Both ^{13}C and ^{1}H NMR spectra were analyzed for understanding the structure. Structures of the molecules were optimized in solvent media for recording the NMR spectra. The solvents were elected as per the availability of the experimental spectra for the ease of comparison. Pinocembrin and Alpinetin were optimized in dimethyl sulphoxide (DMSO) media and pinostrobin in chloroform media. The solvent model chosen was conductor-like polarizable continuum model (CPCM) [14]. NMR spectra is then taken using the gauge-including atomic orbital (GIAO) [15] method. Tetra methyl silane (TMS) is taken as the reference and the spectra of TMS are recorded in the solvent phase. The isotopic shielding tensors so obtained were converted to chemical shift in ppm using the following equation:

$$\delta_i = \sigma_{TMS} - \sigma_i \qquad (3.1)$$

The chemical shifts were then compared with experimentally available spectral data for conforming the structure obtained theoretically. Presence or absence of intramolecular hydrogen bonding which has good significance in antioxidant activity of a molecule [16, 17] is also analyzed.

Frontier Molecular Orbital (Highest occupied molecular orbital (HOMO) and Lowest unoccupied molecular orbital (LUMO)) analysis is carried out to decide optical and electronic properties of molecules. This could also predict the reactivity of the molecule. To understand the reactive sites of the molecule, Molecular electrostatic potential (MEP) [8] was calculated at B3LYP/ 6-31+G (d, p) level of theory for the molecules studied here. It plots electrostatic potential mapped onto constant electron density surface and is a very useful descriptor in identifying sites for electrophilic attack and nucleophilic attack. All the calculations are carried out using Gaussian 09 software [18].

3.3. Result and Discussion

3.3.1. Conformational Analysis

Structure of pinocembrin was downloaded from pubchem [19] (pubchem ID: 68071) and was optimized to global minima *via* the following steps. To begin with, the dihedral C6'-C1'-C2-C3 was scanned from 0 to 360º through 12 steps of 30º intervals. The result was as shown in Fig. 3.1. There were two low energy conformers, conformer 4 and 10. The lowest energy conformer 10 was selected for subsequent scans. Structure of pinocembrin involves two OH groups located on C5 and C7 carbon atoms. Orientation of these OH groups is crucial as they participate in intramolecular H bonding and is

influential in antioxidant activities exerted by the molecule which is discussed in subsequent chapter.

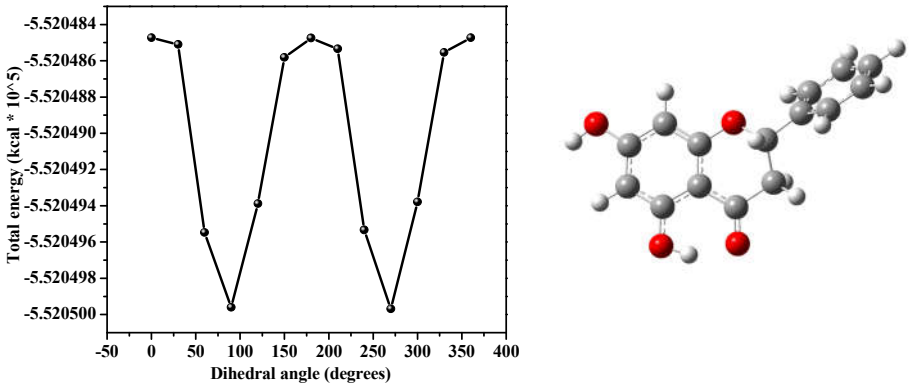

Fig 3.1: Potential energy scan of pinocembrin for the dihedral C6'-C1'-C2-C3.

The lowest conformer from the first scan is subjected to C7-OH scan. The dihedral C8-C7-O7-H7 was scanned from 0 to 360º through 12 steps of interval 30º. There were three low energy conformers, conformer 1, 7 and 13. Of these the lowest conformer, conformer 7 with a dihedral angle of -180º was subjected to C5-OH scan (Fig.3.2a). The dihedral C10-C5-O5-H5 was scanned from 0 to 360º through 12 steps at an interval of 30º. The lowest structure so obtained had the dihedral angle C10-C5-O5-H5 to be 0º (Fig.3.2b). This shows that OH group was oriented towards carbonyl oxygen which indicates a possibility of intramolecular H-bonding. The structure so obtained was further refined with a higher basis set to get the final structure for pinocembrin.

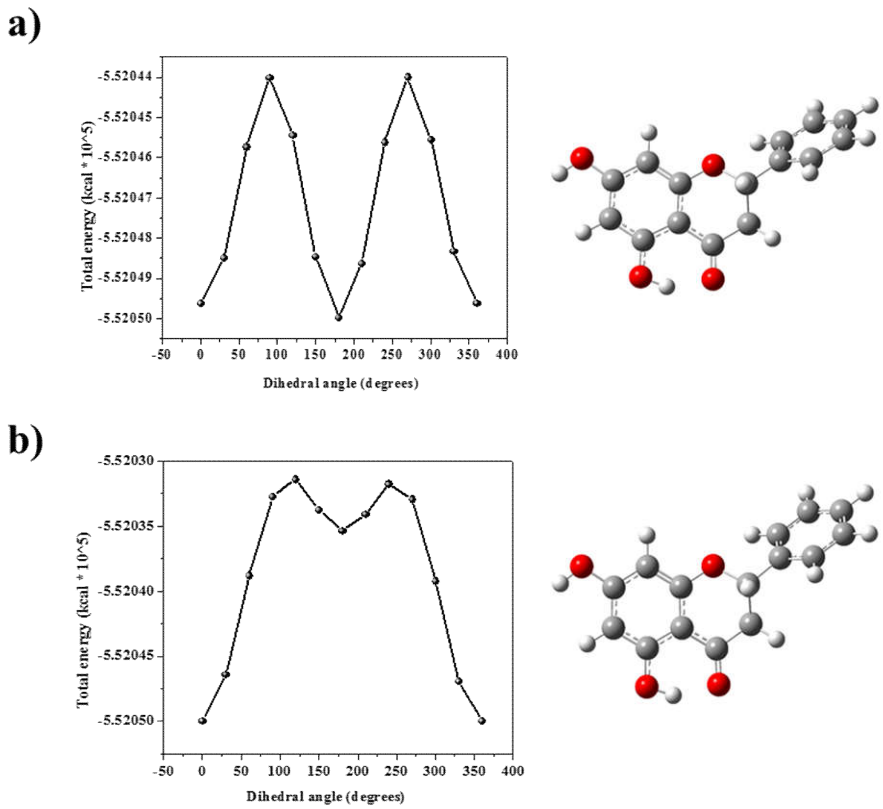

Fig 3.2: Potential energy scan of pinocembrin for the dihedral a) C8-C7-O7-H7 b) C10-C5-O5-H5.

Pinostrobin had a structure very similar to pinocembrin except that C7-OH was replaced by -OMe group. Thus, the structural framework obtained after energy minimization of pinocembrin was taken as the starting geometry for the potential energy scan of pinostrobin. The dihedral C8-C7-O7-O11 was scanned from 0 to 360º through 12 steps of interval 30º (Fig.3.3). The lowest energy conformer, conformer 7 was selected as the starting geometry for geometry optimization.

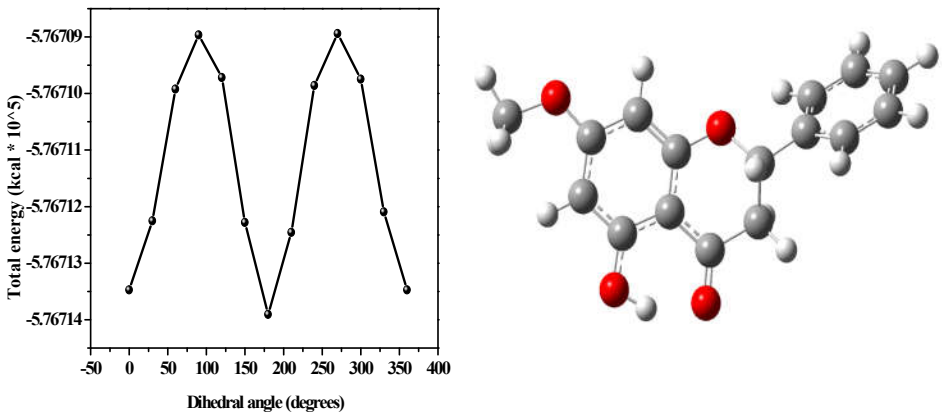

Fig 3.3: Potential energy scan of pinostrobin for the dihedral C8-C7-O7-O11.

Alpinetin also had a structure close to pinocembrin. Here 5-OH was replaced by -OMe group. Starting from the energy minimized structure of pinocembrin, dihedral C10-C5-O5-C11 was scanned from 0 to 360º through 12 steps of interval 30º to get the lowest conformer of alpinetin (Fig. 3.4). The lowest conformer had the dihedral C10-C5-O5-C11 to be 180º.This rotation of C5-O5 bond may be attributed to the bulkier nature of -OMe group and incapability of -OMe group in participating in H-bonding interaction. This structure was further subjected to geometry optimization.

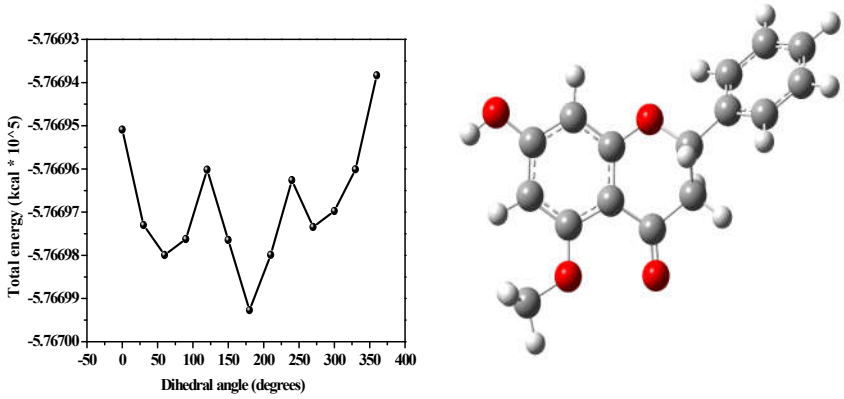

Fig 3.4: Potential energy scan of alpinetin for the dihedral C10-C5-O5-C11.

3.3.2. Basis set selection

The structure obtained from potential energy scan of pinocembrin was further subjected to geometry optimization using three higher basis sets namely, B3LYP/6-31+G(d,p), 6-311+G(d,p) and 6-311++G(d,p). Experimental crystal structure data was available only for pinocembrin and hence the theoretically obtained bond length parameters of pinocembrin using the three different basis sets were compared with the experimental data [4]. Correlation coefficient was calculated for structures optimized with different basis sets. It could be seen that correlation coefficient (R) was 0.928 and R^2 = 0.86 for all the basis sets (Table 3.1). Slight variations are expected as theoretical calculations are done in gas phase and do not consider any molecular interactions unlike experimental structures.

Table 3.1. Bond lengths of pinocembrin optimized in different basis sets are compared to experimental bond length

	Experiment	B3LYP/6-31+G (d,p)	B3LYP/ 6-311+G(d,p)	B3LYP/ 6-311++Gdp
C2-C3	1.391(11)	1.53	1.5	1.53
C3-C4	1.503(8)	1.52	1.51	1.51
C5-C6	1.371(8)	1.39	1.39	1.39
C6-C7	1.402(8)	1.40	1.40	1.40
C7-C8	1.393(8)	1.40	1.40	1.40
C8-C9	1.366(8)	1.39	1.38	1.38
C4-C10	1.420(8)	1.45	1.45	1.45
C5-C10	1.416(8)	1.43	1.42	1.42
C9-C10	1.417(8)	1.42	1.42	1.42
C2-C1'	1.509(10)	1.51	1.51	1.51
C1'-C2'	1.497(22)	1.40	1.40	1.40
C1'-C6'	1.230(30)	1.40	1.40	1.40
C2'-C3'	1.399(25)	1.40	1.39	1.39
C3'-C4'	1.229(24)	1.40	1.39	1.39
C4'-C5'	1.360(30)	1.40	1.39	1.39
C5'-C6'	1.430(3)	1.40	1.39	1.39
C2-H2	1.183(24)	1.10	1.10	1.10
C3-H3(a)	1.087(21)	1.09	1.09	1.09
C3-H3(b)	1.109(21)	1.10	1.10	1.10
C6-H6	1.098(16)	1.09	1.08	1.08
C8-H8	1.099(23)	1.08	1.08	1.08
C2'-H2'	1.090(30)	1.09	1.08	1.08
C3'-H3'	1.160(30)	1.09	1.08	1.08
C4'-H4'	1.072(17)	1.09	1.08	1.08
C5'-H5'	1.150(3)	1.09	1.08	1.08
C6'-H6'	1.080(3)	1.09	1.09	1.09
C2-O1	1.391(9)	1.45	1.45	1.45
C4-O4	1.268(7)	1.25	1.24	1.24
C5-O5	1.360(7)	1.34	1.34	1.34
C7-O7	1.351(7)	1.36	1.36	1.36
C9-O1	1.369(7)	1.36	1.36	1.36
O5-H5	1.090(20)	0.99	0.99	0.99
O7-H7	1.100(21)	0.97	0.96	0.96
	Correlation Coefficient (R)	0.9283	0.9279	0.9279
	R^2	0.8618	0.8610	0.8610

By comparing the correlation coefficients for different basis sets used, we could understand that B3LYP/6-31+G (d,p) basis set has stronger correlation to experimental data set. Also considering computational cost and time this (B3LYP/6-31+G (d,p)) basis set was selected for geometry optimization of pinocembrin, pinostrobin and alpinetin for a major portion of our study.

3.3.3. Geometry Optimization and Structural parameters

Optimized structures of pinocembrin, pinostrobin and alpinetin are given in Fig. 3.5. Atom numbering scheme followed in this thesis are according to that given in the figure. Structure of these flavonone molecules are composed of three rings, two phenyl rings A and B and a chromone ring C. These rings are not planar and there exists a dihedral angle O1-C2-C1'-C2'of -42.82º (pinocembrin) and -41.35º (pinostrobin) and -38.23º (alpinetin) between them. As seen from the figure, pinocembrin has OH groups at position 5 and 7 whereas pinostrobin and alpinetin have 7-OH and 5-OH groups methylated respectively. From the analysis of molecular structure, there exists a probability of intramolecular H-bonding between 5-OH and 4 C=O groups in pinocembrin and pinostrobin unlike that reported by Vargas Sánchez *et. al.* [20] for pinocembrin. This hydrogen bond formation in pinocembrin is also evident in the work by Bertelli *et.al.* [21] using experimental NMR studies. Alpinetin fails to have this H-bond as 5-OH group is methylated and hence the molecule does not have any intramolecular hydrogen bonds. On comparing the bond lengths of C=O bond in pinocembrin, pinostrobin and alpinetin, it could be seen that C=O bond is elongated in pinocembrin and pinostrobin (1.246 Aº)

compared to alpinetin (1.225 Aº), supporting the formation of H-bond in pinocembrin and pinostrobin. Structural parameters of pinostrobin and alpinetin are tabulated in Table 3.2.

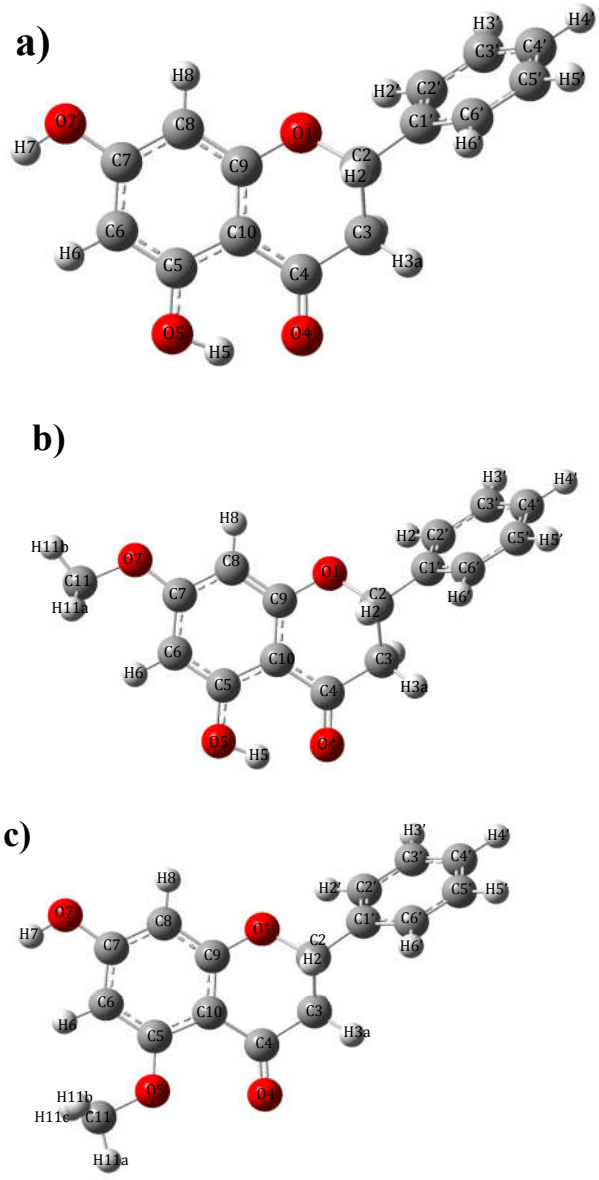

Fig. 3.5. : Optimized structures of a) Pinocembrin b) Pinostrobin and c) Alpinetin

Table 3.2. Theoretically computed interatomic bond distances in pinostrobin and alpinetin molecule.

Bond length	Pinostrobin	Alpinetin
	B3LYP/6-31+G (d, p)	B3LYP/6-31+G (d, p)
C2-C3	1.534	1.526
C3-C4	1.516	1.527
C5-C6	1.397	1.398
C6-C7	1.400	1.403
C7-C8	1.409	1.39
C8-C9	1.383	1.395
C4-C10	1.445	1.477
C5-C10	1.424	1.428
C9-C10	1.423	1.419
C2-C1’	1.512	1.512
C1’-C2’	1.402	1.401
C1’-C6’	1.400	1.401
C2’-C3’	1.396	1.397
C3’-C4’	1.398	1.398
C4’-C5’	1.397	1.397
C5’-C6’	1.397	1.397
C2-H2	1.100	1.100
C3-H3(a)	1.093	1.093
C3-H3(b)	1.099	1.099
C6-H6	1.081	1.084
C8-H8	1.083	1.083
C2’-H2’	1.085	1.085
C3’-H3’	1.086	1.086
C4’-H4’	1.086	1.086
C5’-H5’	1.086	1.086
C6’-H6’	1.087	1.087
C2-O1	1.447	1.444
C4-O4	1.246	1.225
C5-O5	1.341	1.349
C7-O7	1.356	0.966
C9-O1	1.363	1.362
O5-H5	0.995	----
O5-C11	----	1.423
O7-H7	----	0.966
O7-C11	1.356	----
C11-H11a	1.096	1.097
C11-H11b	1.090	1.097
C11-H11c	1.096	1.090

3.3.4. Spectral Characterization – NMR Spectra

^{13}C and ^{1}H-NMR spectra were recorded for all the molecules studied at B3LYP/6-31+G (d, p) level of theory using GIAO formalism inbuilt in Gaussian 09. For the ease of comparison with the existing experimental results, NMR spectra were recorded in dimethyl sulphoxide (DMSO) medium for pinocembrin, chloroform medium for pinostrobin and DMSO medium for alpinetin. The isotopic shielding tensors so obtained were converted to chemical shifts in ppm using the values obtained for TMS under similar conditions. Chemical shifts (δ) so obtained were correlated with the available experimental chemical shift values of pinocembrin [22], pinostrobin [23] and alpinetin [24]. These values (Tables 3.3 and 3.4) showed close correlation, thereby confirming the structure.

^{13}C NMR spectra of pinocembrin (R = 0.9978) showed 15 signals including 8 methine, 1 methylene and 6 quaternary carbon atoms. Ring A showed 6 signals located at 162.71 (C-5), 94.40 (C-6), 162.68 (C-7), 93.30 (C-8), 161.73 (C-9) and 103.48 ppm (C-10). 6 carbon atoms of the mono substituted ring B showed signals at 139.24 (C-1'), 123.27 (C-2'), 127.09(C-3'), 126.48 (C-4'), 125.98 (C-5') and 125.88 ppm (C-6'). For Ring C, carbonyl carbon showed a peak at 193.94 ppm and two carbon atoms C-2 and C-3 showed up at δ values 85.83 and 47.20 ppm respectively.

Table 3.3. Comparison of ^{13}C NMR chemical shifts of pinocembrin, pinostrobin and alpinetin with the experimental results.

	Pinocembrin		Pinostrobin		Alpinetin	
	B3LYP/ 6-31+G(d,p) (ppm)	Expt [22] (ppm)	B3LYP/ 6-31+G(d,p) (ppm)	Expt [23] (ppm)	B3LYP/ 6-31+G(d,p) (ppm)	Expt [24] (ppm)
C2	85.8	78.20	85.6	78.89	85.6	78.10
C3	47.2	42.00	48.1	43.05	50.0	45.00
C4	193.9	195.50	193.1	197.25	188.5	187.40
C5	162.7	164.30	164.0	163.80	161.7	164.10
C6	94.4	96.73	90.4	94.80	90.5	95.80
C7	162.7	164.59	166.2	167.62	159.5	164.40
C8	93.3	95.48	94.9	93.93	94.0	93.50
C9	161.7	162.60	160.6	167.62	164.1	162.20
C10	103.5	101.60	102.9	102.80	105.8	104.44
C11	---	----	55.5	55.36	55.5	52.79
C1’	139.2	138.22	139.9	138.02	139.5	136.80
C2’	123.3	126.13	122.6	125.81	123.5	120.48
C3’	127.1	128.88	127.0	128.54	126.7	123.49
C4’	126.4	128.91	125.8	128.54	126.5	122.27
C5’	126.0	128.88	125.3	128.54	126.1	122.58
C6’	125.9	126.13	125.7	125.81	125.8	120.41

^{13}C NMR spectra of pinostrobin (R =0.9976) showed 16 signals including one methyl, one methylene, 8 methine and 6 quaternary carbon atoms. The signals for ring A showed up at 164.00 (C-5), 90.35 (C-6), 166.15 (C-7), 94.89 (C-8), 160.63 (C-9) and 102.86 ppm (C-10). Ring B has all aromatic carbons, which peaks up at 139.98 (C-1’), 122.56 (C-2’), 127.01 (C-3’), 125.77 (C-4’), 125.29 (C-5’) and 125.70 ppm (C-6’). Ring A shows carbonyl carbon signal at 193.11, C-2 carbon at 85.57 and C-3 at 43.05 ppm. C-11 carbon appears at 55.45 ppm.

^{13}C NMR spectra of alpinetin (R =0.9965) also showed 16 signals one methyl, one methylene, 8 methine and 6 quaternary carbon atoms. Signals for ring A showed up at 161.67 (C-5), 90.50 (C-6), 159.52 (C-7), 94.02 (C-8), 164.06 (C-9) and 105.83 ppm (C-10). Aromatic carbon atoms of ring B appears at 139.52 (C-1'), 123.51 (C-2'), 126.71 (C-3'), 126.47 (C-4'), 126.08 (C-5') and 125.79 ppm (C-6'). Carbonyl carbon of ring A is found at 188.51 ppm, C-2 carbon at 85.64 ppm and C-3 carbon at 50.03 ppm. C-11 carbon appears at 55.52 ppm.

^{1}H-NMR spectra were also recorded for the molecules studied in solvent phase. The chemical shifts obtained in experiments were well reproduced theoretically. In pinocembrin (R = 0.9992), 5-OH showed up at δ = 12.00 which confirms the presence of H-bond between this H and 4 C=O. Other OH at C-7 showed a peak at 5.5 ppm. Meta hydrogens at C-6 and C-8 positions were found respectively at 6.07 and 6.18 ppm. Two hydrogen atoms at C-3, characteristic of flavanones appeared at 2.48 and 3.21 ppm and C-2 hydrogen at 5.39 ppm. Five hydrogen atoms of ring B appeared in the range 7.58 - 8.01 ppm.

Similarly, ^{1}H-NMR spectra of pinostrobin (R = 0.9983) also showed 5-OH signal at 13.09 ppm. This downshift of 5-OH proton confirms the existence of H-bond. Ring A had two Meta hydrogens C-6 and C-8 very close by at 6.13 and 6.14 ppm. There are also three hydrogens from the -OMe group at around 3.8 - 4.2 ppm. Ring B had five hydrogens around 7.58-7.90 ppm. Ring C shows C-2H at 5.38 ppm and two hydrogens at C3 at 2.47 and 3.13 ppm.

Table 3.4. Comparison of ^{1}H NMR chemical shifts of pinocembrin, pinostrobin and alpinetin with the experimental results

	Pinocembrin		Pinostrobin		Alpinetin	
	B3LYP/ 6-31+G(d,p) (ppm)	Expt [22] (ppm)	B3LYP/ 6-31+G(d,p) (ppm)	Expt [23] (ppm)	B3LYP/ 6-31+G(d,p) (ppm)	Expt [24] (ppm)
2-H	5.39	5.58	5.38	5.40	5.34	5.44
3-H	2.48	2.72	2.47	2.85	2.38	2.59
	3.21	3.23	3.13	3.10	3.12	2.98
5-OH	12.82	12.13	13.09	12.00	----	----
6-H	6.07	5.90	6.14	6.03	5.73	5.98
7-OH	5.51	---	----	----	5.24	----
8-H	6.18	5.93	6.13	6.03	6.36	6.06
2'-H	8.01	7.41-7.55	7.90	7.40	7.94	7.40
3'H	7.75	7.41-7.55	7.65	7.40	7.74	7.40
4'H	7.77	7.41-7.55	7.71	7.40	7.76	7.40
5'H	7.67	7.41-7.55	7.59	7.40	7.70	7.40
6'H	7.58	7.41-7.55	7.58	7.40	7.58	7.40
H11a			4.16	3.90	3.70	3.72
H11b			3.84	3.90	4.34	3.72
H11c			3.82	3.90	3.74	3.72

^{1}H-NMR spectra of alpinetin (R = 0.9923) was quite similar to pinocembrin and pinostrobin, but the absence of hydrogen bond is reflected in the spectra with the absence of the peak around 12.00. 7-OH which does not have any hydrogen bond appeared at 5.24 ppm. Meta hydrogens of ring A at C-6 and C-8 appeared at 5.73 ppm and 6.36 ppm. Three hydrogens of the – OMe group attached occurs around 3.70 - 4.34 ppm. Ring B showed five signals for hydrogens

attached to aromatic carbon atoms in the range 7.60-7.90 ppm. Hydrogens attached to C-2 and C-3 carbon atoms of ring C shows up at 5.34, 2.38 and 3.12 ppm.

3.3.5. Frontier Molecular Orbital Analysis

Highest occupied molecular orbital (HOMO) and lowest unoccupied molecular orbital (LUMO) are together termed frontier molecular orbitals. They decide the optical and electronic properties as well as reactivity of a molecule. HOMO gives information regarding the donation of electron whereas LUMO gives information regarding the molecule's tendency to accept electrons [25]. The energy difference between HOMO and LUMO (ΔE) can be associated with the reactivity of the molecule. A molecule with smaller energy gap (ΔE) is found to be more reactive when compared to a molecule with larger energy gap [26][27]. For the molecules studied here, the calculated values of E_{HOMO} and E_{LUMO} in the gas phase are: E_{HOMO} (pinocembrin) = - 6.43 eV and E_{LUMO} (pinocembrin)= -1.88 eV ; E_{HOMO} (pinostrobin)= - 6.31 eV and E_{LUMO} (pinostrobin)= -1.8 eV and E_{HOMO} (alpinetin)= -6.35 eV and E_{LUMO} (alpinetin)= -1.44 eV respectively. These are comparable to the E_{HOMO} and E_{LUMO} values of quercetin, -5.69 eV and -2.3 eV respectively [28]. The computed values of energy gap are ΔE (pinocembrin) = 4.55 eV, ΔE (pinostrobin) = 4.51 eV and ΔE (alpinetin) = 4.91 eV (Fig. 3.6). From these values, it can be inferred that pinostrobin is highly chemically reactive and alpinetin is least reactive.

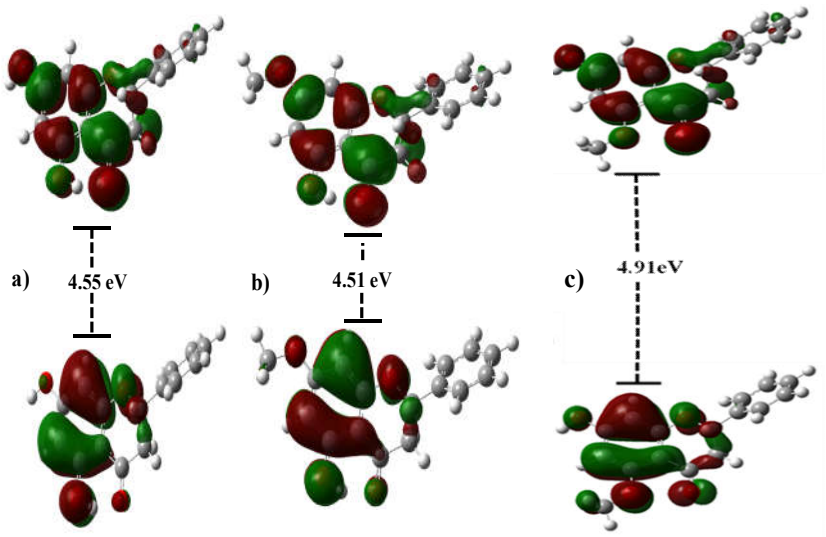

Fig 3.6: Molecular orbitals and energies for the HOMO and LUMO for a) pinocembrin and b) pinostrobin and c) alpinetin

3.3.6. Molecular Electrostatic Potential (MEP)

Electrostatic potential mapped onto constant electron density surface is a very useful descriptor in identifying sites for electrophilic attack and nucleophilic attack. This is described by a descriptor called molecular electrostatic potential (MEP) [8]. The molecular electrostatic potential V(r) in the space around a molecule created by its nuclei and electrons is given by the equation below:

$$V(r) = \sum_{A} \frac{Z_A}{R_A - r} - \int \frac{\rho(r')}{(r' - r)dr} \qquad (3.2)$$

where Z_A is the charge of nucleus A, which is located at R_A, $\rho(r')$ is the electronic density function for the molecule and r' is the dummy integration variable. V(r) at any point is the interaction between the

electric charge generated by the molecule and a proton at a distance r [29][8].

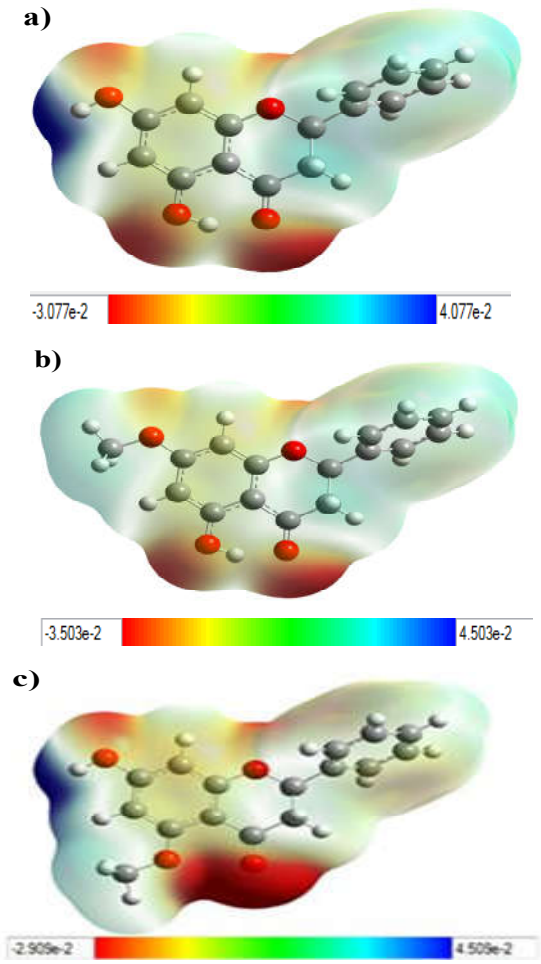

Fig: 3.7 Molecular electrostatic potential map of a) pinocembrin b) pinostrobin and c) alpinetin

Electron rich regions are indicated by red, green represents neutral sites and electron deficient regions are represented by blue. Light blue represents slightly electron deficient regions and yellow represents slightly electron rich regions. As can be seen from the 3D

plot of MEP (Fig. 3.7), electron rich regions (red) are generally centered on electronegative oxygen atoms and electron deficient regions (blue) on hydrogen atoms. This gives information regarding the intermolecular interactions which is likely to be displayed by the molecule.

3.4. Conclusions

DFT calculations are done on pinocembrin and o-methyl derivatives of pinocembrin namely pinostrobin and alpinetin. Structures were carefully optimized following conformational analysis and optimal basis set selection. The computed molecular structural parameters and the NMR data are compared against the experimental data available to validate the theoretical results. They are found to have good correlation. Frontier molecular orbitals analysis was performed to understand the reactivity of these molecules. The values of E_{HOMO} and E_{LUMO} are comparable to that of well-known anti-oxidant flavonoid quercetin. Molecular electrostatic potential mapping shows that electronegative oxygen centers are the negative centers and the others are positive centers. These molecules tend to have a much therapeutic application which needs to be explored.

References

[1] D. Barreca, G. Gattuso, E. Bellocco, A. Calderaro, D. Trombetta, A. Smeriglio, G. Laganà, M. Daglia, S. Meneghini, S.M. Nabavi, BioFactors. 43 (2017) 495–506.

[2] Y. Murti, P. Mishra, Int. J. ChemTech Res. 6 (2014) 3160–3178.

[3] A. Rasul, F.M. Millimouno, W.A. Eltayb, M. Ali, J. Li, X. Li, BioMed Res. Int. 2013 (2013).

[4] J.W. Fahey, K.K. Stephenson, J. Agric. Food Chem. 50 (2002) 7472–7476.

[5] A.Y.L. Ching, T.S. Wah, M.A. Sukari, G.E.C. Lian, M. Rahmani, K. Khalid, Malaysian J. Anal. Sci. 11 (2007) 154–159.

[6] Q. Yang, Y. Tong, F. Chen, Y. Qi, W. Li, S. Wu, Chin. J. Chem. 30 (2012) 1315.

[7] W.A. Roman Junior, D.B. Gomes, B. Zanchet, A.P. Schönell, K.A.P. Diel, T.P. Banzato, A.L.T.G. Ruiz, J.E. Carvalho, A. Neppel, A. Barison, C.A.M. Santos, Brazilian J. Pharmacogn. 27 (2017) 592–598.

[8] P. Politzer, D.G. Truhlar, Chemical Application of Atomic and Molecular Electrostatic Potentials, Plenum, New York, 1981.

[9] A.D. Becke, J. Chem. Phys. 98 (1993) 5648–5652.

[10] C. Lee, W. Yang, R.G. Parr, Phys. Rev. B 37 (1988) 785–789.

[11] J. Zhang, Y. Xiong, B. Peng, H. Gao, Z. Zhou, Comput. Theor. Chem. 963 (2011) 148–153.

[12] R. Amorati, A. Baschieri, A. Cowden, L. Valgimigli, Biomimetics 2 (2017) 9.

[13] D. Zhang, L. Chu, Y. Liu, A. Wang, B. Ji, W. Wu, F. Zhou, Y. Wei, Q. Cheng, S. Cai, L. Xie, G. Jia, J. Agric. Food Chem. 59 (2011) 10277–10285

[14] J. Tomasi, B. Mennucci, R. Cammi, Chem.Rev. 105 (2005) 2999–3094.

[15] R. Ditchfield, Mol. Phys. 27 (1974) 789–807.

[16] S. Aparicio, Int. J. Mol. Sci. 11 (2010) 2017–2038.

[17] S.A.B.E. Van Acker, M.J. De Groot, D. Van Den Berg, M.N.J.L. Tromp, G.D.-O. den Kelder, W.J.F. van der Vijgh, A. Bast, Chem. Res. Toxicol. 9 (1996) 1305–1312.

[18] M.J. Frisch, G.W. Trucks, H.B. Schlegel, G.E. Scuseria, M.A. Robb, J.R. Cheeseman, G. Scalmani, V. Barone, B. Mennucci, G.A. Petersson, H. Nakatsuji, M. Caricato, X. Li, H.P. Hratchian, A.F. Izmaylov, J. Bloino, G. Zheng, J.L. Sonnenberg, M. Hada, M. Eha, D.J. Fox, (2009).

[19] https://pubchem.ncbi.nlm.nih.gov.

[20] R.D. Vargas-Sánchez, A.M. Mendoza-Wilson, R.R. Balandrán-Quintana, G.R. Torrescano-Urrutia, A. Sánchez-Escalante, Comput. Theor. Chem. 1058 (2015) 21–27.

[21] D. Bertelli, G. Papotti, L. Bortolotti, G.L. Marcazzan, M. Plessi, Phytochem. Anal. 23 (2012) 260–266.

[22] Y. Liu, D.K. Ho, J.M. Cassady, J. Nat.Prod. 55 (1992) 357–363.

[23] B. Burke, M. Nair, Phytochemistry 25 (1986) 1427–1430.

[24] H. Itokawa, M. Morita, S. Mihashi, Phytochemistry 20 (1981) 2503–2506.

[25] A.M. Mendoza-Wilson, D. Glossman-Mitnik, J. Mol. Struct. 761 (2006) 97–106.

[26] I. Fleming, Frontier Orbitals and Organic Chemical Reactions, John Wiley & Sons., New York, 1976.

[27] S. Muthu, T. Rajamani, M. Karabacak, A.M. Asiri, Spectrochim. Acta Part A Mol. Biomol. Spectrosc. 122 (2014) 1–14.

[28] A.M. Mendoza-Wilson, D. Glossman-Mitnik, J. Mol. Struct. Theo-Chem 716 (2005) 67–72.

[29] P. Politzer, J.S. Murray, Theor. Chem. Acc. 108 (2002) 134–142.

Chapter 4

Antioxidant properties and druggability studies

4.1. Introduction

4.1.1. Free radicals and Oxidative stress

According to IUPAC Compendium of Chemical Terminology, Gold Book [1], free radical is a molecular entity such as $CH3^{\cdot}$, $SnH3^{\cdot}$, $Cl^{\cdot}$, which possess unpaired electron [2, 3]. They are generally very reactive to complete their octet [4]. They complete their octet by abstracting an electron from the neighboring entities thereby triggering a chain reaction.

Biologically, most relevant free radicals are reactive oxygen species (ROS) and reactive nitrogen species (RNS) [5]. ROS is a collective term and comprises of a broad class of oxygen centered reactive species like superoxide ($O_2^{\cdot -}$), hydroxyl radical ($OH^{\cdot}$), hydrogen peroxide (H_2O_2), singlet oxygen, hypohalites, alkoxyl radicals ($RO^{\cdot}$), peroxyl radicals ($ROO^{\cdot}$) and the like [2]. RNS [6] on

the other hand include nitrogenous products like nitric oxide ($NO^{\cdot}$), nitroxyl (HNO), nitrogen dioxide ($NO_2^{\cdot}$), peroxynitrite anion ($ONOO^{-}$), nitrite (NO_2^{-}), nitrosonium cation (NO^{+}), etc.

Radicals may be produced endogenously or exogenously in our body [2][7]. The major endogenous sources are oxygen leakage that occurs during photosynthesis and respiration [8]. Other sources being NADPH oxidases (Nox's) [9], xanthine oxidase [10, 11], cytochrome P450 2E1 (CYP2E1) [12] and nitric oxide synthases (NOSs) [13]. Ionizing and non-ionizing radiations, exposure to cigarette smoking, pesticides, drugs and other pollutants contribute exogenously towards the production of free radicals. An excess of free radicals either endogenously or exogenously may result in a predisposing condition referred to as oxidative stress [3].

Free radicals are not always harmful to our body as usually portrayed. They have some important role in our immune system [14] and also in some signal transductions inside our body. They are also involved in cell cycle regulation, cell apoptosis and redox homeostasis [15,16]. But the extent of production, regulation and reversibility are crucial in maintaining their balance.

As the free radicals have ability to attack biological components like proteins [17], carbohydrates [18], nucleic acid [19], etc., they have implications in aging and other age related conditions, infections and inflammations. Many of the environmental pollutants have their implications via the production of free radicals [20]. In the current pathological condition, there are quite a lot of diseases which

are caused due to free radicals or oxidative stress. The list includes neuro-inflammatory conditions such as Alzheimer's and Parkinson's diseases, cardiac failure, atherosclerosis, diabetes, chronic obstructive pulmonary disease (COPD), asthma, pneumococcal meningitis, ischemia/reperfusion injuries and even cancer [21]. Thus, there is a necessity to maintain a balance in the amount of free radicals produced and consumed in our body.

4.1.2. Antioxidants

Antioxidants are referred to as substances which are capable of preventing, retarding or terminating radical chain reactions [22]. Antioxidants may be enzymatic or non-enzymatic, exogenous or endogenous, water soluble or lipid soluble. Enzymes such as catalase, superoxide dismutases, glutathione reductase, glutathione peroxidases, conjugation enzymes, NAD(P)H: quinone oxidoreductase, proteases, phospholipases etc. are enzymatic endogenous antioxidants whereas non-enzymatic endogenous antioxidants are melatonin, glutathione, cysteine, α-lipoic acid/dihydrolipoic acid, urate, bilirubin etc. [23]. Common exogenous antioxidants are those derived from fruits, vegetables etc. like α-tocopherol (vitamin E), ascorbic acid (vitamin C), carotenoids, omega-3-fatty acids, secondary plant metabolites flavonoids, chalcones, tannins and some phenolic acids [24].

Dietary intake of antioxidants may help in maintaining oxidative balance and normal physiological functioning of the human body [25]. There has been increasing interest in studying the

mechanism of action of antioxidants and whether they specifically intercept or remove free radicals from the human body [26, 27].

Flavonoids are well characterized for their ability to act as radical scavengers [28, 29]. Consumption of flavonoid rich foods are found to increase the amount of antioxidants in the body [30 -32]. In this context, we attempt to explore the anti-oxidant mechanism exhibited by the selected flavanones pinocembrin, pinostrobin and alpinetin, theoretically.

4.2. Computational Methodology

Global reactivity descriptors calculated by means of DFT gives insight regarding the global reactivity of a molecule. Reliable calculations of these descriptors are necessary as they are powerful tools to predict the relationship between the structure with reactivity. Calculation of various global descriptors involves ionization potential and electron affinity values of corresponding molecules. Computationally, ionization potential and electron affinity can be calculated using two methods namely energy vertical method and orbital vertical method. In energy vertical method, Ionization potential (IP_E) is calculated as the difference in total electronic energy between N-1 (cation) and N (neutral) electron systems. Similarly, electron affinity (EA_E) is calculated as the difference between N (neutral) and N+1 (anion) electron systems. This method is slightly computationally demanding, hence one can resort to orbital vertical method wherein ionization potential (IP_O) and electron affinity (EA_O) is calculated as negative of E_{HOMO} and as negative of E_{LUMO} respectively.

$$IP_E = E_{cation} - E_{neutral} \quad (4.1)$$

$$EA_E = E_{neutral} - E_{anion} \quad (4.2)$$

$$IP_O = - E_{HOMO} \quad (4.3)$$

$$EA_O = - E_{LUMO} \quad (4.4)$$

Using the values of ionization energy and electron affinity, global descriptors like electronegativity (χ), electrophilicity (ω), softness (S), hardness (η) and chemical potential (μ) are calculated using equations (4.5) – (4.9) as follows [33-35]:

$$\text{Electronegativity } (\chi) = \frac{IP+EA}{2} \quad (4.5)$$

$$\text{Electrophilicity index } (\omega) = \frac{\mu^2}{2\eta} \quad (4.6)$$

$$\text{Softness}(S) = \frac{1}{2\eta} \quad (4.7)$$

$$\text{Hardness } (\eta) = \frac{IP-EA}{2} \quad (4.8)$$

$$\text{Chemical potential } (\mu) = -\chi \quad (4.9)$$

In literature, there are several pathways of antioxidant action. Antioxidants follow any of these available pathways based on the energetic advantage. The important pathways are hydrogen atom transfer (HAT) mechanism [36] which follows homolytic bond cleavage resulting in the generation of free radicals; Single-electron transfer followed by proton transfer (SET-PT) which involves electron

transfer followed by proton dissociation; Sequential proton loss electron transfer (SPLET) which involves heterolytic bond cleavage. The chemical pathways entailing these mechanisms are as follows:

1) HAT (*Hydrogen atom transfer*) mechanism:

$$ArOH + X^{\bullet} \rightarrow ArO^{\bullet} + XH \quad (4.10)$$

2) SET-PT (*Single-electron transfer followed by proton transfer*):

$$ArOH + X^{\bullet} \rightarrow ArOH^{\bullet+} + X^{-} \quad (4.11)$$

$$ArOH^{\bullet+} \rightarrow ArO^{\bullet} + H^{+} \quad (4.12)$$

3) SPLET (*Sequential proton loss electron transfer*):

$$ArOH \rightarrow ArO^{-} + H^{+} \quad (4.13)$$

$$ArO^{-} + X^{\bullet} + H^{+} \rightarrow ArO^{\bullet} + XH \quad (4.14)$$

HAT mechanism is governed by the physical parameter called bond dissociation energy (BDE). It is calculated as

$$B.D.E = H(ArO^{\bullet}) + H(H^{\bullet}) - H(ArOH) \quad (4.15)$$

SET-PT mechanism is a two-step process. The first step involving the loss of electron is governed by the thermodynamic variable Adiabatic Ionization potential (IP). The second step involves proton transfer and is governed by Proton dissociation enthalpy (PDE). Of these two steps, initial step which involves the loss of electron is the limiting step of the reaction. Adiabatic ionization potential and proton dissociation enthalpy are calculated as:

$$I.P. = H(ArOH^{\bullet+}) + H(e^{-}) - H(ArOH) \quad (4.16)$$

$$P.\ D.\ E. = H(ArO^{\bullet}) + H(H^{+}) - H(ArOH^{\bullet+}) \quad (4.17)$$

SPLET is again a two-step process, the initial step involving proton loss and is governed by proton affinity (PA). Second step is governed by electron transfer enthalpy (ETE). These can be calculated as:

$$P.\ A. = H(ArO^{-}) + H(H^{+}) - H(ArOH) \quad (4.18)$$

$$E.\ T.\ E. = H(ArO^{\bullet}) + H(e^{-}) - H(ArO^{-}) \quad (4.19)$$

The enthalpies of electron (e), proton (H^{+}) and hydrogen atom ($H^{\bullet}$) are taken to be 3.145 kJ/ mol,6.197 kJ/ mol and -1306.55 kJ/ mol [37, 38] respectively in the gas phase.

Inside the body, these flavonone molecules have to be functional in aqueous polar media. To analyze the antioxidant mechanism in this media, the descriptors were calculated in polar aqueous media. The molecules were separately optimized in these solvent media using conductor-like polarizable continuum model (CPCM) [39]. For the solvent phase calculation ΔH (hydration) of electron (e), proton (H^{+}) and hydrogen atom (H^{-}) are respectively taken to be -105 kJ/ mol, -1090 kJ/ mol and -4.0 kJ/ mol [40 - 43].

Pharmacokinetic properties of molecules can be analyzed in-silico by checking whether they satisfy ‘Lipinski’s rule of five’ [44]. Lipinski’s rule of five states five conditions for the molecules to be orally active. These are a) Molecular weight should be less than 500,

b) calculated octanol/water partition coefficient (log P) should be less than 5, c) number of H bond donors should be less than 5 and d) number of hydrogen bond acceptors should be less than 10. There are two extensions to this rule of five, these are polar surface area should be less than or equal 140 $Å^2$ [45] and number of rotatable bonds should be less than or equal to 10. Rotatable bonds decide the conformational flexibility of the molecule. Total polar surface area is cumulative of surface areas of all polar atoms like oxygen, nitrogen and the attached hydrogen. It is an important property in determining the transport property of a molecule. It is predicted that a molecule is orally active if they do not violate more than one rule. There could be exceptions to this as well.

Druggability studies were carried out using molinspiration [46] and OSIRIS property explorer softwares [47] available online. Molinspiration software could calculate log P, total polar surface area, number of hydrogen bond donors and acceptors, molecular weight, volume, number of rotatable bonds, etc. Toxicity studies (mutagenicity, tumorigenicity, irritation and reproduction) were conducted using OSIRIS property explorer [47].

4.3. Results and Discussion

4.3.1. Global reactivity Descriptors

Ionization potential calculated for the title compounds pinocembrin, pinostrobin and alpinetin using orbital vertical methods are found to be 6.43 eV, 6.31 eV and 6.35 eV. Electron affinity values are 1.88 eV, 1.8 eV and 1.44 eV respectively for pinocembrin,

pinostrobin and alpinetin. Ionization potential calculated using energy vertical method gives the following values, for pinocembrin 8.12 eV, for pinostrobin 7.92 eV and alpinetin 7.89 eV whereas electron affinity of pinocembrin, pinostrobin and alpinetin have values 0.28 eV, 0.23 eV and 0.09 eV. Difference in the values calculated using both these methods is because Koopman's theorem is not accurately verified for commonly used exchange-correlation functional like B3LYP, B3PW91 etc. This theorem is only an approximation; it does not consider electron correlation and orbital relaxation.

The values are in accordance with the ionization values and electron affinity values of (+)-Catechin (IP_E = 7.20 eV; EA_E = -0.40 eV), (-)-epicatechin [48] (IP_E = 7.21 eV; EA_E = -0.49 eV) and quercetin [49] (IP_E = 7.22 eV, IP_O = 5.69 eV; EA_E = 0.76 eV, EA_O = 2.31 eV); studied using CHIH (medium)-DFT model chemistry.

Table 4.1. Ionization enthalpy and Electron affinity global reactivity descriptors for pinocembrin, pinostrobin and alpinetin calculated through orbital vertical and energy vertical methods.

ORBITAL VERTICAL METHOD (acc. Koopmann's theorem)									
Sample	E_{LUMO} (eV)	E_{HOMO} (eV)	IP (eV)	EA (eV)	η	χ	μ	ω	S
PINOCEMBRIN	-1.88	-6.43	6.43	1.88	2.28	4.16	-4.16	3.78	0.22
PINOSTROBIN	-1.8	-6.31	6.31	1.8	2.26	4.06	-4.06	3.66	0.22
ALPINETIN	-1.44	-6.35	6.35	1.44	2.46	3.9	-3.9	3.10	0.20
QUERCETIN[49]					1.69	4	-4	4.72	0.30

ENERGY VERTICAL METHOD										
Sample	Cation (Ha)	Neutral (Ha)	Anion (Ha)	IP (eV)	EA (eV)	η	χ	μ	ω	S
PINOCEMBRIN	-879.49	-879.79	-879.80	8.12	0.28	3.92	4.20	-4.20	2.25	0.13
PINOSTROBIN	-918.80	-919.09	-919.10	7.98	0.23	3.87	4.11	-4.11	2.18	0.13
ALPINETIN	-918.78	-919.07	-919.07	7.89	0.09	3.99	3.90	-3.90	1.91	0.13
QUERCETIN [49]						3.23	3.99	-3.99	2.47	0.15

Electronegativity index is a measure of tendency to attract a bonded pair of electrons and electrophilicity index measure affinity of electrons. Escaping tendency of an electron from equilibrium is studied using chemical potential, and it is given by the first derivative of energy with respect to the number of electrons [50]. Resistance to charge transfer is reflected in the hardness descriptor and inverse of hardness is another descriptor called softness [51]. Electronegativity and electrophilicity index follows the order alpinetin < pinostrobin < pinocembrin whereas hardness follows the order pinostrobin < pinocembrin < alpinetin. These descriptors for the title molecules are tabulated in Table 4.1. These descriptors had values comparable to quercetin which is a potent antioxidant molecule [49]. From the Table 4.1, all the values associated with chemical potential is found to be low, thus these molecules will have a tendency to release electrons than accept them. This is quite favourable for anti-oxidant activity.

4.3.2. Antioxidant Mechanism

Flavonone molecules can adopt any of the antioxidant pathways depending on the energetic advantage. Different mechanisms

are dictated by descriptors associated with different steps involved in that mechanism. The different parameters involved are Bond dissociation enthalpy (B.D.E), ionization potential (I.P) and proton affinity (P.A); which governs HAT, SET-PT and SPLET pathways, respectively.

Table 4.2. Calculated Bond dissociation enthalpy (B.D.E), Ionization potential (I.P), Proton dissociation enthalpy (P.D.E), proton affinity (P.A) and Electron transfer enthalpy (E.T.E.) values of pinocembrin, pinostrobin and alpinetin in gas phase.

Molecules	B.D.E. (kcal/ mol)	I.P. (kcal/ mol)	P.D.E. (kcal/ mol)	P.A. (kcal/ mol)	E.T.E. (kcal/ mol)
Pinocembrin5-OH	99.15	181.88	231.78	345.92	67.73
Pinocembrin7-OH	89.59		222.22	328.02	76.08
Pinostrobin 5-OH	98.62	178.59	234.53	346.92	66.20
Alpinetin 7-OH	86.23	178.82	221.91	329.32	71.42

Comparing the energetics of each of these pathways it could be seen that B.D.E has a lower value compared to I.P and P.A. This point out that hydrogen atom transfer via homolytic bond cleavage is the preferred pathway in vaccuo. Flavonoids are generally known for their ease of $H^{\cdot}$ removal producing another radical Fl-$O^{\cdot}$ which is more stable than the attacking radical. Weaker the OH bond, lower the B.D.E value and higher the antioxidant activity.

Optimization of the radical species was performed starting from the optimized global minima of neutral molecule. $H^{\cdot}$ were removed from the OH groups of the neutral molecule and were reoptimized using unrestricted wavefunction in the gas phase. During

the optimization of radical species, no geometric constraints were employed.

On comparing the B.D.E values of the three flavanone molecules studied, it could be seen that their B.D.E values in vaccuo were in the following order: alpinetin < pinocembrin < pinostrobin. In pinocembrin, there are two OH groups likely to undergo homolytic cleavage. On comparing B.D.E values of these two -OH groups we could understand that B.D.E of 5-OH outweighs B.D.E of 7-OH, making H abstraction from 7-OH easier compared to that from 5-OH. This could be attributed the existence of hydrogen bond between 5-OH and the neighboring ketonic group.

4.3.3. Solvent Effects

Effect of solvents on the antioxidant mechanism needs to be necessarily evaluated as these molecules have to act under physiological conditions wherein they have to encounter polar solvents. As a representative example water is taken as the polar solvent.

On comparing the energetics of the three mechanisms of antioxidant action in polar medium, it was understood that proton affinity had considerably low values compared to B.D.E and I.P. Thus SPLET becomes the mechanism of choice of flavanones in polar media. This pathway is governed by ease of deprotonation, which as expected is more favourable in polar aqueous media. P.A values of these molecules are in the following order pinocembrin < alpinetin < pinostrobin. Comparing the PA values of 5-OH and 7-OH of

pinocembrin, it follows the same trend as observed in gas phase. 5-OH has a higher PA value compared to 7-OH making its cleavage difficult.

Table 4.3. Calculated Bond dissociation enthalpy (B.D.E), Ionization potential (I.P), Proton dissociation enthalpy (P.D.E), proton affinity (P.A) and Electron transfer enthalpy (E.T.E) values of pinocembrin, pinostrobin and alpinetin in aqueous phase.

Molecules	B.D.E. (kcal/ mol)	I.P. (kcal/ mol)	P.D.E. (kcal/ mol)	P.A. (kcal/ mol)	E.T.E. (kcal/ mol)
Pinocembrin 5-OH	92.64	118.14	4.33	35.36	87.11
Pinocembrin 7-OH	88.42		0.11	24.36	93.89
Pinostrobin 5-OH	92.16	116.95	5.05	35.68	86.32
Alpinetin 7-OH	86.48	117.22	-0.91	25.53	90.77

4.3.4. Druggability

Lipinski's rule of five was analyzed for pinocembrin, pinostrobin and alpinetin using molinspiration software. According to the very first criteria of Lipinski's rule of five, molecular weight of the molecule should be less than 500. Molecular weight of the molecules studied here are in the range 250 - 270 g. In order to penetrate biological membranes, log P values should be less than 5 according to Lipinski's rule of 5. For the title molecules, log P values are in the range 2.60 - 3.13. It varies in the order pinocembrin < alpinetin < pinostrobin. The last two conditions are number of hydrogen donors should be less than 5 and acceptors less than 10. These are also not violated by the molecules under study. Total polar surface area should be less than 140 $Å^2$. These values give a good insight regarding the

drug absorption including intestinal absorption, bioavailability, Caco-2 permeability and blood–brain barrier penetration. TPSA of the studied molecules are well below 100 $Å^2$. Conformational flexibility of the molecules are decided by the number of rotatable bonds. This is important for analyzing the conformational changes which are important in the binding of molecules to receptors or channels. Oral viability criteria have set the number of rotatable bonds preferably to be less than or equal to 10. These are also very few in the studied molecules. Hence, it could be concluded that none of the studied molecules violate the oral bioavailability criteria set by Lipinski. In the current study calculated Global reactivity descriptors and Lipinski's parameters seems to have no correlation.

Table 4.5. Lipinski parameters and its extension for the molecules studied

Molecule	Lipinski's Parameters					Extension	
	milogP	MW	HBD	HBA	Violations	TPSA	nrot
Pinocembrin	2.60	256.26	2	4	0	66.76	1
Pinostrobin	3.13	270.28	1	4	0	55.77	2
Alpinetin	2.66	270.28	1	4	0	55.77	2

Toxicity studies were done in-silico using OSIRIS property explorer software. It checks for fragments in the molecule which is likely to be toxic. Preliminary information of toxicity of molecules are required in the field of drug design. Toxicity risks included in the current study are mutagenicity, tumorigenicity, irritation and reproductive effect. None of the title molecules show any chance of toxicity.

Table 4.6. Results of the toxicology studies conducted on the molecules.

Molecules	Mutagenic	Tumorigenic	Reproductive effective	Irritant
Pinocembrin	none	none	none	none
Pinostrobin	none	none	none	none
Alpinetin	none	none	none	none

4.4. Conclusions

Quantum chemical descriptors like electronegativity (χ), electrophilicity (ω), softness (S), hardness (η) and chemical potential (μ) were calculated using energy vertical and orbital vertical methods. These values were comparable to that of well-known antioxidant quercetin. This point out towards the antioxidant potentiality of the molecules studied. Further different anti-oxidant mechanisms were studied using thermodynamic parameters. Influence of solvents on these mechanisms was also analyzed. Hydrogen atom transfer was the mechanism of choice in vacuum but the mechanism switches to Sequential proton loss electron transfer mechanism in polar solvents whereas in non-polar solvents there is likely to be a competition between the above two mechanisms. Having described the antioxidant mechanism, druggability and toxicity studies were also conducted. These molecules satisfied conditions for oral bioavailability proposed by Lipinski and also turn out to be non-mutagenic, non- tumorigenic, non-irritant and have no reproductive effects according to Osiris property explorer.

References

[1] IUPAC Compendium of Chemical Terminology - the Gold Book, http://goldbook.iupac.org, n.d.

[2] B. Halliwell, C.E. Cross, Env. Heal. Perspect. 102 (1994) 5–12.

[3] J. Kehrer, J. Robertson, C. Smith, Free Radicals and Reactive Oxygen Species in Comprehensive Toxicology, Oxford: Elsevier, 2010.

[4] M. Saran, W. Bors, Radiat. Environ. Biophys 29 (1990) 249–62.

[5] F. Di Virgilio, Curr. Pharm. Des. 10 (2004) 1647–52.

[6] M. Gutowski, S. Kowalczyk, Acta Biochim. Pol. 60 (2013) 1–16.

[7] G. Aseervatham, T. Sivasudha, R. Jeyadevi, D. Arul Ananth, Environ. Sci. Pollut. R. 20 (2013) 4356–69.

[8] R. Banerjee, Redox Metabolism and Life in Redox Biochemistry, Wiley-Interscience, 2008.

[9] D. Brown, K. Griendling, Free Radic. Biol. Med. 47 (2009) 1239–53.

[10] R. Harrison, Free Radic. Biol. Med 33 (2002) 774–97.

[11] N. Cantu-Medellin, E. Kelley, Redox Biol. 1 (2013) 353–8.

[12] T.-M. Leung, N. Nieto, J Hepatol. 58 (2013) 395–8.

[13] M. Forrester, M. Foster, Free Radic. Biol. Med. 52 (2012) 1620–33.

[14] M. Valko, D. Leibfritz, J. Moncol, M. Cronin, M. Mazur, J. Telser, Int. J. Biochem. Cell Biol. 39 (2007) 44–84.

[15] H. Forman, J. Fukuto, T. Miller, H. Zhang, A. Rinna, S. Levy, Arch. Biochem. Biophys. 477 (2008) 183–95.

[16] J. Matés, J. Segura, F. Alonso, J. Márquez, Arch. Toxicol . 82 (2008) 273–99.

[17] J. Keller, E. Dimayuga, Q. Chen, J. Thorpe, J. Gee, Q. Ding, Int. J. Biochem. Cell Biol. 36 (2004) 2376–91.

[18] P. Manini, P. La Pietra, L. Panzella, A. Napolitano, M. D'Ischia, Carbohydr. Res. 341 (2006) 1828–33.

[19] T. Kryston, A. Georgiev, P. Pissis, A. Georgakilas, Mutat. Res. 711 (2011) 193–201.

[20] M. Miller, C. Shaw, J. Langrish, Futur. Cardiol. 8 (2012) 577–602.

[21] S. Saeidnia, M. Abdollahi, Toxicol. Appl. Pharmacol. 273 (2013) 442–455.

[22] B. Halliwell, J. Gutteridge, Free Rad. Biol. Med. 18 (1995) 125–6.

[23] I. Young, J. Woodside, J. Clin. Pathol. 54 (2001) 176–86.

[24] P. Sailaja Rao, S. Kalva, A. Yerramilli, S. Mamidi, Free Radicals Antioxidants 1 (2011) 2–7.

[25] H. Boeing, A. Bechthold, A. Bub, S. Ellinger, D. Haller, A. Kroke, E. Leschik-Bonnet, M.J. Mu¨ller, H. Oberritter, M. Schulze, P. Stehle, B. Watzl, Eur. J. Nutr. 51 (2012) 637–663.

[26] J. Alamed, W. Chaiyasit, D.J. McClements, E.A. Decker, J. Agr. Food Chem.Agri. Food Chem. 57 (2009) 2969–2976.

[27] E.N. Bentz, A.B. Pomilio, R.M. Lobayan, Comput. Theor. Chem. 1110 (2017) 14–24.

[28] C. Kandaswami, E. Middleton, in:, Free Radicals Diagnostic Med. Adv. Exp. Med. Biol., Springer, Boston, MA, 1994.

[29] W. Bors, W. Heller, C. Michel, M. Saran, Methods Enzym. 186 (1990) 343–355.

[30] S.B. Lotito, B. Frei, Free Rad. Biol. Med. 41 (2006) 1727–1746.

[31] A. Martínez, E. Hernández-Marin, A. Galano, Food Funct. 3 (2012) 442.

[32] V.K. Gupta, R. Kumria, M. Garg, M. Gupta, Asian J Plant Sci Res 9 (2010) 108–117. [33] R.G. Parr, R.G. Pearson, J. Am. Chem. Soc. 105 (1983) 7512–7516.

[34] R.G. Parr, L. V. Szentpály, S. Liu, J. Am. Chem. Soc. 121 (1999) 1922–1924.

[35] K. Sadasivam, R. Kumaresan, Spectrochim Acta A Mol Biomol Spectrosc 79 (2011) 282–293.

[36] J. Zhang, Y. Xiong, B. Peng, H. Gao, Z. Zhou, Comput. Theor. Chem.

963 (2011) 148–153.

[37] J.E. Bartmess, J. Phys. Chem. 98 (1994) 6420.

[38] J.S. Wright, E.R. Johnson, G.A. DiLabio, J. Am. Chem. Soc. 123 (2001) 1173–1183.

[39] J. Tomasi, B. Mennucci, R. Cammi, Chem.Rev. 105 (2005) 2999–3094.

[40] P.W. Atkins, Physical Chemistry, 6th edn., Oxford University Press, Oxford, 1998.

[41] M.M. Bizarro, B.J.C. Cabral, R.M.B. dos Santos, J.A.M. Simoes, Pure. Appl. Chem. 71 (1999) 1249–1256.

[42] V.D. Parker, J. Am. Chem. Soc. 114 (1992) 7458–7462.

[43] J. Rimarcik, V. Lukes, E. Klein, M. Ilcin, J. Mol. Struct 952 (2010) 25–30.

[44] C.A. Lipinski, F. Lombardo, B.W. Dominy, P.J. Feeney, Adv. Drug Deliv. Rev. 46 (2001) 3–26.

[45] D.F. Veber, S.R. Johnson, H.Y. Cheng, B.R. Smith, K.W. Ward, K.D. Kopple, J. Med.Chem. 45 (2002) 2615–2623.

[46] http://www.molinspiration.com/.

[47] http://www.organic-Chemistry.org/prog/peo.

[48] A.M. Mendoza-Wilson, D. Glossman-Mitnik, J. Mol. Struct. 761 (2006) 97–106.

[49] A.M. Mendoza-Wilson, D. Glossman-Mitnik, J. Mol. Struct. Theo-Chem 716 (2005) 67–72.

[50] D. Young, Computational Chemistry: A Practical Guide for Applying Techniques to Real World Problems, John Wiley & Sons, Inc., New York, 2001.

[51] R.G. Parr, W. Yang, Density Functional Theory of Atoms and Molecules, Oxford University Press, New York, 1989.

Chapter 5

Improving the radical scavenging activity

5.1. Introduction

Free radicals are beneficial to human body in low to moderate concentration as they take part in defense mechanism. Excess production of free radicals through extracellular stress, exposure to environmental pollutants, etc., can disturb the balance and can cause oxidative stress in our body [1,2]. As we already know, several plant secondary metabolites like flavonoids, chalcones, tannins, etc., act as effective antioxidants. Dietary intake of these antioxidants has beneficial role in regulating oxidative stress as well as in preventing deadly diseases caused by free radicals [3,4].

Apart from natural antioxidants, there are synthetic antioxidants already in use in food industry. Though there is a general aversion in the use of synthetic antioxidants in food, they possess the advantage that they will be of high purity, can be subjected to safety

evaluation and they also open room for research towards finding new and improved antioxidants [5]. In India, Food Safety and Standards Authority of India (FSSAI) enlist several food additives which are safer to use [6]. This list includes several synthetic antioxidants. Some of the most common synthetic antioxidants are butylated hydroxytoluene (BHT), butylated hydroxyanisole (BHA) and propylgallate (PG) [7].

In this direction, we try to improve the antioxidant ability of the flavonone molecules studied here by substituting them with two classes of substituents namely: electron donors and electron acceptors. We also attempt to elucidate the use of different indices to predict the nature of electron transfer and feasibility of the reaction instead of going into the intricacies of studying the reaction mechanisms. Finally, we have also checked the toxicity of the new molecules designed.

5. 2. Computational Methodology

To improve the antioxidant potential of parent compounds namely pinocembrin, pinostrobin and alpinetin, electron donating and electron withdrawing substituents were added to these molecules. Electron donating groups chosen were methyl (-Me), hydroxyl (-OH) and methoxy ($-OCH_3$) groups whereas electron withdrawing groups chosen were ester ($-COOCH_3$) and keto (-C=O) groups.

Full geometry optimization was performed on all cations, anions, radicals and neutral species using Becke's exchange functional [8] in conjunction with Lee-Yang–Parr correlational functional (B3LYP) [9] within the framework of Density Functional Theory

(DFT) [10] in the gas phase. All calculations are performed using Gaussian 09 software [11]. The basis set used for the study was B3LYP/6-31+G (d, p). Prior to geometry optimization potential energy scans were performed using the semi-empirical PM6 method to confirm the relative orientation of groups attached to 5-C, 6-C and 7-C. Harmonic frequency calculations were carried out to confirm the obtained structures as global minima. Solvent effects were included to the obtained stationary point, *a posteriori* by single point calculations using integral equation formalism-polarizable continuum model (IEFPCM) with water as the solvent as described by A. Martinez et. al.[12].

Different mechanisms followed for radical scavenging action namely Hydrogen atom transfer (HAT), Single-electron transfer followed by proton transfer (SET-PT) and Sequential proton loss electron transfer (SPLET) were examined theoretically at 298.15 K in gas phase and solvent effects included by single point calculations. Different thermodynamic parameters control the different mechanisms that operate. These thermodynamic parameters dictate the mechanism of choice as described in previous chapter.

Ionization energy (IE) and electron affinity (EA) of deprotonated ligands (monoanionic species) were calculated from the single point energy calculations of corresponding neutral (cation) and dianion (corresponding anion) species to analyze the charge transfer process. To understand the role of the ligands, their accepting and donating powers were compared to two free radicals $O_2^{\cdot -}$ (electron donor) and $^{\cdot}OH$ (electron acceptor). Using these values, a donor

acceptor map was plotted. Enthalpy change and Gibb's free energy change were calculated in the aqueous phase as single point electronic energy. Thermal corrections were taken from the gas phase calculations done in the same level of theory. We have also checked the druggability and toxicity of the substituted molecules using molinspiration [13] and datawarrior softwares [14].

5.3. Results and Discussion

In an attempt to increase the anti-oxidant ability of the parent naturally occurring flavanone molecules, we have substituted them with electron donating and electron withdrawing substituents. Electron donating groups chosen were methyl, hydroxyl and methoxy groups and electron withdrawing groups chosen were ester and keto groups. Structures of the substituted flavanones are depicted in Fig. 5.1. The substitution was done at the 6^{th} position in the A-ring of the flavonone molecule. This position was chosen so that the inductive effect exerted by the substituents can exert their effects easily on the hydroxyl groups of the neighboring carbon atoms.

5.3.1. Antioxidant activity

There are several pathways of antioxidant action prevalent in literature which may be adopted by free radical scavengers. Of these, the most important pathways are Hydrogen atom transfer (HAT), Single-electron transfer followed by proton transfer (SET-PT) and Sequential proton loss electron transfer (SPLET). Thermodynamic parameters involved for each of these mechanisms was studied in detail using the enthalpy change (ΔH) associated with each process and

is tabulated in Table 5.1. The parameters controlling various steps of these mechanisms are Bond dissociation enthalpy (B.D.E.), Adiabatic Ionization potential (I.P.), proton dissociation enthalpy (P.D.E.), proton affinity (P.A.) and electron transfer enthalpy (E.T.E.).

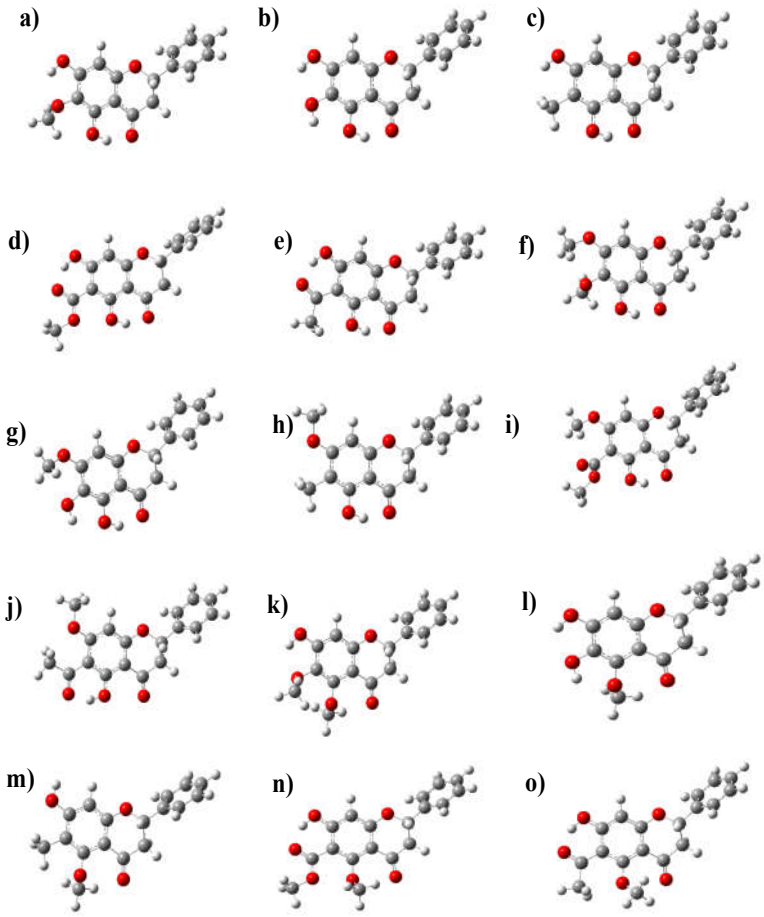

Fig. 5.1: Structures of the flavanone molecules with substitution a) OMe-pinocembrin b) OH-pinocembrin c)Me-pinocembrin d) COOMe-pinocembrin e) COMe-pinocembrin f) OMe-pinostrobin g) OH- pinostrobin h)Me- pinostrobin i) COOMe- pinostrobin j) COMe-pinostrobin k) OMe-alpinetin l) OH- alpinetin m)Me- alpinetin n)COOMe- alpinetin o) COMe- alpinetin

Table 5.1. Thermodynamic parameters governing various antioxidant mechanisms calculated in water and expressed in kcal/mol.

Molecules	B.D.E.	I.P.	P.D.E.	P.A.	E.T.E.
1	92.42	117.64	4.61	35.85	86.40
2	88.40		0.59	25.01	93.22
3	85.52	106.32	9.02	34.83	80.51
4	83.09		6.60	26.54	86.38
5	81.37	107.54	3.67	30.84	80.36
6	70.93		-6.77	28.58	72.18
7	81.06		3.36	25.69	85.20
8	89.88	112.92	6.79	37.03	82.67
9	85.11		2.02	25.46	89.48
10	100.44	122.30	7.98	31.78	98.49
11	105.27		12.80	29.43	105.67
12	100.75	122.26	8.32	29.78	100.80
13	100.06		7.63	32.99	96.90
14	91.98	116.52	5.29	36.08	85.73
15	84.77	105.45	9.14	34.99	79.61
16	79.92	105.95	3.80	29.75	80.00
17	72.86		-3.25	33.73	68.97
18	89.13	110.35	8.61	38.47	80.49
19	91.86	119.26	2.43	32.62	89.07
20	96.03	126.27	-0.42	34.29	91.57
21	86.37	116.80	-0.61	25.94	90.25
22	84.63	107.77	6.70	26.92	87.54
23	71.26	107.75	3.63	27.98	73.12
24	81.54		3.63	25.92	85.45
25	93.58	112.44	2.27	26.15	88.55
26	105.00	121.11	13.72	27.58	107.25
27	99.62	120.76	8.70	31.59	97.86

From Table 5.1, it could be seen that, of the different thermodynamic parameters studied in aqueous media, it is evident that proton affinity has the lowest values. Thus, SPLET will be the preferred mechanism of action in aqueous media. Second step in the SPLET pathway, which involves loss of electron, is governed by electron transfer enthalpy (ETE). On analyzing the role of substituents

on the thermodynamic parameters governing SPLET, we could see that substituents do not have much influence on the P.A values. On the contrary, electron transfer enthalpy has undergone considerable modifications. It could be seen that molecules with electron donating groups have lower ETE values compared to the molecules with electron withdrawing groups. Electron donating substituents have even lowered the electron transfer enthalpy of the derivatives compared to that of the parent molecules. The lowest value among electron donating substituents is attained on -OH substitution. This indicates that electron transfer properties of flavanones can be influenced through derivatization.

Further, we went ahead in analyzing the influence of the substituents on the electron transfer capability of the deprotonated monoanions (DA) in the vicinity of other free radicals. Flavonoids like quercetin are known to exist mainly as deprotonated species at physiological pH [15,16]. Structures of the 27 different monoanions formed through deprotonating different hydroxyl sites are shown in the Fig. 5.2. Electron affinity and Ionization potential of all the 27 monoanions were calculated in water medium by energy vertical method (Table 5.2). Superoxide radical anion ($O_2^{\cdot -}$) and $^{\cdot}OH$ free radicals were chosen for comparison as these are common free radicals found in human body. Superoxide radical anion generally donates electrons and $^{\cdot}OH$ radical generally accepts electrons.

To qualitatively comment on the electron donor and acceptor powers of monoanions, a plot of Ionization energy v/s electron affinity was drawn. From the literature, the molecules situated in the lower left corner are considered as good electron donors and those situated in the

upper right corner are considered as good acceptors. Thus the direction of electron flow will be from lower left to upper right [12].

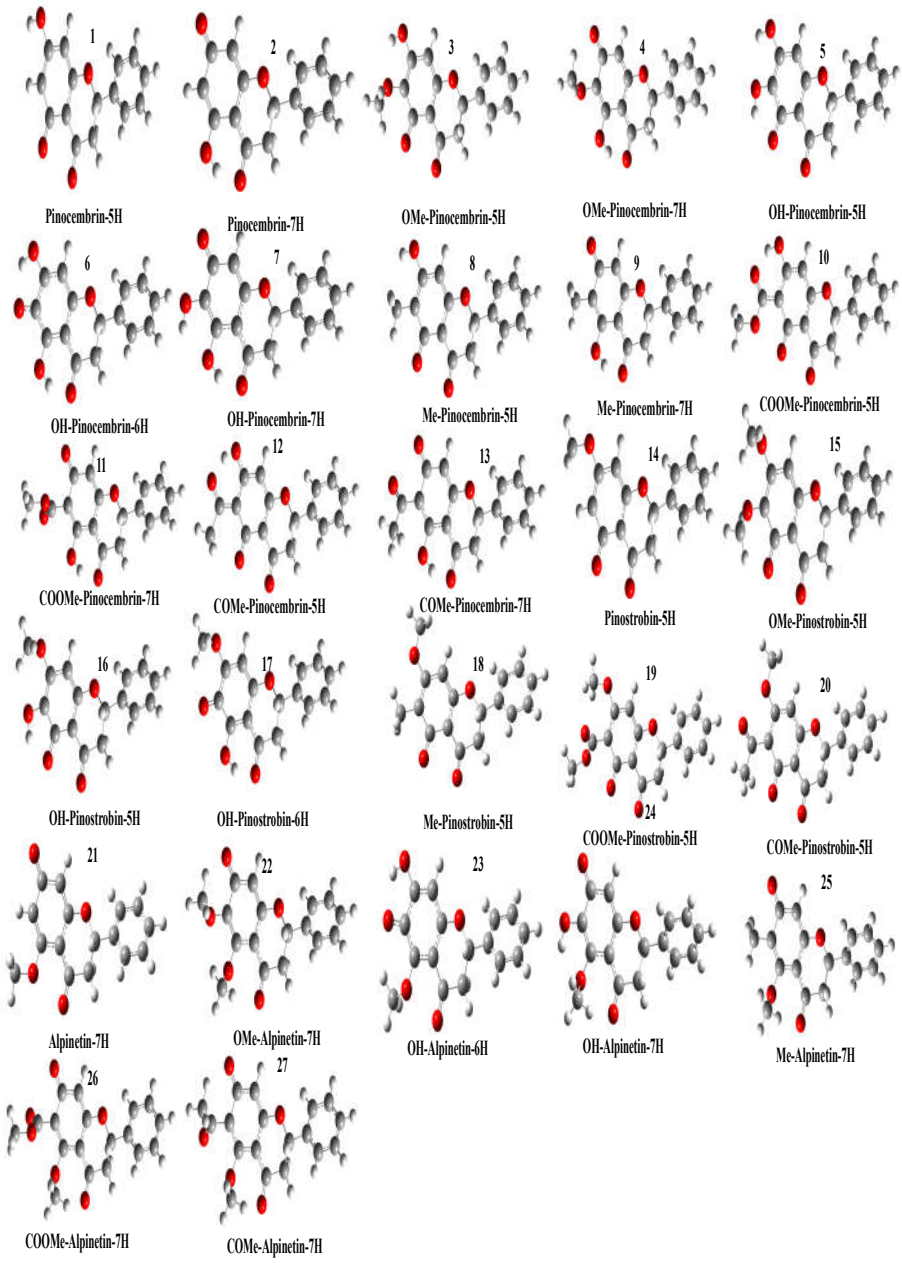

Fig. 5.2. Optimized structures of the monoanionic species under study.

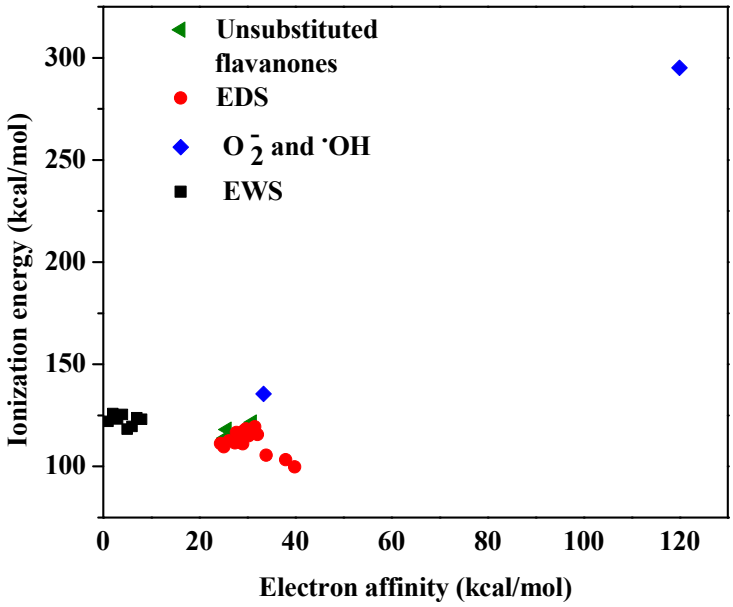

Fig. 5.3. A plot of ionization energy v/s electron affinity of the molecules under study.

The plot of ionization energy and electron affinity (Fig. 5.3) of all the DAs along with $O_2^{\cdot -}$ and $^{\cdot}OH$ shows that all the DAs are localized near the superoxide radical anion. Thus, there won't be any electron transfer between the molecules under study and superoxide radical anion. But, these molecules are situated down to the left compared to $^{\cdot}OH$ radical. These molecules can hence be predicted to be capable of donating electrons to deactivate $^{\cdot}OH$ free radical.

The molecules could now be categorized as electron donors or acceptors but further thermodynamic feasibility of the reaction could not be commented upon. For a quantitative picture, a thermodynamic

variable called energetic index is reported [17] for full electron transferability within the framework of chemical reactivity theory as:

$$\Delta E = \chi_d - \chi_a + \frac{1}{2}(\eta_d - \eta_a) \tag{5.1}$$

Here'd' denotes electron donor, 'a' denotes acceptor, 'χ' represents electronegativity and η represents hardness. $\chi = \frac{IE + EA}{2}$ and $\eta = IE - EA$. Substituting these values, ΔE can be represented as

$$\Delta E = IE_d - EA_a \tag{5.2}$$

ΔE gives the probability of charge transfer in terms of electron donating and accepting capacities. A reaction to be thermodynamically feasible, the value of ΔE should be negative, i.e., I. E. (donor) should be less than the E. A. (acceptor).

In polar aqueous media, $^{\cdot}OH$ radical is likely to act as an electron acceptor. Thus, all those molecules which have ionization energy less than the electron affinity of $^{\cdot}OH$ (119.93 kcal/ mol) will be good electron donors. On the other hand, $O_2^{\cdot -}$ is likely to be a good electron donor and hence all the molecules which have electron affinity greater than the ionization energy of $O_2^{\cdot -}$ (135.45 kcal/ mol) will be good electron acceptors.

From Table 5.2, it could be understood that ionization energy of all the DAs with electron donating substituents are less than the electron affinity of $^{\cdot}OH$ free radical. Among electron withdrawing

substituents, some of them attached to pinostrobin also shows ionization enthalpy lower than electron affinity of $^{\cdot}OH$. Energetic index of all these DAs turns out to be negative, indicating that the reactions between these DAs and $^{\cdot}OH$ will be exergonic. On comparing the energetic index of substituted DAs to that of unsubstituted parent monoanions (deprotonated), it could be seen that electron donating substituents considerably lowers the energetic index whereas electron withdrawing substituents increases the ΔE value. On the other hand, electron affinities of the molecules studied is not greater than the ionization energy of $O_2^{\cdot -}$, making the energy index positive. Thus, the flavanone molecules studied here are likely to act as electron donors and not acceptors upon deprotonation.

To further verify our results, Gibb's free energy change was calculated. These were again calculated for deprotonated monoanions. It was calculated as follows [12] :

$$\Delta G_{ET}^{0} = [G(anti^{+}) + G(R^{-})] - [G(anti) + G(R^{\cdot})] \qquad (5.3)$$

Table 5.2. Vertical ionization energy and vertical electron affinity of the molecules. ΔE (I) calculated with deprotonated monoanions (anti) as electron donors and ΔE (II) calculated with (anti) as electron acceptors in kcal/ mol in water medium.

Molecule	Ionization energy	Electron affinity	ΔE (I)(OH) IE(anti)-EA($^{\cdot}$OH)	ΔE (II) ($O2^{-\cdot}$) IE($O2^{-\cdot}$)-EA(anti)
OH^-	295.10	119.93		
$O2^{-\cdot}$	135.49	33.38		
1	114.64	26.02	**-5.28**	109.47
2	121.62	31.01	1.70	104.48
3	112.58	26.17	**-7.34**	109.32
4	119.41	31.56	**-0.51**	103.93
5	111.51	27.44	**-8.42**	108.05
6	103.28	37.97	**-16.64**	97.52
7	115.66	32.11	**-4.27**	103.38
8	111.22	24.43	**-8.70**	111.06
9	118.38	29.74	**-1.55**	105.75
10	122.07	33.68	2.14	101.81
11	125.80	33.86	5.87	101.63
12	123.18	36.88	3.26	98.61
13	125.42	34.43	5.50	101.07
14	113.88	25.33	**-6.05**	110.16
15	111.70	28.62	**-8.22**	106.87
16	111.01	29.02	**-8.92**	106.47
17	99.80	39.85	**-20.12**	95.64
18	109.56	25.11	**-10.36**	110.38
19	118.22	31.20	**-1.70**	104.29
20	119.57	34.53	**-0.35**	100.97
21	118.14	25.73	**-1.78**	109.77
22	117.45	29.27	**-2.48**	106.22
23	105.55	33.90	**-14.38**	101.59
24	114.99	30.31	**-4.94**	105.19
25	116.58	27.73	**-3.35**	107.76
26	123.83	31.79	3.90	103.71
27	123.04	32.50	3.12	102.99

From Table 5.3, it could be seen that all the deprotonated monoanions with electron donating substituents gives negative value for ΔG and all those with electron withdrawing substituents gives positive value of ΔG. Except in pinostrobin, where both substitutions

show negative ΔG values. This shows that the reactions are thermodynamically feasible. However, on comparing ΔG values of deprotonated monoanions of substituted molecules with that of parent molecules, ΔG values of only those carrying electron donating substituents are lower than that of the parent molecules. Analyzing the molecules with electron donating groups, it could be further deduced that OH substitution is more effective in lowering ΔG than other groups. On comparing both the tables (Tables 5.2 and 5.3), it could be seen that the in most of the cases deprotonated monoanions with a negative energetic index turn out to have a negative value for ΔG as well.

Table 5.3. Adiabatic Gibb's free energy (ΔG) for reaction I between radical and radical scavengers in kcal/mol.

Molecule	ΔG	Molecule	ΔG
1	**-9.72**	15	**-16.64**
2	**-2.69**	16	**-16.13**
3	**-16.26**	17	**-26.88**
4	**-9.85**	18	**-15.03**
5	**-15.45**	19	**-7.07**
6	**-23.42**	20	**-2.76**
7	**-10.53**	21	**-5.72**
8	**-13.55**	22	**-8.55**
9	**-6.18**	23	**-22.67**
10	3.70	24	**-10.84**
11	11.17	25	**-7.69**
12	5.84	26	12.25
13	2.37	27	3.73
14	**-10.26**		

5.3.2. Druggability and Toxicity studies

Druggability of the substituted molecules was studied using molinspiration online software. It could be found out that all the

molecules satisfy Lipinski's rule of five. All the molecules have log P values less than 5, molecular weight less than 500, number of hydrogen bond donors less than 5 and acceptors less than 10. Total polar surface area of the molecules are less than the prescribed limit of 140 $Å^2$. Number of rotatable bonds (nrot) which decides the conformational flexibility is also well below 10 which is the prescribed upper limit. Thus all the substituted molecules are likely to be orally bioavailable. We have also checked the toxicity of the molecules using DataWarrior software. The molecules appear to be non-toxic under the different heads studied like mutagenic, tumorigenic, reproductive effect and irritant.

Table 5.4. Lipinski parameters and its extension for the molecules studied

Molecule	Lipinski's Parameters					Extension	
	milogP	MW	HBD	HBA	Violations	TPSA	nrot
OMe-Pinocembrin	2.40	286.28	2	5	0	76.00	2
OH-Pinocembrin	2.13	272.26	3	5	0	86.99	1
Me-Pinocembrin	3.23	270.28	2	4	0	66.76	1
COOMe-Pinocembrin	2.62	314.29	2	6	0	93.07	3
COMe-Pinocembrin	2.68	298.29	2	5	0	83.83	2
OMe-Pinostrobin	2.71	300.31	1	5	0	65.00	3
OH- Pinostrobin	2.44	286.28	2	5	0	76.00	2
Me- Pinostrobin	3.30	284.31	1	4	0	55.77	2
COOMe-Pinostrobin	2.68	328.32	1	6	0	82.07	4
COMe- Pinostrobin	2.75	312.32	1	5	0	72.84	3
OMe-Alpinetin	2.68	300.31	1	5	0	65.00	3
OH- Alpinetin	2.40	286.28	2	5	0	76.00	2
Me- Alpinetin	3.51	284.31	1	4	0	55.77	3
COOMe- Alpinetin	2.89	328.32	1	6	0	82.07	4
COMe- Alpinetin	2.96	312.32	1	5	0	72.84	3

Table 5.5. Results of the toxicology studies conducted on the molecules.

Molecule	Mutagenic	Tumorigenic	Reproductive effective	Irritant
OMe-Pinocembrin	none	none	none	none
OH-Pinocembrin	none	none	none	none
Me-Pinocembrin	none	none	none	none
COOMe-Pinocembrin	none	none	none	none
COMe-Pinocembrin	none	none	none	none
OMe-Pinostrobin	none	none	none	none
OH- Pinostrobin	none	none	none	none
Me- Pinostrobin	none	none	none	none
COOMe- Pinostrobin	none	none	none	none
COMe- Pinostrobin	none	none	none	none
OMe-Alpinetin	none	none	none	none
OH- Alpinetin	none	none	none	none
Me- Alpinetin	none	none	none	none
COOMe- Alpinetin	none	none	none	none
COMe- Alpinetin	none	none	none	none

5.4. Conclusions

Pinocembrin, Pinostrobin and Alpinetin were derivatized with an aim to improve their anti-oxidant properties. Different mechanisms of antioxidant action were examined by calculating thermodynamic parameters involved. Sequential proton loss and electron transfer (SPLET) seems to be the favored mechanism due to low value of proton affinity. Substituents have not much effect on proton affinity but have marked effect on electron transfer enthalpy.

This effect on electron transfer enthalpy was qualitatively analyzed from I.E. v/s E. A. plot. It could be understood that deprotonated monoanions of the flavanones created upon proton loss could serve as electron donors to deactivate $^{\cdot}OH$ free radical. Further energetic index and Gibb's free energy change calculated, ascertains that electron donating ability of deprotonated monoanions increases with electron donating substituents. From these data, it could be concluded that electron donating groups are likely to increase anti-oxidant potential whereas electron withdrawing groups are likely to decreases it. But, lowering of ionization potential beyond a limit is likely to trigger pro-oxidant nature in some molecules. Thus effective and careful derivatization can help to improve the antioxidant capability of the flavanone molecules without triggering prooxidant nature. Druggability and toxicity studies conducted on the substituted molecules showed that all the molecules satisfied Lipinski's rule of five and are also non-toxic under the heads studied.

References

[1] J. Kehrer, J. Robertson, C. Smith, Free Radicals and Reactive Oxygen Species in Comprehensive Toxicology, Oxford: Elsevier, 2010.

[2] P. Sailaja Rao, S. Kalva, A. Yerramilli, S. Mamidi, Free Radicals Antioxidants 1 (2011) 2–7.

[3] P.G. Pietta, J. Natur. Prod. 63 (2000) 1035–1042.

[4] S.B. Lotito, B. Frei, Free Rad. Biol. Med. 41 (2006) 1727–1746.

[5] N. Nenadis, D. Siskos, Food Res. Int. 76 (2015) 506–510.

[6] http://www.fssai.gov.in/home.

[7] I.D. Thorat, D.D. Jagtap, D. Mohapatra, D.C. Joshi, R.F. Sutar, S.S. Kapdi, Int. J. Food Stud. 2 (2013) 81–104.

[8] A.D. Becke, J. Chem. Phys. 98 (1993) 5648–5652.

[9] C. Lee, W. Yang, R.G. Parr, Phys. Rev. B 37 (1988) 785–789.

[10] W. Kohn, a D. Becke, R.G. Parr, J. Phys Chem (1996) 12974–12980.

[11] M.J. Frisch, G.W. Trucks, H.B. Schlegel, G.E. Scuseria, M.A. Robb, J.R. Cheeseman, G. Scalmani, V. Barone, B. Mennucci, G.A. Petersson, H. Nakatsuji, M. Caricato, X. Li, H.P. Hratchian, A.F. Izmaylov, J. Bloino, G. Zheng, J.L. Sonnenberg, M. Hada, M. Eha, D.J. Fox, (2009).

[12] A. Martínez, E. Hernández-Marin, A. Galano, Food Funct. 3 (2012) 442.

[13] http://www.molinspiration.com/.

[14] http://www.openmolecules.org/datawarrior/download.html.

[15] M. Medvidović-Kosanović, M. Šeruga, L. Jakobek, I. Novak, Croat. Chem. Acta 75 (2010) 547–561.

[16] J.S. Barnes, Characterization of Flavonoid Reactivities and Degradation Productsusing Online Continuous Flow Kinetic Measurements and Higher Order Mass Spectrometry, The University of Texas, Arlington, 2013.

[17] A. Martinez, R. Vargas, A. Galano, Phys. Chem. B 113 (2009) 12113–12120.

Chapter 6

Flavanones as UVB filters - TDDFT and NLMO study

6.1. Introduction

Solar electromagnetic spectrum consists harmful UV radiation, which can be classified into three: UV A (320-400 nm), UV B (290-320 nm) and UV C (200-280 nm) [1,2]. Among this, UV C is highly damaging but is fully absorbed by earth's atmosphere. Exposure to UV A and UV B can cause serious skin damages, including erythema (sunburn), photo aging of the skin and increased risk of skin cancer [1][3]. To protect the skin from these damaging effects sunscreens are widely available in the market. One of the main ingredients contained in topical sunscreens is organic UV filters which can absorb these harmful radiations [4]. Organic filters absorb these harmful radiations generally by exciting an electron from ground state to excited state with the help of unsaturated electrons (π orbitals) or unpaired electrons

(n orbitals) [1]. An ideal UV filter should absorb both UV A and UV B radiations, adhere well to the skin and should resist removal by water.

Recently, there is great demand for sunscreens which not only filter out harmful UV radiations but also has ingredients for photo protection. Antioxidants can be a good choice of a substance as they can trap the free radicals formed as a result of UV exposure. Some of the prime candidates explored include resveratrol, green tea polyphenols, flavonoids and the like. UV B induced tumor in mice is found to be suppressed by epigallocatechin-3-gallate (EGCG) is one of the important polyphenols observed in green tea. Flavonoids like silimaryn, quercetin, apigenin genistein, etc., are found to be effective against skin carcinogenesis, sunburn, DNA damage etc. [5].

Simulation of UV-Visible spectra using TD-DFT provides crucial information regarding the absorption properties and the influence of molecular structure on absorption. Time dependent density functional theory (TD-DFT) also provides information regarding the excited states and excitation energies [6]. Natural localized Molecular Orbital (NLMO) clusters were developed from the Natural bond orbital (NBO) theory to better understand the nature of the orbitals involved. UV-Visible spectrum can be better explained by NLMO clusters than the Kohn- Sham orbitals as they involve structure factors [7, 8].

6.2. Computational Methodology

Generally UV-Visible spectral studies using TDDFT a carried out with basis functions with added diffuse and polarization functions

[9,10]. Thus the structures optimized at B3LYP/6-311++ G (d,p)[11, 12] level of theory in gas phase using the Gaussian 09 [13] computational software package were used. Harmonic frequency calculations were performed to confirm the structures as a global minimum. The theoretical ^{13}C and ^{1}H NMR spectra taken in gas phase were compared to experimental spectra recorded in solvent phase.

UV-Visible spectra are generated using TD-DFT method inherent in Gaussian 09. Herein a time dependent oscillating electric field is applied to model an excited state and various excitations and transition vectors to this state are studied. Lowest six excitations were studied in each case. Solvation models were studied using the default IEFPCM solvation model using two solvents namely water and methanol. NLMOs were constructed using the NBO 3.1. version [14] inbuilt in Gaussian 09. Visualization softwares used were Chemission [15] and Chemcraft [16].

6.3. Results and Discussion

6.3.1. Structural parameters

Optimized parameters of the molecules in the B3LYP/6-311++ G (d,p) are tabulated in Table 1. ^{13}C and ^{1}H -NMR spectra of these molecules in solvent phase (DMSO for pinocembrin and alpinetin and chloroform for pinostrobin) were compared with experimental NMR spectra available in the same solvents. These are shown in tables 6.2 and 6.3 respectively. The flavanone molecules selected namely pinocembrin, pinostrobin and alpinetin are already established to have free radical scavenging (antioxidant) capabilities. If these molecules

can screen UV radiations also, then it will be very useful for sunscreen applications.

Table 6.1. Optimized parameters of pinocembrin, pinostrobin and alpinetin at the B3LYP/6-311++ G (d,p) level of theory.

Bond length	Theoretical (B3LYP/6-311++G (d,p))		
	Pinocembrin	Pinostrobin	Alpinetin
C2-C3	1.53	1.53	1.52
C3-C4	1.51	1.51	1.53
C5-C6	1.39	1.39	1.39
C6-C7	1.40	1.40	1.40
C7-C8	1.40	1.40	1.39
C8-C9	1.38	1.38	1.39
C4-C10	1.44	1.44	1.48
C5-C10	1.42	1.42	1.42
C9-C10	1.42	1.42	1.42
C2-C1’	1.51	1.51	1.51
C1’-C2’	1.40	1.40	1.40
C1’-C6’	1.40	1.40	1.40
C2’-C3’	1.39	1.39	1.39
C3’-C4’	1.39	1.39	1.39
C4’-C5’	1.39	1.39	1.39
C5’-C6’	1.39	1.39	1.39
C2-H2	1.10	1.10	1.10
C3-H3(a)	1.09	1.09	1.09
C3-H3(b)	1.10	1.10	1.10
C6-H6	1.08	1.08	1.08
C8-H8	1.08	1.08	1.08
C2’-H2’	1.08	1.08	1.08
C3’-H3’	1.08	1.08	1.08
C4’-H4’	1.08	1.08	1.08
C5’-H5’	1.08	1.08	1.08
C6’-H6’	1.08	1.08	1.08
C2-O1	1.45	1.44	1.44
C4-O4	1.24	1.24	1.22
C5-O5	1.34	1.34	1.34
C7-O7	1.36	1.35	1.36

C9-O1	1.36	1.36	1.36
O5-H5	0.99	0.99	---
O7-C11	---	1.43	---
O7-H7	0.96	---	0.96
O5-C11	---	---	1.42
C11-H11a	---	1.09	1.09
C11-H11b	---	1.09	1.09
C11-H11c	---	1.09	1.09

Table 6.2. Comparison of chemical shift of pinocembrin, pinostrobin and alpinetin molecule computed using ^{13}C NMR spectroscopy with the experimental results.

	Pinocembrin		Pinostrobin		Alpinetin	
	Theory	Experiment [17]	Theory	Experiment [18]	Theory	Experiment [19]
C2	88.82	78.2	88.43	78.89	88.40	78.1
C3	49.54	42	49.72	43.05	52.74	45
C4	205.42	195.5	203.64	197.25	198.68	187.4
C5	173.78	164.3	174.09	163.8	172.54	164.1
C6	100.67	96.73	96.19	94.8	95.91	95.8
C7	174.45	164.59	176.79	167.62	172.66	164.4
C8	100.00	95.48	101.24	93.93	100.76	93.5
C9	173.12	162.6	171.25	167.62	175.61	162.2
C10	109.20	101.6	109.02	102.8	111.87	104.6
C11	----	----	58.88	55.36	59.04	55.7
C1'	148.71	138.22	148.65	138.02	149.36	139.2
C2'	134.23	126.13	133.82	125.81	134.09	126.4
C3'	136.19	128.88	135.78	128.54	136.26	128.5
C4'	136.34	128.91	135.90	128.54	136.07	128.3
C5'	135.87	128.88	135.41	128.54	135.73	128.5
C6'	135.00	126.13	134.07	125.81	134.83	126.4
R	0.9990		0.9984		0.9964	

Table 6.3. Comparison of chemical shift of pinocembrin, pinostrobin and alpinetin molecule computed using ^{1}H NMR spectroscopy with the experimental results.

	Pinocembrin		Pinostrobin		Alpinetin	
	Theory	Experiment [17]	Theory	Experiment [18]	Theory	Experiment [19]
2-H	5.37	5.58	5.32	5.4	5.31	5.44
3-H	2.55	2.72	2.48	2.85	2.40	2.59
	3.18	3.23	3.08	3.1	3.09	2.98
5-OH	12.37	12.13	12.64	12.00	----	----
6-H	6.16	5.9	6.13	6.03	5.93	5.98
7-OH	5.26	-----	----	-----	5.14	----
8-H	6.15	7.55	6.14	6.03	6.26	6.06
2'-H	8.00	7.55	7.94	7.4	8.00	7.04
3'H	7.77	7.41	7.68	7.4	7.79	7.4
4'H	7.79	7.41	7.78	7.4	7.74	7.4
5'H	7.68	7.55	7.61	7.4	7.64	7.4
6'H	7.60	7.55	7.54	7.4	7.58	7.4
11Ha	----	5.58	3.81	3.9	3.81	3.72
11Hb	----	3.23	4.15	3.9	3.79	3.72
11Hc	----	2.72	3.82	3.9	4.33	3.72
R	0.9988		0.9984		0.9936	

6.3.2. Optical signatures

Electronic transition in polyphenols is attributed generally to the transition between π- molecular orbitals extended over the molecular structure [10]. Flavonoids are characterized by two absorption bands: Band II around 240- 290 nm and Band I around 300 – 350 nm arising from the conjugation between B and C rings [20]. Flavanones in particular are characterized by a broad absorption band between 270 and 290 nm (Band II) and a small shoulder around 320 nm (Band I)[21, 22]. The substitution done to the flavanone ring have considerable effect in shifting the absorption maxima.

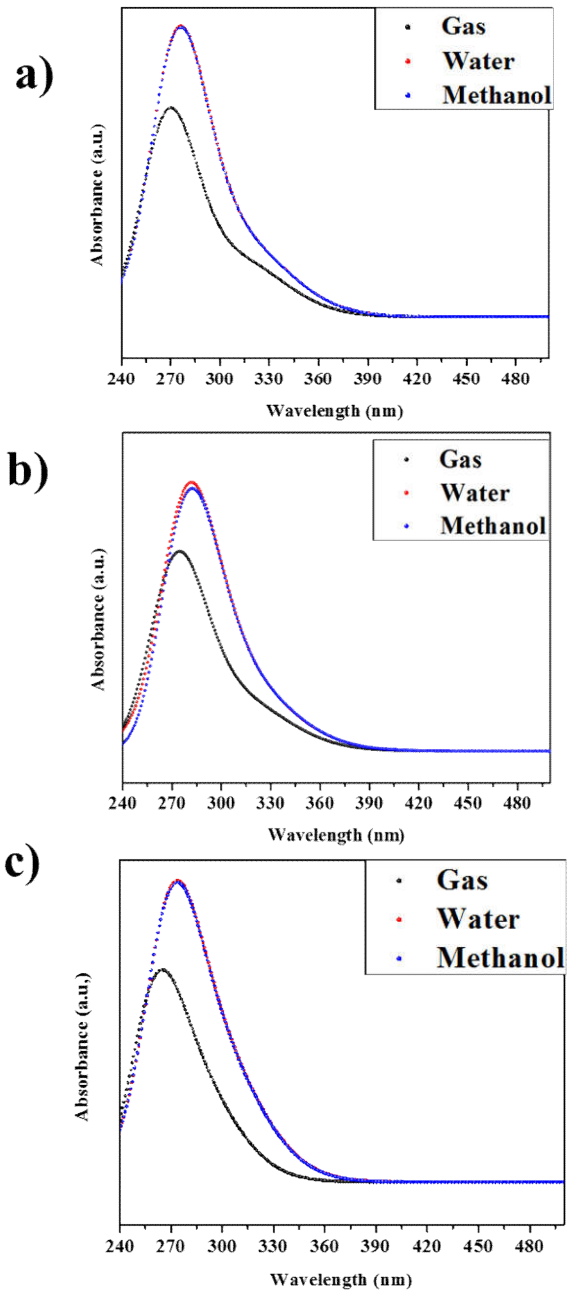

Fig. 6.1. Theoretical UV-Visible absorbance spectra of a) Pinocembrin b) Pinostrobin and c) Alpinetin.

Here in we have studied the UV-Visible spectra corresponding six low energy transitions for all molecules. In gas phase, it could be seen that the most intense band in pinocembrin is around 270 nm and shoulder is around 319 nm. The maxima arise from the electron transfer from HOMO-1 to LUMO primarily (~87%) and the shoulder results from HOMO to LUMO transition (~93%). For pinostrobin, the intense band is red shifted to 274 nm in gas phase with a shoulder around 320 nm. Similar to pinocembrin the maxima arises from electron transfer from HOMO-1 to LUMO (~85%) and shoulder is due to HOMO–LUMO transition (~89%). In alpinetin, the main transition in gas phase is from HOMO-2 to LUMO electron transfer and hence occurs at a lower wavelength of 263 nm. The shoulder appears at 294 nm and is due to HOMO–LUMO transition similar to other molecules. Absorption spectra of the studied molecules are shown in Fig 6.1.

On comparing the oscillator strengths of the different bands, it could be seen that significant transitions are HOMO-1 to LUMO, HOMO to LUMO and HOMO-2 to LUMO. In pinocembrin and pinostrobin, the most intense band in longer wavelength region is due to HOMO-1 to LUMO transition (f = 0.2361 for pinocembrin and 0.2976 for pinostrobin) and the shoulder is due to HOMO–LUMO transition (f = 0.0516 for pinocembrin and 0.0556 for pinostrobin). In alpinetin, the intense band in longer wavelength region is a transition from HOMO-2 to LUMO (f =0.2223) and the shoulder is due to HOMO–LUMO transition (f = 0.0709). For a band to have maximum intensity, there should be a good overlap between the orbitals involved in the electronic transition. The orbitals contributing towards the main absorption band and shoulder are shown in Fig. 6.2.

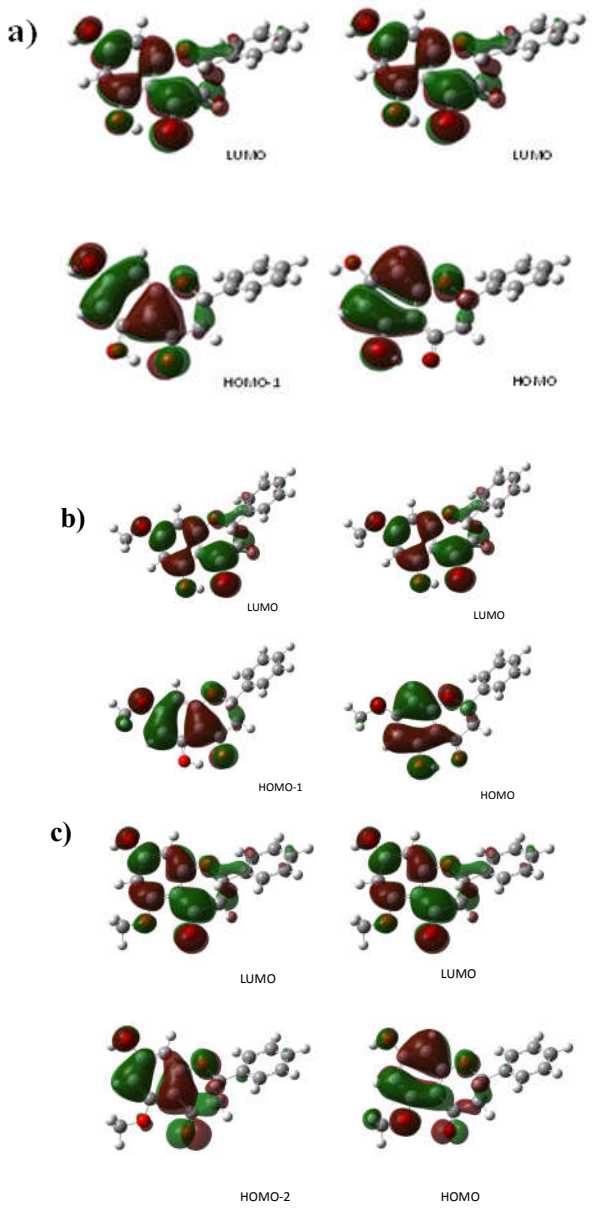

Fig 6.2. Topology of orbitals having maximum contribution towards intense band and shoulder band in the longer wavelength regime for a) Pinocembrin b) Pinostrobin and c) Alpinetin in gas phase.

As can be seen from Fig. 6.1, absorption band of the title molecules spans the entire UVB region. Electrons are promoted generally from the occupied molecular orbitals to the vacant molecular orbitals. Maximum absorption wavelength corresponds to the smallest gap between filled and vacant orbitals which is given by the difference between HOMO and LUMO orbitals. As could be understood from frontier molecular orbital studies, the energy gap of the studied molecules is around 4.5 eV which very well lies in the UV region of the electromagnetic spectrum. Absorption maxima of the compounds lie in the harmful UVB region (around 280 nm) and the shoulder lies in the UVA region (around 320 nm). But oscillatory strengths are appreciable only for absorption maxima and hence it could be inferred that these molecules are likely to effectively screen harmful UV B radiations.

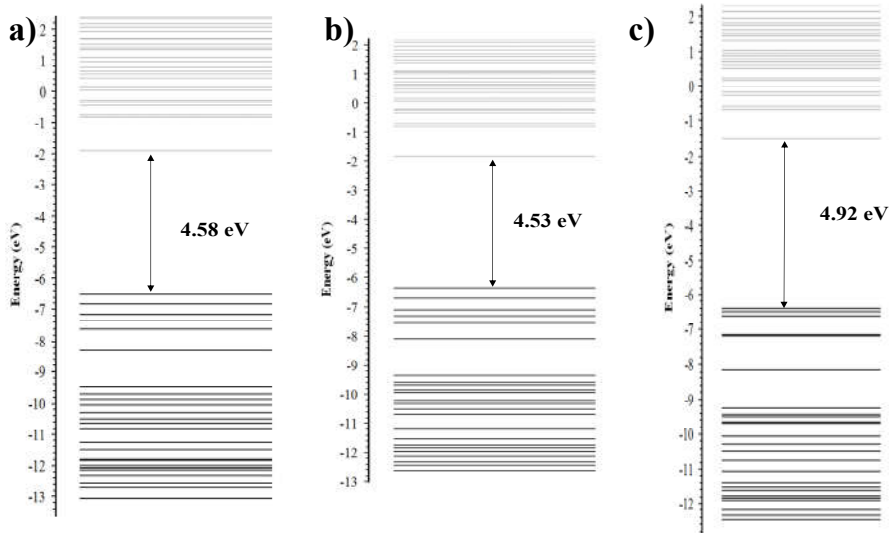

Fig 6.3. Molecular orbital energy level diagram of pinocembrin, pinostrobin and alpinetin portraying the energy gap.

Table 6.4. Theoretical absorption wavelength (nm), energies (eV), molecular orbital contributions and oscillator strengths (f) of pinocembrin, pinostrobin and alpinetin in gas phase.

Molecules	λ (nm)	Energy (eV)	MO involved	% contribution	Oscillator strength (f)
Pinocembrin	270.42	4.58	HOMO-1 ->LUMO	86.71	0.24
	319.8	3.88	HOMO ->LUMO	92.86	0.05
Pinostrobin	274.4	4.52	HOMO-1 ->LUMO	84.55	0.30
	321.7	3.85	HOMO ->LUMO	89.39	0.06
Alpinetin	263.16	4.71	HOMO-2 ->LUMO	56.86	0.22
	293.81	4.22	HOMO ->LUMO	71.93	0.07

6.3.3. Solvent effects

Low energy transitions of the molecules are also studied in polar solvents like water and methanol. It is observed that all the absorption bands are red shifted in polar media. In pinocembrin, HOMO-1 to LUMO transition shifts to around 276 nm and the HOMO to LUMO transition to 324 nm. Similarly in pinostrobin, the main peak shifts to 281 nm and shoulder shifts to 325 nm. In alpinetin, the main absorption band shifts to 272 nm and is due to HOMO- 11 to LUMO transition and shoulder continues to be HOMO–LUMO transition but is shifted to 306 nm as shown in Fig 7.1.

Table 6.5. Theoretical absorption wavelength (nm), energies (eV), molecular orbital contributions and oscillator strengths (f) of pinocembrin, pinostrobin and alpinetin in methanol and water media.

	λ (nm)	Energy (eV)	MO involved	% contribution	Oscillator strength (f)
Methanol					
Pinocembrin	276.19	4.49	HOMO-1 ->LUMO	88.64	0.32
	323.95	3.83	HOMO ->LUMO	95.51	0.06
Pinostrobin	281.05	4.41	HOMO-1 ->LUMO	85.18	0.39
	325.58	3.81	HOMO ->LUMO	91.48	0.07
Alpinetin	272.29	4.55	HOMO-1 ->LUMO	82.35	0.32
	306.5	4.05	HOMO ->LUMO	83.12	0.09
Water					
Pinocembrin	276.29	4.49	HOMO-1 ->LUMO	88.66	0.32
	324.01	3.83	HOMO ->LUMO	95.56	0.06
Pinostrobin	281.14	4.41	HOMO-1 ->LUMO	85.12	0.39
	325.6	3.81	HOMO ->LUMO	91.51	0.07
Alpinetin	272.54	4.55	HOMO-1 ->LUMO	82.93	0.32
	306.88	4.04	HOMO ->LUMO	83.07	0.09

This red shift of absorption bands is reasonable as polar solvents are known to stabilize the π* orbitals more compared to π orbitals [23]. This increased stabilization leads to observed bathochromic shift of the absorption bands (Table 6.2). Theoretical

values in methanol medium are compared to experimentally reported λ_{max} values. Experimental absorption maxima of pinocembrin, pinostrobin and alpinetin are 289 nm, 288 nm and 285 nm respectively in methanol media [24]. It is also observed that there is an increase in oscillator strength in polar media. This could be attributed to better orbital overlap. In methanol, the HOMO-1 to LUMO transition in pinocembrin, pinostrobin and alpinetin has oscillator strengths of values f = 0.3202, 0.3857 and 0.3172 respectively, and in water, it further increases to f = 0.3214, 0.3869 and 0.3194 respectively. There is thus an increase in oscillator strength with increase in polarity of the medium.

6.3.4. NLMO study

As a representative example, NLMO study is performed on pinocembrin. The construction of NLMO clusters are carried out as follows. All the NBOs , bonding and anti-bonding are arranged in decreasing order of energy. Attention is then focused on high lying bonding and low lying anti-bonding orbitals [8].

NLMO cluster is formed of NLMOs which have spatial proximity and energetic closeness. Among the bonding orbitals, energetically and spatially closer π (C-C) NLMOs of the B ring forms the HOMO cluster whereas three π (C-C) NLMOs of the A ring forms the HOMO-1 cluster, HOMO-2 cluster is formed by p NLMOs on oxygen atoms. In the antibonding region, LUMO cluster is made up of π* (C-O) NLMO of the carbonyl group on the C ring and π* (C-C) NLMO of the A ring and LUMO+1 cluster is formed by three π* (C-C)

NLMOs of the B ring (Table 7.3). NLMOs are formed by delocalization of the corresponding NBOs. Those NLMOs which contribute to significant absorptions are shown in the Fig.7.4, NBOs are localized orbitals whereas NLMOs are spread over the entire ring.

Table 6.6. Data related to bonding and antibonding NLMOs of pinocembrin.

NBO		Occupancy	Energy	NLMO cluster
Anti-bonding Orbitals				
74.	BD*(2) C 2' - C 3'	0.3179	0.0238	LUMO+1
73.	BD*(2) C 1' - C 6'	0.3526	0.0236	
72.	BD*(2) C 5' - C 4'	0.3272	0.0218	
71.	BD*(2) C 5 - C 6	0.3790	0.0077	LUMO
70.	BD*(2) C 8 - C 7	0.4208	0.0065	
69.	BD*(2) C 10 - C 9	0.5035	-0.0008	
68.	BD*(2) O 4 - C 4	0.2478	-0.0066	
Bonding Orbitals				
67.	BD (2) C 2' - C 3'	1.6602	-0.2594	HOMO
66.	BD (2) C 5'- C 4'	1.6618	-0.2602	
65.	BD (2) C 1'- C 6'	1.6646	-0.2628	
64.	BD (2) C 8 - C 7	1.6275	-0.2674	HOMO-1
63.	BD (2) C 10 - C 9	1.6232	-0.2702	
62.	BD (2) C 5 - C 6	1.6749	-0.2716	
61.	LP (2) O 4	1.8679	-0.3116	HOMO-2
60.	LP (2) O 5	1.8102	-0.3224	
59.	LP (2) O 1	1.8414	-0.3423	
58.	LP (2) O 7	1.8566	-0.3452	
57.	BD (2) O 4 - C 4	1.9782	-0.3906	HOMO-3

Anti-bonding orbitals

LUMO cluster

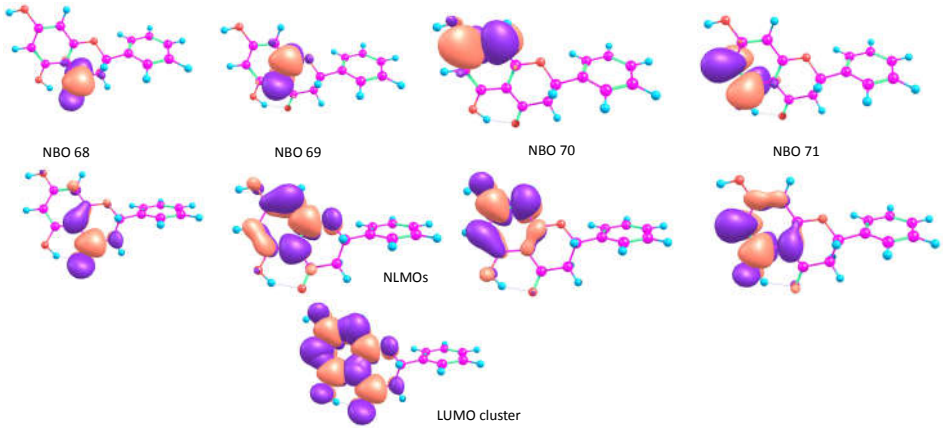

Fig 6.4. Anti-bonding NLMO clusters of pinocembrin

Bonding orbitals

HOMO cluster

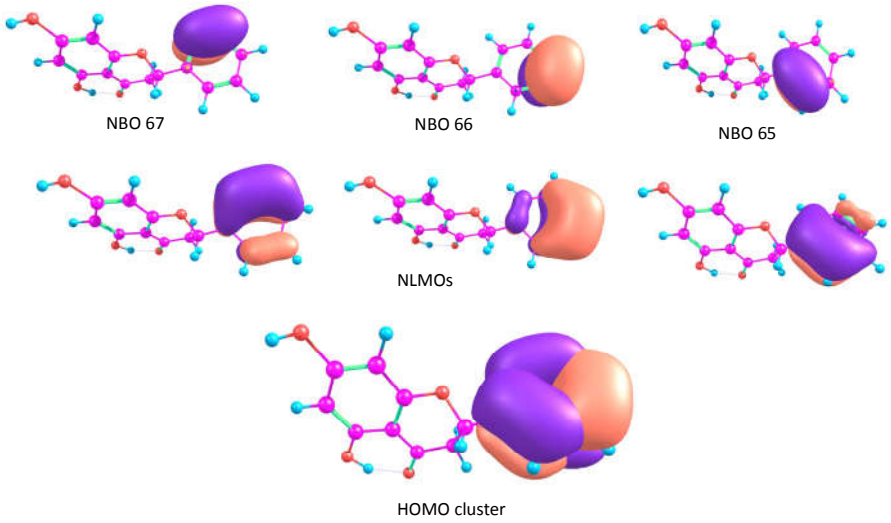

HOMO-1 cluster

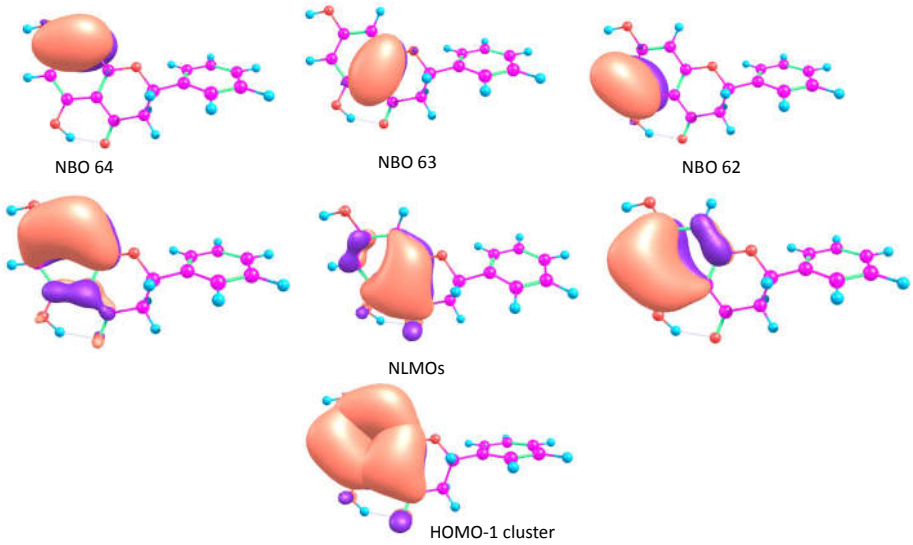

Fig 6.5. Bonding NLMO clusters of pinocembrin

On deeper analysis, it can be seen from the NLMO clusters that HOMO–>LUMO transition involves electron transition from B ring to A and C rings, whereas electron transition from HOMO-1–>LUMO involves transfer from A and C rings to A and C rings. As discussed earlier, oscillator strength requires maximum overlap between orbitals involved. Thus, as per NLMO analysis the most intense band in higher wavelength region of UV spectra of pinocembrin should be a band corresponding to HOMO-1–LUMO transition. HOMO–LUMO transition should be weaker compared to this. The TD-DFT results corroborate this finding. The intense band at 270 nm in pinocembrin corresponds to HOMO-1 to LUMO transition and the HOMO to LUMO transition appears as a shoulder around 319 nm. NLMO study thus explains the observed TD-DFT results conclusively.

As could be understood, in the low energy window, flavanones exhibit absorption maxima around 280 nm which extends as a shoulder to around 320 nm. Thus almost the entire window of UV B radiation from 290nm-320nm is spanned by the absorption spectrum. Thus these molecules could be used for UVB screening purposes.

6.4. Conclusions

The flavanone molecules, namely pinocembrin, pinostrobin and alpinetin selected for current study are known antioxidant molecules capable of free radical scavenging activity. This helps in photoprotection. The UV absorption characteristics of these molecules studied, using TDDFT and NLMO formalism, indicates that the absorption spectra of these molecules cover the UV B region (290 nm – 320 nm) of the electromagnetic spectrum almost completely in gaseous medium. In polar solvents like water and methanol the spectra are slightly red shifted as expected. NLMO studies carried out in pinocembrin gives a thorough understanding of the orbitals involved in the electronic transitions. These molecules with photoprotection and UV filtering capabilities can be a potential candidate for the sunscreen applications.

References

[1] B.A.M. Corrêa, A.S. Gonçalves, A.M.T. De Souza, C.A. Freitas, A.S. Gonc, M. Cabral, M.G. Albuquerque, H.C. Castro, E.P. Santos, C.R. Rodrigues, J. Phys. Chem. A 116 (2012) 10927–10933.

[2] N. Serpone, D. Dondi, A. Albini, Inorganica Chim. Acta 360 (2007) 794–802.

[3] N. Saewan, A. Jimtaisong, J. Appl. Pharm. Sci. 3 (2013) 129–141.

[4] T. Suresh, S. Sarveswari, N. Arul murugan, V. Vijayakumar, P. Iniyavan, A. Srikanth, J.P. Jasinski, J. Mol. Struct. 1099 (2015) 560–566.

[5] S. González, M. Fernández-Lorente, Y. Gilaberte-Calzada, Clin. Dermatol. 26 (2008) 614–626.

[6] M.E. Casida, J.Mol. Struc.-Theochem. 914 (2009) 3–18.

[7] S. Marković, J. Tošović, J. Phys. Chem. A 119 (2015) 9352–9362.

[8] J. Tošović, S. Markovic, Chem. Pap. 74 (2017) 543–552.

[9] R.D. Garcia, V.G. Maltarollo, K.M. Honório, G.H.G. Trossini, J. Mol. Model. 21 (2015).

[10] E.H. Anouar, J. Gierschner, J.L. Duroux, P. Trouillas, Food Chem. 131 (2012) 79–89.

[11] A.D. Becke, J. Chem. Phys. 98 (1993) 5648–5652.

[12] C. Lee, W. Yang, R.G. Parr, Phys. Rev. B 37 (1988) 785–789.

[13] M.J. Frisch, G.W. Trucks, H.B. Schlegel, G.E. Scuseria, M.A. Robb, J.R. Cheeseman, G. Scalmani, V. Barone, B. Mennucci, G.A. Petersson, H. Nakatsuji, M. Caricato, X. Li, H.P. Hratchian, A.F. Izmaylov, J. Bloino, G. Zheng, J.L. Sonnenberg, M. Hada, M. Eha, D.J. Fox, (2009).

[14] E.D. Glendening, A.E. Reed, J.E. Carpenter, F. Weinhold., NBO Version 3.1. (n.d.).

[15] L.V. Skripnikov, Chemissian Version 4.43 Visualization Computer Program, n.d.

[16] G.A. Zhurko, D.A. Zhurko, Chemcraft 1.6, Chemcraft Graphical Program for Working with Quantum Chemistry Results, 2009.

[17] Y. Liu, D.K. Ho, J.M. Cassady, J. Nat.Prod. 55 (1992) 357–363.

[18] B. Burke, M. Nair, Phytochemistry 25 (1986) 1427–1430.

[19] H. Itokawa, M. Morita, S. Mihashi, Phytochemistry 20 (1981) 2503–2506.

[20] C. Santos-Buelga, C. García-Viguera, F.A. Tomás-Barberán, Methods in Polyphenol Analysis, The Royal Society of Chemistry, Cambridge, UK, 2003.

[21] A. Marston, K. Hostettmann, Flavonoids: Chemistry, Biochemistry, and Applications, CRC Press, Taylor & Francis Group, Boca Raton, USA., 2006.

[22] D. Tsimogiannis, M. Samiotaki, G. Panayotou, V. Oreopoulou, Molecules 12 (2007) 593–606.

[23] L.D.S. Yadav, Organic Spectroscopy, Kluwer Academic Publishers and Ananmaya Publishers, 2005.

[24] T. Panphadung, Antioxidant Activity and Quality Control by HPLC Method of Constituents from Boesenbergia Pandurata Rhizomes (PhD Thesis), Prince of Songkla University, 2004.

Chapter 7

Flavonones as antidotes for metal overdose

7.1. Introduction

Metals are an integral part of the structural and functional components of our body and play a critical role in physiological and pathological processes. Metallo pharmacology and metallotoxicology deals with altering the concentrations of metal in our body and their after effects. Deficiency of essential metals has to be cleared by directly administering them whereas excess metals should be removed from the body as well. Metals are also used for tagging biomolecules for diagnosis, for drug delivery purposes as carriers for targeted delivery etc. Metal toxicity may occur in two ways, either due to heavy metal exposure or due to metal overload. These metals and metal compounds will interfere with the functioning of several organ systems like central nervous system, liver, kidneys etc. Diagnostic testing for the presence of heavy metals and subsequently decreasing the level of

the metal in the body is an integral part of treatment of metal poisoning [1].

One of the prime methods for treating metal poisoning is chelation therapy [2]. Chelating agents can reduce the metal toxicity by forming a stable complex with the metal thereby shielding it from other biomolecules and more effectively by mobilizing toxic metals to urine. Several effective chelating agents used till date are dimercaprol (also called British Anti-Lewisite or BAL) [3], meso 2,3-dimercaptosuccinic acid (DMSA) [4], sodium 2,3-dimercaptopropane 1-sulfonate (DMPS) [5], Ethylenediaminetetraacetic acid (EDTA) [6] and the like. These conventional antidotes though effective have several limitations [7]. For faster action and for minimizing side effects, new trend followed in chelation therapy is combination therapy in which two described drugs are administered resulting in synergistic action. This combined therapy aims at enhanced mobilization of the metal and reduction in dose of the metal chelators [8]. Combined administration of DMSA and Monoisoamyl DMSA (MiADMSA) in arsenic poisoning was able to control hepatic DNA damage [9]. Combined administration of thiol chelator MiADMSA and $CaNa_2EDTA$ is prescribed for lead toxicity [10].

Oxidative stress may be considered as one of the prime mechanism in metal toxicity [1]. Metal toxicity in general, induces reactive oxygen species which leads to oxidative stress. Most of the common heavy metals like arsenic (As), cadmium (Cd), mercury (Hg), lead (Pb), etc., induces free radicals directly or indirectly. This provides a good rationale for including antioxidants in chelation

therapy. Combined treatment of thiol chelator and herbal antioxidant C*entella asiatica* is proven to be beneficial for oxidative stress induced by lead toxicity [11]. Combinational therapy using antioxidants like *N*-acetylcysteine (NAC) [12], lipoic acid (LA) [13], melatonin [12], and gossypin have shown considerable effect in metal intoxication. Phenolic compounds may act as terminators of free radicals and also chelate redox-active metal ions. Mishra et.al have reported that combined administration of quercetin and MiADMSA could abate toxic effects of arsenic [14].

From the literature, it is known that flavonoids can form complexes with metals [15]. Some of the experimentally studied complexes include $[Fe^{II}(3HF)_2Cl(CH_3OH)]$[16], $[Cu^{II}(3HF)_2]$[17][18], $Na_2[Zn(MSA)_2(H_2O)]$, $[Zn(MSA)(H_2O)_2]_n$ [19], etc. Here 3HF is 3-hydroxy flavone and MSA is morin-5-sulfonic acid. Some literature data are also available on theoretical study of metal chelation of flavonoids though largely for essential metals like iron (Fe) and copper (Cu). Ren et.al., [20] reported electronic structure calculations for Fe complexes of quercetin, luteolin, galangin, kaempferol and chrysin. Lekka et al [21] attempted a detailed DFT investigation on Cu-flavonoid complexes. Leopoldini et al. [22] carried out an extensive study on Fe - quercetin complexes. Aluminium – apigenin [23] complexes were studied by Amat et.al.

In this context, we have tried to have an insight into the interaction that antioxidant flavanones namely pinocembrin, pinostrobin and alpinetin, is likely to have with heavy metals using theoretical calculations. We have also analyzed their UV-Visible

absorption characteristics using TD-DFT formalism implemented in Gaussian 09. These flavanones may be helpful to be used in combination with other antidotes for chelation therapy against heavy metals. The metals included in the current study are zinc, cadmium, mercury, lead and palladium. Some of the toxic effects of these metals on human body are as follows:

1) **Zinc (Zn):** Zinc is considered relatively non-toxic among heavy metals. Zinc is an essential trace element not only for humans but for all organisms. However, there are instances of high zinc intake mainly when food is stored in galvanized containers. Brown et. al. [24] describes food poisoning with zinc which leads to epigastric pain, nausea and vomiting, abdominal cramps, and diarrhea. Excessive zinc intake may also lead to copper deficiency [25].

2) **Cadmium (Cd):** Cadmium is one of the most toxic metal ions in our environment. It is listed by environmental protection agency as one among the 126 priority pollutants. Cadmium has also been classified as a #1 category human carcinogen by the International Agency for Research on Cancer, Lyon, France [26]. Chronic human exposure to Cd results in anemia, renal dysfunction, osteotoxicities, hepatic dysfunction, cancers of the prostate, lung, pancreas, and kidney [27]. Cadmium also alters the antioxidant defense mechanism of our body [28]. This oxidative damage may result in lipid peroxidation and inhibition of enzyme action [29]. ROS so produced have

implications in nephrotoxicity, immunotoxicity and carcinogenesis [30].

3) **Mercury (Hg):** Mercury can exist in three forms in the environment like metallic form, non-metallic element and organic compounds. Mercury is highly toxic and is bioaccumulative [31,32]. Methylmercury is a neurotoxic compound which is responsible for microtubule destruction, mitochondrial damage, lipid peroxidation and accumulation of neurotoxic molecules. Exposure to significant levels of mercury can cause respiratory, renal, reproductive, immunologic, dermatologic and a variety of other effects. Minamata disease is a classic example of mercury toxicity. Minamata disease has sever neurological consequences. Mercury poisoning is the second most common cause of toxic metal contamination [33][30].

4) **Lead (Pb):** Lead poisoning is considered as a classic disease and its manifestations are more prominent in children than in adults. The clinical term for disorders due to lead poisoning is plumbism. Lead is also treated as a carcinogen. Lead toxicity affects central nervous, hematopoietic, hepatic and renal system [34,35]. Chronic exposure to lead may lead to persistent vomiting, lethargy, encephalopathy, delirium, convulsions and coma [36,37].

5) **Palladium (Pd):** Palladium is accumulating in the environment due to human activities and is a toxic metal when entered into

the food chain or leached into water bodies [38]. Inorganic form of palladium is found to be more toxic than organic form. Palladium is found to accumulate mostly in liver, kidney, lung, spleen, bone and heart in animal models. Inorganic Pd could induce oxidative stress[39], inhibit DNA and protein synthesis and cause DNA damage in mouse lymphoma cell lines, lead to depression in heart function via a change in cardiomyocyte membrane potential [40] and the like.

7.2. Computational Methodology

Optimized structures of these flavanones shows that Pinocembrin and Pinostrobin has a possible site for metal chelation at 4 C=O and 5-O. According to Leopolidini et.al. [22], this site is the most probable site for metal chelation in flavonoids as it will produce a six membered ring with metal ion at one of the vertices. Flavanones being acidic, tend to be protonated, pinocembrin and pinostrobin were deprotonated at 5-OH and were optimized using B3LYP/ 6-31+ G (d,p) as anion [Fl-O^-]. These anions were then reacted with several metal cations. Complex was optimized using a combination of basis sets. LANL2DZ for the metal and 6-31+G (d,p) for the chelator. Those which form stable ring structures were taken up for further studies. The complexes were also optimized using the hybrid basis sets in aqueous media using the IEF-PCM formalism. We have studied the 1:1 metal-ligand interactions.

Stability of the complex was determined by calculating interaction energy of the complex using the Eq. 1:

$$E_{inter} = E_{complex} - E_{metal\text{-}ion} - N \times E_{flav} \quad (7.1)$$

Here $E_{complex}$ is the energy of the complex, $E_{metal\text{-}ion}$ is the energy of the free metal, N is the number of ligands associated (for monomer N=1) and E_{flav} is the energy of the free deprotonated flavanone molecule.These energies include zero point energy (ZPE) corrections and thermal corrections.

Natural population analysis (NPA) was carried out on all metal-flavanone complex to have a notion of effective nuclear charge prevailing on metals after complex formation.

UV-Visible absorption spectra of the flavonone-metal complexes were studied in polar aqueous media using TDDFT formalism and compared with that of the neutral non-chelated flavanone molecule. We have analyzed absorption bands above 240 nm. Frontier molecular analysis was performed to understand the nature of charge transfer possibly taking place in the metal complexes.

7.3. Results and Discussion

Pinocembrin and Pinostrobin were deprotonated at 5-OH and were optimized as anions using 6-31+G (d, p) basis set. Alpinetin was not considered as there is no free hydroxyl group at C-5 for alpinetin. These anions formed stable complexes with metal cations like Zn^{2+}, Cd^{2+}, Hg^{2+}, Pb^{2+} and Pd^{2+}. These metal ions formed a six membered ring structure linking 4 C=O and 5-O. Monomer complexes with metal and ligand in the ratio 1:1 were analyzed. All these complexes had an overall uni positive charge.

7.3.1 Structural parameters

Table **7.1.** Structural parameters for pinocembrin and pinostrobin complexes with those of aqueous solvents inside the parenthesis.

Pinocembrin metal complex			
Metal ion	$d_{M\text{-}5O}$	$d_{M\text{-}4O}$	$\theta_{O5\text{-}M\text{-}O4}$
Zn^{2+}	1.86 (1.95)	1.90 (2.02)	107.51 (93.40)
Pd^{2+}	1.95 (1.94)	2.02 (1.98)	93.47 (94.64)
Pb^{2+}	2.05 (2.10)	2.14 (2.20)	84.31 (82.28)
Cd^{2+}	2.10 (2.21)	2.15 (2.28)	89.22 (79.47)
Hg^{2+}	2.30 (2.34)	2.41 (2.50)	75.95 (72.96)
Pinostrobin metal complex			
Zn^{2+}	1.86 (1.96)	1.89(2.01)	107.63 (93.30)
Pd^{2+}	1.96 (1.95)	2.00 (1.98)	94.66 (94.15)
Pb^{2+}	2.05 (2.10)	2.14 (2.19)	84.44 (82.34)
Cd^{2+}	2.10 (2.20)	2.15 (2.27)	89.03 (80.56)
Hg^{2+}	2.31 (2.33)	2.42 (2.52)	75.36 (72.56)

Optimized geometries are shown in Figure 7.1. It could be seen that stable positively charged monomer complexes are formed for Zn^{2+}, Cd^{2+}, Hg^{2+}, Pb^{2+} and Pd^{2+}. The important geometrical parameters involved in chelation with the metal would be $d_{M\text{-}5O}$, $d_{M\text{-}4O}$ and $\theta_{O5\text{-}M\text{-}O4}$ for monomers (Table7.1). The values for bond length and bond angles for a particular metal are almost the same for both pinocembrin and pinostrobin. Bond length of the metal – oxygen bond varies in the order Zn-complex < Pd-complex < Pb-complex < Cd-complex < Hg-complex. Aqueous solvents like water also do not alter the geometric parameters of the complex much. Slight variation in the order of variation of bond lengths could be observed.

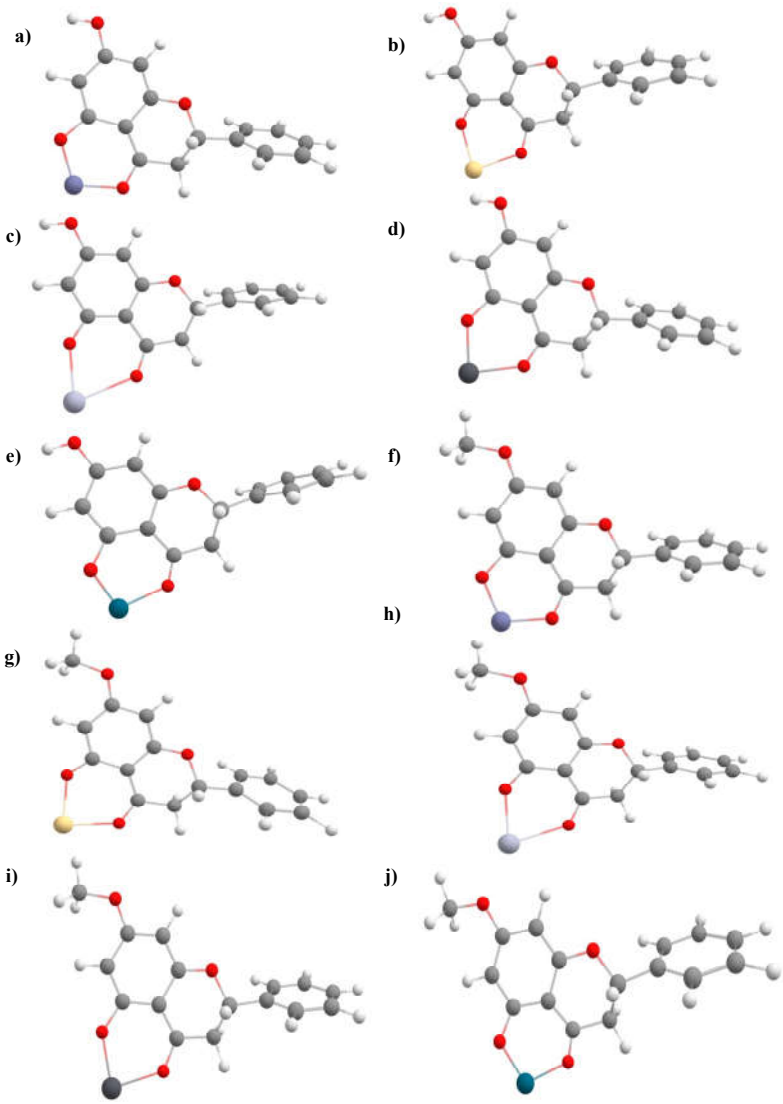

Fig 7.1. Optimized structures of metal flavanone complexes a) pinocembrin-Zn complex b) pinocembrin-Cd c) pinocembrin-Hg d) pinocembrin-Pb e) pinocembrin-Pd f) pinostrobin-Zn complex g) pinostrobin-Cd h) pinostrobin-Hg i) pinostrobin-Pb j) pinostrobin-Pd.

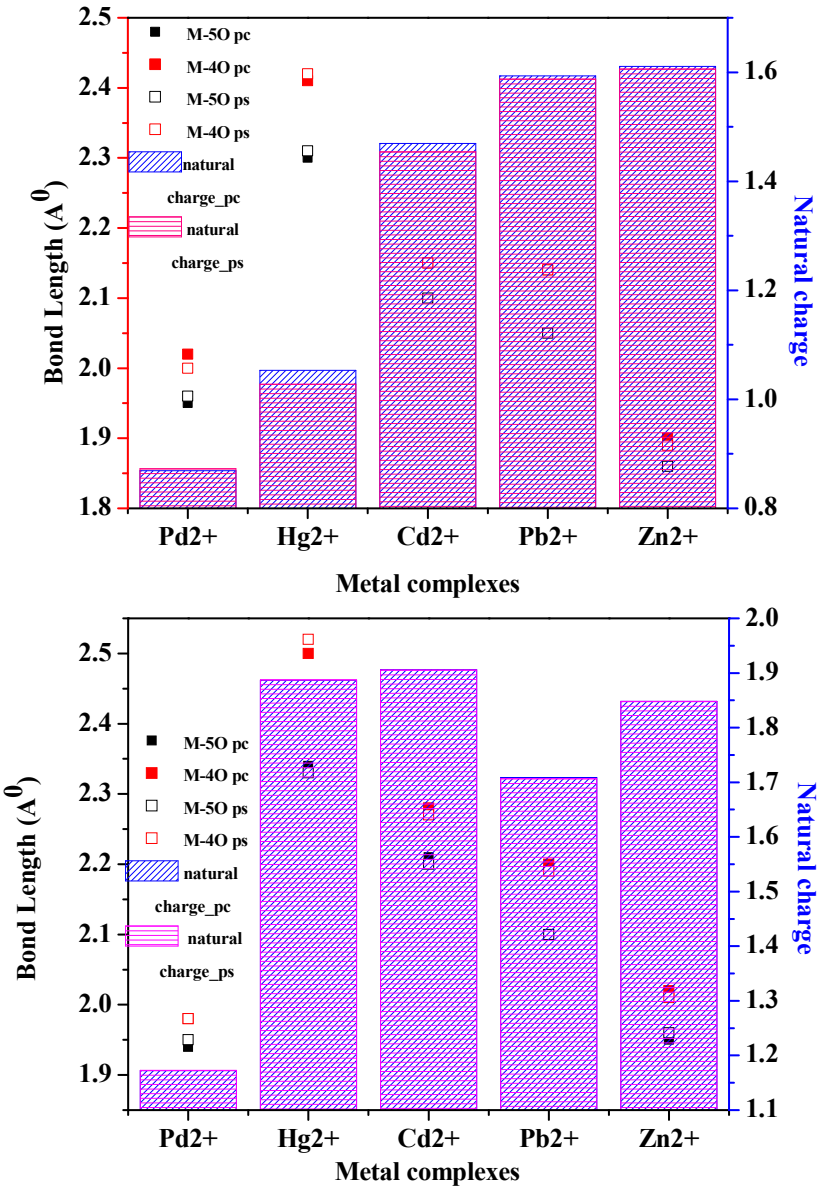

Fig 7.2. Graph depicting variation of bond lengths of M-5O bond and M-4O with natural charge on the metal a) gas phase b) aqueous phase.

Effective nuclear charge on the metal after forming a stable complex was calculated using natural population analysis. The variation of nuclear charge with metal is plotted in Fig. 7.2. It could be seen that natural charge on the metal ion varies as Pd^{2+}< Hg^{2+}< Cd^{2+}< Pb^{2+}< Zn^{2+} in gaseous phase. On comparing the effective nuclear charge of metals with the bond length of M-O bonds, it could be inferred that bond length is inversely proportional to charge on the metal except for Pd^{2+}, which does not show an elongation in M-O bond even though the effective nuclear charge is the lowest. In aqueous solvents, bond length variation follows the same trend as in gaseous phase but it does not have much correlation with the natural charge on the metal.

Table 7.2. Natural charge calculated from NPA analysis on pinocembrin and pinostrobin complexes in gaseous and aqueous phase.

Metal ions	Pinocembrin		Pinostrobin	
	Gas	Aqueous	Gas	Aqueous
Zn^{2+}	1.61	1.85	1.61	1.85
Pb^{2+}	1.59	1.71	1.59	1.71
Cd^{2+}	1.47	1.90	1.45	1.90
Hg^{2+}	1.05	1.89	1.03	1.89
Pd^{2+}	0.87	1.17	0.87	1.17

Table 7.3. Interaction energies of pinocembrin and pinostrobin in gaseous and aqueous phase in units of kcal/mol.

Metal ions	Pinocembrin		Pinostrobin	
	Gas	Aqueous	Gas	Aqueous
Pd^{2+}	-516.81	-105.61	-519.56	-105.96
Zn^{2+}	-417.87	-35.71	-420.09	-35.84
Hg^{2+}	-382.02	-0.40	-384.71	-0.02
Cd^{2+}	-371.20	-13.22	-373.40	-13.15
Pb^{2+}	-369.09	-85.38	-371.31	-85.49

7.3.2. Interaction energies

Interaction energies of the metal-ligand complexes were calculated to quantify the interactions between metal and ligands. The more negative the interaction energy, the strongest the intermolecular chelator – ion interaction. Interaction energies are calculated for complexes in gaseous as well as aqueous media. These are tabulated in Table 7.3.

Interaction energy is found to vary with the central metal ion. For monomer complexes in vaccuo, interaction energy varies as Pd-complex < Zn-complex < Hg-complex < Cd-complex < Pb-complex for both pinocembrin and pinostrobin. This entails that the most stable complexes are those formed between ligands and Pd^{2+} ions. These variations in stability could be correlated to the amount of charge transfer from ligands to metal. Amount of charge transfer could be determined from the difference between the charge on the isolated

cation and the charge on the metal in complexes. The greater the suppression of charge on the metal indicates stronger interaction between ligand and the metal. This difference of charge for different metal complexes is tabulated in Table 7.4. $dQ(M^{n+})$ is plotted alongside interaction energies in Fig. 7.3 a) for monomer complexes in gaseous media and Fig. 7.3 b) for monomer complexes in aqueous media. On examining the $dQ(M^{n+})$ values and interaction energies, it could be understood that in gaseous media the interaction energies decreases with increased suppression of charge on metal except for Zn – complex. This shows that more the net charge $dQ(M^{n+})$ on metal more stable is the complex. But in the case of zinc complexes although the suppression of charge is weak, the complexes formed shows favourably good interaction energies.

Stability of complexes in physiologically relevant polar media is important for application purposes. Interaction energy in aqueous complexes follow a different trend, it varies as Pd-complex < Pb-complex < Zn-complex <Cd-complex < Hg-complex. The charge transfer in aqueous media is also different from that of gaseous media. This could be due to solvent effects. Lead shows more efficient charge transfer in polar media and the complex formed is also comparatively more stable. On the contrary, Mercury complexes show very weak interaction energies aqueous media. Correlation between net charge and interaction energies is very smooth in solvent phase (Fig 7.3 b).

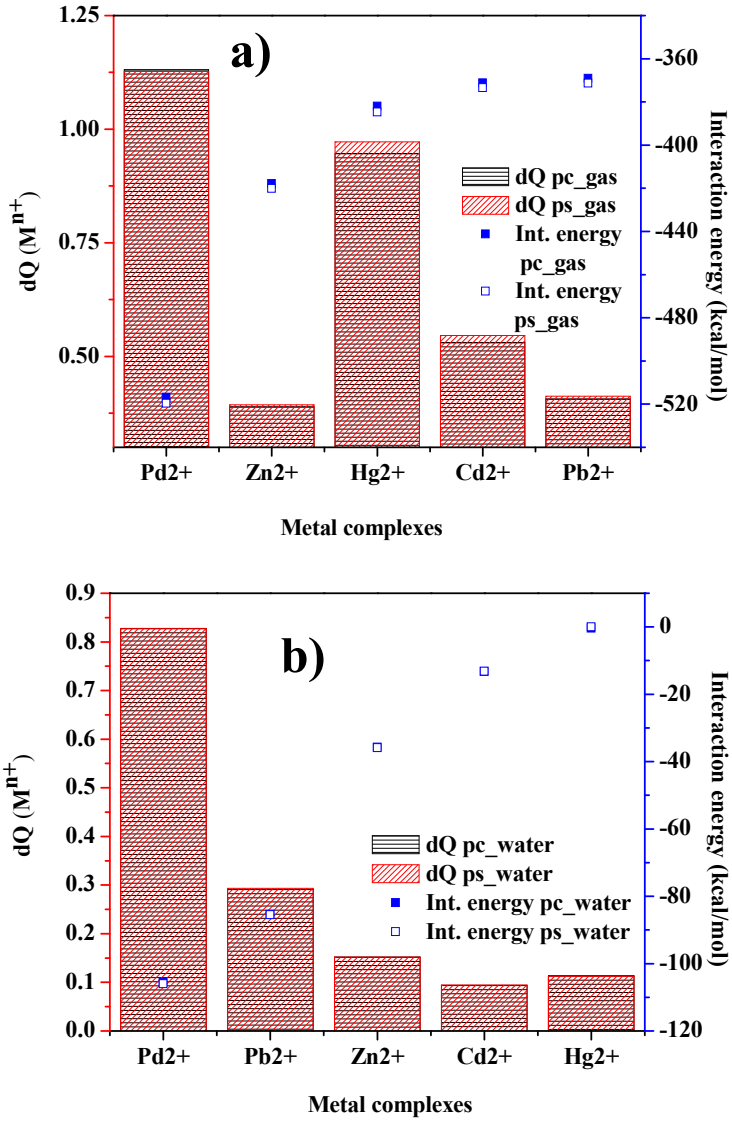

Fig. 7.3. Graphs showing correlation between net charge on the metal and interaction energies in a) gas phase and b) aqueous phase.

Table 7.4. Net charge (dQ) calculated for pinocembrin and pinostrobin complexes in gaseous and aqueous phase.

Metal ions	Pinocembrin		Pinostrobin	
	Gas	Aqueous	Gas	Aqueous
Zn^{2+}	0.39	0.15	0.39	0.15
Pd^{2+}	0.41	0.83	0.41	0.83
Cd^{2+}	0.53	0.09	0.54	0.09
Hg^{2+}	0.95	0.11	0.97	0.11
Pb^{2+}	1.13	0.29	1.13	0.29

From these structural studies, we could conclude that the interaction energies of complexes are related to the charge transfer from ligand to metal. As the charge transfer increases, net charge on metal dQ (M^{n+}) decreases and the interaction energy becomes more and more negative making the complex more stable. From crystal field theory's stand point interaction between metal and ligand is partly electrostatic in nature whereas according to molecular orbital theory, atomic overlap is possible for orbitals of metals and flavonoids having same.

7.3.3. Optical signatures:

Complexation of flavonoids with metals and the structural changes associated with it will be reflected in optical spectroscopy. Optical signatures of the molecules under study were calculated using TDDFT calculations for wavelengths above 240 nm. Upon complexation with metals, the bands in the absorption spectra show

significant changes. We have studied the optical properties of these complexes in polar aqueous media as it is physiologically significant.

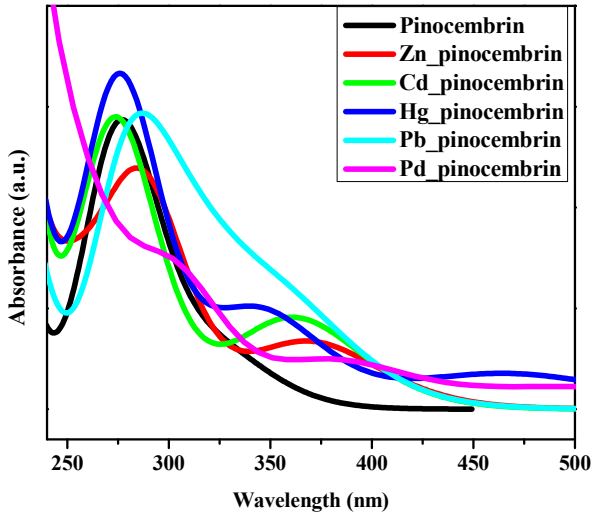

Fig 7.4. Absorption spectra of flavanone and flavanone metal complexes of pinocembrin

Flavanones unlike flavonoids are characterized by a broad absorption between 270 nm and 290 nm (Band II) and a small shoulder around 320 nm (Band I). On complexation, the bands undergo significant changes in position. The peaks are shifted to longer wavelength and the shoulder at 320 nm became more prominent. The absorption band at ~277 nm for pinocembrin is red shifted in the order: Hg-complex < Pb-complex < Zn-complex < Pd-complex. An exemption here is that of cadmium-pinocembrin complex were the band undergoes no shift or can be said to have slight blue shift (275.33 nm compared to 276.94 nm for pinocembrin). Hg-complex also does not show any considerable red shift compared to other metal complexes. The shoulder observed in pinocembrin at 325.83 nm becomes more pronounced and is also red shifted in metal complexes.

The extent of red shift varies in the order Hg-complex < Pb-complex <Cd-complex < Zn-complex < Pd-complex. Here Pb-complex also has a peak of comparable oscillatory strength at 317 nm. This red shift in the absorption bands of metal complexes may be attributed to the extended electron delocalization observed in these complexes due to the formation of a fourth ring involving the metal [20].

Lower energy transitions in all complexes are predominantly due to HOMO to LUMO transitions and it keeps shifting with change in metal. Examining the different orbitals involved we could see that the HOMOs are centered mainly on A and C rings of the flavanone molecule whereas LUMO has a large lobe centered on the metal. Only exception being palladium complex, in which there are lobes on the metal in both HOMO and LUMO but there is an increase in size of the lobe in LUMO. This indicates that these higher wavelength transitions might be due to charge transfer from ligand to metal. But the oscillatory strength of these transitions are relatively low.

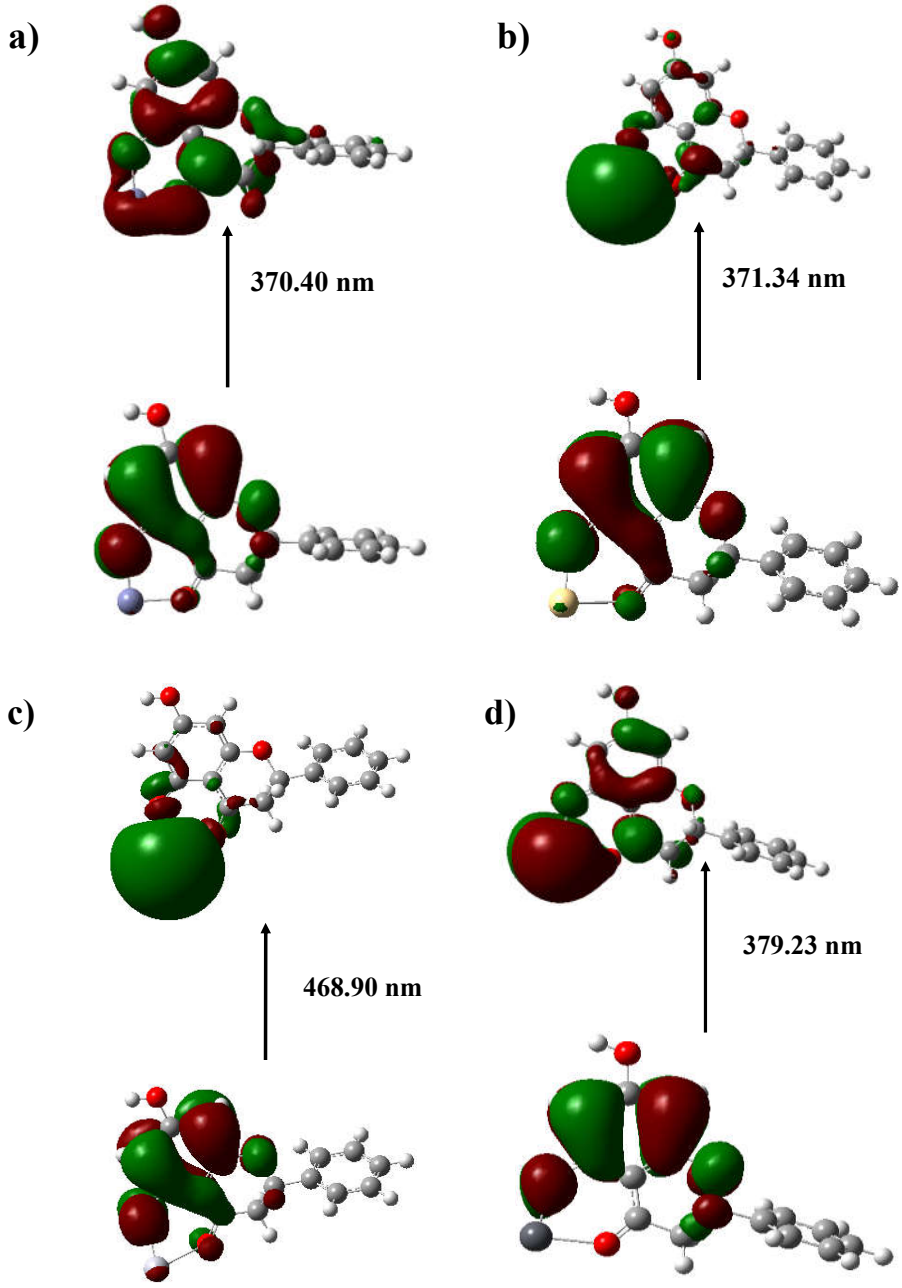
a)
370.40 nm
b)
371.34 nm
c)
468.90 nm
d)
379.23 nm

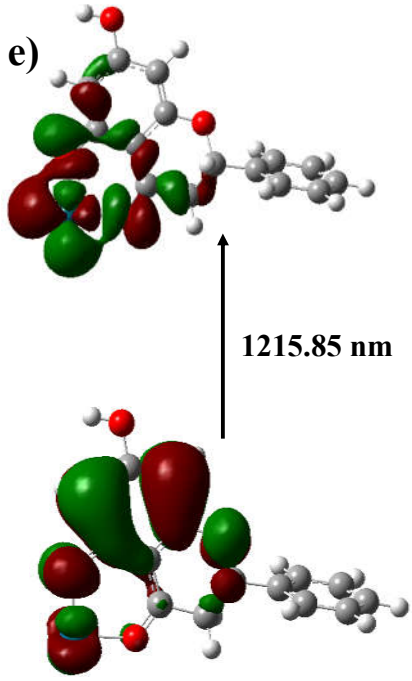

Fig 7.5. Frontier molecular orbitals involved in the transition at maximum wavelength of pinocembrin complexes with a) Zinc b) Cadmium c) Mercury d) Lead and e) Palladium complexes

Table 7.5. Theoretical absorption wavelength (nm), energy (eV), MOs involved, % contribution and oscillator strengths of metal complexes of pinocembrin.

	Pinocembrin				
	Wavelength (nm)	Energy (eV)	MO involved	%contribution	Oscillator strength (f)
Zn	252.10	4.92	H-2->L+1	45.87	0.1107
	289.00	4.29	H-1->L	79.32	0.2171
	370.40	3.35	H->L	97.36	0.0800
Cd	260.66	4.76	H-3->L+1	49.92	0.0537

	275.32	4.50	H-1->L+1	55.02	0.2952
	361.21	3.43	H->L+1	93.92	0.0947
	371.34	3.34	H->L	96.28	0.0158
Hg	263.36	4.71	H-5->L	53.71	0.0488
	277.95	4.46	H-1->L+1	75.21	0.3110
	344.10	3.60	H->L+1	67.95	0.1114
	468.90	2.64	H->L	98.06	0.0423
Pb	279.82	4.43	H-3->L+1	52.37	0.2286
	283.60	4.37	H-2->L+1	51.36	0.0449
	317.04	3.91	H-1->L	70.41	0.1202
	356.90	3.47	H->L+1	87.96	0.0960
	379.23	3.27	H->L	89.57	0.0207
Pd	248.46	4.99	H-12->L	30.68	0.1410
	308.33	4.02	H-1->L+1	48.75	0.0982
	383.87	3.23	H->L+1	95.60	0.0559
	1215.85	1.02	H->L	77.58	0.0011

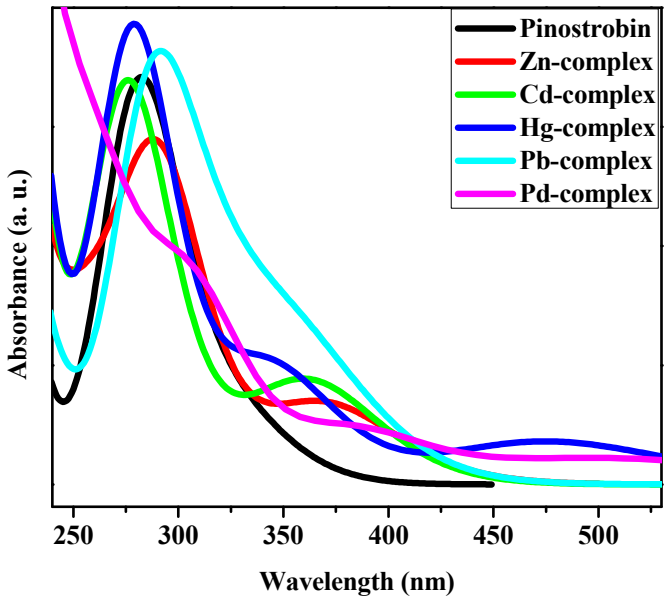

Fig 7.6. Absorption spectra of flavanone and flavanone metal complexes of pinostrobin

Pinostrobin metal complexes show absorbance characteristics similar to that of pinocembrin metal complexes. The absorption band at 281.76 nm for free pinostrobin is red shifted in Zn-complex, Pd-complex and Pb-complex in the order: Pb-complex< Zn-complex< Pd-complex. Hg-complex and Cd-complex are blue shifted slightly. The shoulder at 327.31 nm observed in pinostrobin becomes more pronounced and is red shifted in the order: Hg-complex< Pb-complex< Cd-complex < Zn-complex and Pd-complex. Pb-complex shows a peak of comparable oscillatory strength at 324.34 nm as well. Anamolous shifting of absorption bands around 270 nm to lower wavelength in case of Cd-complex and Hg-complex may be due to longer M-O bond length in these complexes which may lead to poorer delocalization.

Table 7.6. Theoretical absorption wavelength (nm), energy (eV), MOs involved, % contribution and oscillator strengths of metal complexes of pinostrobin.

	Pinostrobin				
	Wavelength (nm)	Energy (eV)	MO involved	%contribution	Oscillator strength (f)
Zn	254.53	4.87	H-2->L+1	42.09	0.1221
	281.76	4.40	H-1->L+1	91.30	0.0420
	291.37	4.26	H-1->L	69.94	0.2406
	297.65	4.16	H-4->L	48.37	0.0524
	370.65	3.34	H->L	96.61	0.0805
Cd	276.02	4.49	H-1->L+1	48.86	0.3550
	297.11	4.17	H-2->L	43.82	0.0507
	361.14	3.43	H->L+1	93.96	0.0935
	374.13	3.31	H->L	96.71	0.0129

Hg	268.22	4.62	H-6->L	84.10	0.0628
	280.44	4.42	H-1->L+1	76.44	0.3563
	343.61	3.61	H->L+1	70.10	0.1151
	477.71	2.60	H->L	98.19	0.0437
Pb	242.38	5.12	H-4->L+1	68.62	0.0475
	286.44	4.33	H-1->L+1	35.94	0.2612
	293.23	4.23	H-1->L+1	40.56	0.0889
	324.34	3.82	H-1->L	89.07	0.1204
	359.16	3.45	H->L+1	85.80	0.0972
	379.53	3.27	H->L	86.70	0.0230
Pd	247.82	5.00	H-13->L	53.30	0.0465
	253.30	4.89	H-11->L	55.32	0.1311
	271.04	4.57	H-9->L	53.37	0.0602
	275.36	4.50	H-5->L+1	67.86	0.0827
	310.57	3.99	H-1->L+1	72.78	0.1532
	384.52	3.22	H->L+1	94.09	0.0531
	1246.75	0.99	H->L	78.64	0.0008

Similar to pinocembrin, lower energy transition in pinostrobin-metal complexes are predominantly due to HOMO to LUMO transition. In almost all complexes HOMOs are centered on A and C rings, whereas LUMO is extended to the ring containing metal as well. The exception here is palladium complex, in which HOMOs and LUMOs have density on metal. But on comparison, LUMO lobes are greater in size compared to HOMO. These frontier molecular pictures is an indication that ligand to metal charge transfer is possible in pinostrobin metal complexes also.

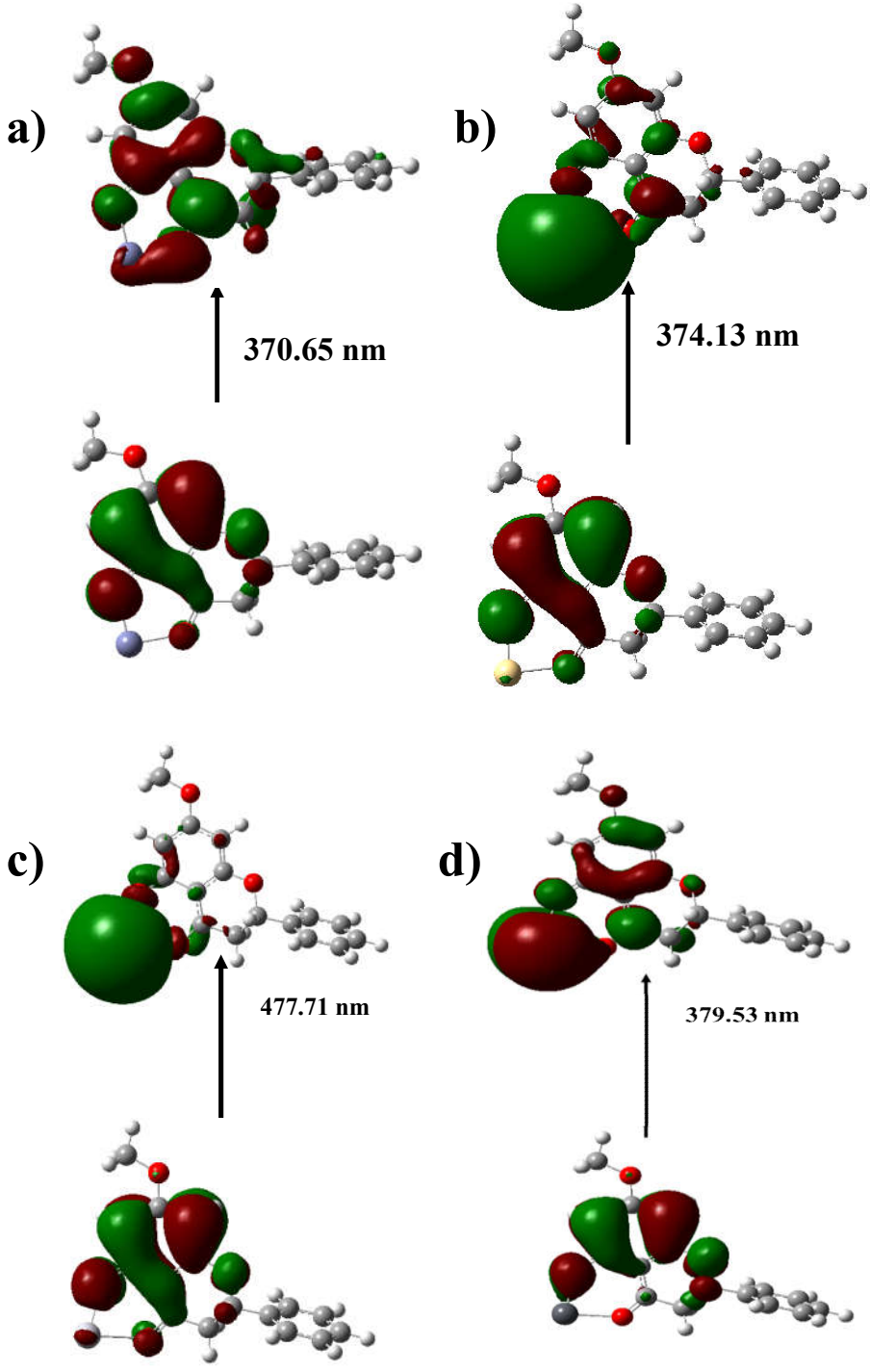
a)
370.65 nm
b)
374.13 nm
c)
477.71 nm
d)
379.53 nm

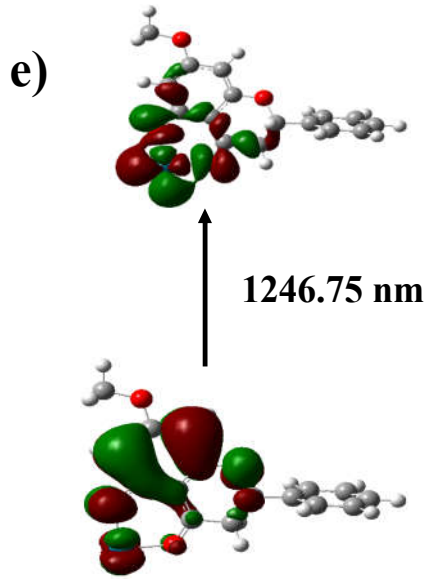

Fig 7.7. Frontier molecular orbitals involved in the intense transition of pinostrobin complexes with a) Zinc b) Cadmium c) mercury d) Lead and e) Palladium complexes

7.4. Conclusions

Metal complexes of flavanone molecules pinocembrin and pinostrobin are investigated using DFT calculation. The metals subjected to study were zinc, cadmium, mercury, palladium and lead. The flavanone molecules showed favorable interaction with heavy metals in gaseous and aqueous media. The strongest interaction was towards palladium metal in physiologically relevant aqueous media and least was towards mercury. The complexes showed characteristic absorption bands in the UV- visible region. On analyzing the orbitals associated with lower energy transitions, ligand to metal charge transfer is largely evident on most of the metal complexes. These antioxidant flavanones may also be capable of forming complexes of

higher co-ordination number 1:2, 1:3 (metal: ligand) geometry or metal: ligand: solvent combination etc. which might be more stable. The fact that flavanones are capable of engaging in favorable interaction with metal could be exploited for metal intoxication purposes.

References

[1] S.J.S. Flora, V. Pachauri, Int. J. Environ. Res. Public Heal. 7 (2010) 2745–2788.

[2] O. Andersen, Chem. Rev. 99 (1999) 2683–2710.

[3] R. Peters, L. Stocken, R. Thompson, Nature 156 (1945) 616–619.

[4] L. Fournier, G. Thomas, R. Garnier, A. Buisine, P. Houze, F. Pradier, Med. Toxicol. 3 (1988) 499–504.

[5] V. Gersl, R. Hrdina, J. Vavrova, M. Holeckova, V. Palicka, J. Vogkova, Y. Mazurova, J. Bajgar, Acta. Medica. 40 (1997) 3–8.

[6] B. Guldager, P.J. Jorgensen, P. Grandjean, Clin. Chem. 42 (1996) 1938–1942.

[7] C.R. Angle, Chelation Therapies for Metal Intoxication in Toxicology of Metals, CRC Press, Boca Raton, FL, USA, 1996.

[8] S.J.S. Flora, R. Bhattacharya, R. Vijayaraghavan, Fund. Appl. Toxicol. 25 (1995) 233–240.

[9] D. Mishra, A. Mehta, S.J.S. Flora, Chem. Res. Toxicol. 21 (2008) 400–407.

[10] S.J.S. Flora, G. Saxena, A. Mehta, J. Pharmacol. Exp. Ther. 322 (2007) 108–116.

[11] G. Saxena, S.J.S. Flora, J. Pharm. Pharmacol. 58 (2006) 547–559.

[12] S.J.S. Flora, M. Pande, G.M. Kannan, A. Mehta, Cell. Mol. Biol. 50 (2004) 543–551.

[13] M. Pande, S.J.S. Flora, Toxicology 177 (2002) 187–196.

[14] D. Mishra, S.J.S. Flora, Biol. Trace Elem. Res. 122 (2008) 137–147.

[15] M.M. Kasprzak, J. Ochocki, RSC Adv., 5 (2015) 45853–45877.

[16] F.B.A. El Amrani, L. Perello, J.A. Real, M. Gonzalez-Alvarez, G. Alzuet, J. Borras, S. Garcia-Granda, J. Montejo-, Bernado, J. Inorg. Biochem. 100 (2006) 1208–1218.

[17] E. Balogh-Hergovich, G.S. and G. Argay, Chem. Commun. (1991) 551–552.

[18] E. Balogh-Hergovich, J. Kaizer, G. Speier, G. Argay, L. Parkanyi, Dalt. Trans. (1999) 3847–3854.

[19] E. Pieniazek, J. Kalembkiewicz, M. Dranka, E. Woznicka, J. Inorg. Biochem 141 (2014) 180–187.

[20] J. Ren, S. Meng, C.E. Lekka, E. Kaxiras, J. Phys. Chem. B 112 (2008) 1845–1850.

[21] C.E. Lekka, J. Ren, S. Meng, E. Kaxiras, J. Phys. Chem. B 113 (2009) 6478–6483.

[22] M. Leopoldini, N. Russo, S. Chiodo, M. Toscano, J. Agric. Food Chem. 54 (2006) 6343–6351.

[23] A. Amat, C. Clementi, C. Miliani, A. Romani, A. Sgamellotti, S. Fantacci, Phys. Chem. Chem. Phys. 12 (2010) 6672– 6684.

[24] M. Brown, J. Thom, G. Orth, P. Cova, J. Juarez, Arch Env. Heal. 8 (1964) 657–60.

[25] L.M. Plum, L. Rink, H. Haase, Int J Env. Res Public Heal. 7 (2010) 1342–1365.

[26] IARC, International Agency for Research on Cancer, Beryllium, Cadmium, Mercury, and Exposures in the Glass Manufacturing Industry, IARC Scientific Publications, Lyon, France, 1993.

[27] R.A. Goyer, M.G. Cherian, Renal Effects of Metals in Metal Toxicology, Academic Press, San Diego, CA, USA, 1995.

[28] S.A. Sheweita, Int. J. Toxicol. 17 (1998) 383–392.

[29] C. Kelley, D.E. Sargent, J.K. Uno, Curr. Pharm. Des. 5 (1999) 229–240.

[30] M. Waisberg, P. Joseph, B. Hale, D. Beyersmann, Toxicology 192 (2003) 95–117.

[31] S. Amler, Contemp. Pediatr. 19 (2002) 37–56.

[32] J.F. Risher, R.A. Nickle, S.N. Amler, Int. J. Hyg. Environ. Hlth. 206 (2003) 371–379.

[33] R.A. Goyer, T.W. Clarkson, Toxic Effects of Metals in Casarett & Doull's Toxicology: The Basic of Poisons, 6th ed., McGraw-Hill, New York, NY, USA, 2001.

[34] G. Flora, D. Gupta, A. Tiwari, Interdiscip. Toxicol. 5 (2012) 47–58.

[35] K Kalia, S.J. Flora., J Occup Heal. 47 (2005) 1–21.

[36] J.M. Pearce, Eur Neurol 57 (2007) 118–9.

[37] S.J.S. Flora, G. Flora, G. Saxena, Environmental Occurrence, Health Effects and Management of Lead Poisoning in Lead, Elsevier B.V., Amsterdam, 2006.

[38] M. Hosseini, I. Jafarian, S. Farahani, R. Khodadadi, S. Tagavi, P. Naserzadeh, A. Mohammadi-Bardbori, N. Arghavanifard, Metallomics. 8 (2016) 252–9.

[39] M. Schmid, S. Zimmermann, H.F. Krug, B. Sures, Environ. Int. 33 (2007) 385.

[40] T. Peric, V.L. Jakovljevic, V. Zivkovic, J. Krkeljic, Z.D. Petrovic, D. Simijonovic, S. Novokmet, D.M. Djuric, S.M. Jankovic, Med Chem 8 (2012) 9.

Chapter 8

Multi-targeted bioactivity: an inverse docking study

8.1. Introduction

Recent advances in the field of genomics have resulted in a paradigm shift in the focus of drug discovery from single-target interaction to comparative analysis of multi-targets network [1]. To map the ligand- target profiling space globally, there is a need to develop fast and efficient methods of screening. High throughput *in vitro* screening of small molecules is unaffordable as it is laborious and time-consuming. In this scenario, *in silico* target profiling is emerging as an efficient alternative to find out therapeutic indications of new molecules as well as existing drugs [2]. The development of multi-target drugs may allow to treat various diseases which involve multiple pathogenic effects like cancer, cardiovascular diseases and neurological disorders [3].

Inverse docking is one such method originally developed by Chen *et. al.*[4] It refers to computational docking of small molecules of interest to a library of receptor structures. Inverse docking can select potential targets of an active compound from a given protein database [5,6]. Given a multi-faceted nature of biological nature of a pharmacologically active compound, it can provide new insights to explain the mechanism of action [7].

PharmMapper [8–10] is one such server which probes the potential ligand binding sites stored in potential drug target database (PDTD) [8]. Pharmacophore is the spatial arrangement which enables a molecule to interact with the receptor. Pharmacophores have been isolated from protein-ligand 3D structures and are stored in a repository. This provides a pool of potential target information required for 'target fishing' [11]. Conventional docking is the method of docking multiple ligands against a single target. It requires optimization of docking parameters which involve preparation of protein target and ligand as pdbqt files, specification of grid parameters etc. and is an involved process [12]. Inverse docking will be very useful as an initial step to screen out potential targets which can then be studied exclusively.

The flavanone molecules studied here namely pinocembrin, pinostrobin and alpinetin were very common in ancient medicine. These had multiple therapeutic implications as anti-bacterial effect, anti-microbial effects, anti-oxidant nature, neuroprotective effects, anti-inflammatory effects and even anti-tumor and anti-cancer characteristics [13–17]. Anti-oxidant action of flavanones is also well

characterized. Apart from this, neuroprotective, anti-inflammatory and anti-cancer effects shown by flavanones are likely to be mediated through interactions with specific proteins. To analyze potential protein targets for these molecules, we performed inverse docking followed by detailed analysis of binding characteristics of ligands with highest binding energies.

8.2. Computational Methodology

Optimized structures of the molecules namely pinocembrin, pinostrobin and alpinetin were converted to mol2 by using the OpenBabel. These were uploaded in mol2 format to the online web server PharmMapper [18]. This online server has an inhouse repository comprising of almost 7000 pharmacophore models isolated from available 3D structures of proteins called PharmTargetDB. Each of the small molecule input is aligned to pharmacophore models and the fit-score is calculated and recorded. All the fit scores are compared against each other to generate a final list of potential protein targets in the decreasing order of their fit score. From the given list of protein targets human protein targets were sorted out and arranged in the decreasing order of their fit-score as shown in Table 8.1. Targets which have a fitscore of 3.000 and above for each of the ligands were mostly subjected to detailed docking analysis using Autodock Vina. Missing residues were reconstructed using SwissPDB [19,20], water molecules were deleted but in some cases relevant water molecules in the active site were retained during docking. For proteins with no docked inhibitor in the PDB active site was selected from literature. Binding

energy values are obtained from the software in kcal/mol. It is then converted to inhibition constant using the expression:

$$K_i = e^{\Delta G/RT} \quad (8.1)$$

where R is gas constant and temperature is 298.15 K.

8.3. Results and Discussion

8.3.1. Inverse docking

Optimized structures of the molecules namely pinocembrin, pinostrobin and alpinetin were uploaded in the mol2 format in PharmMapper server. PharmMapper server undertakes several steps to reach the final output. The first step is the ligand initialization and preparation following that ligand as well as target pharmacophore model features are subjected to triangulation. After pair wise alignment and GA post optimization, solution filtering and ranking of the output is done [8]. Maximum number of target hits was set to 300. Of these 300 compatible protein targets, around 60 were human protein targets. A parameter to indicate the efficiency of interaction is also given in the output termed as the fit score. These targets were identified and are listed in descending order of fit score. The different classes of proteins included were transferases, Oxido reductases, protein kinases, hydrolases etc. Of the several types of proteins listed, human targets were separated and are listed in Table 8.1.

Table 8.1. Table indicating the human targets predicted via inverse docking using PharmMapper for pinocembrin, pinostrobin and alpinetin with protins selected for further analysis highlighted in yellow.

PINOCEMBRIN							
Sl. No.	Pharma Model	Fit	Hydrophobic	HB Acceptor	HB Donor	Name	Class
1.	1XO2	3.811	2	3	0	Cell division protein kinase 6	CELL CYCLE/TRANSFERASE
2.	1L9N	3.772	3	4	1	Protein-glutamine gamma-glutamyltransferase E	TRANSFERASE
3.	2P2I	3.342	4	1	1	Vascular endothelial growth factor receptor 2	TRANSFERASE
4.	1S2A	3.207	4	3	0	Aldo-keto reductase family 1 member C3	OXIDOREDUCTASE
5.	1WMA	3.006	2	2	1	Carbonyl reductase [NADPH] 1	OXIDOREDUCTASE
6.	3BM9	2.985	2	2	1	Heat shock protein HSP 90-alpha	CHAPERONE
7.	1K59	2.976	0	4	0	Angiogenin	HYDROLASE
8.	2HCK	2.974	1	0	2	Tyrosine-protein kinase HCK	TRANSFERASE
9.	1UPV	2.966	5	1	0	Oxysterols receptor LXR-beta	RECEPTOR
10.	1P5Z	2.945	1	1	3	Deoxycytidine kinase	TRANSFERASE
11.	1LHO	2.934	4	1	1	Sex hormone-binding globulin	TRANSPORT PROTEIN
12.	1XBB	2.926	5	0	1	Tyrosine-protein kinase SYK	TRANSFERASE
13.	1OG5	2.906	3	3	0	Cytochrome P450 2C9	ELECTRON TRANSPORT
14.	2OSF	2.902	1	0	2	Carbonic anhydrase 2	LYASE
15.	3BLR	2.894	2	2	0	Cyclin-T1	TRANSCRIPTION

16.	1KBO	2.884	3	0	1	NAD(P)H dehydrogenase [quinone] 1	OXIDOREDUCTASE
17.	1RTK	2.88	1	1	2	Complement factor B	HORMONE/GROWTH FACTOR
18.	2AMB	2.873	3	1	1	Androgen receptor	HORMONE/GROWTH FACTOR RECEPTOR
19.	1A7A	2.865	0	3	2	Adenosylhomocysteinase	HYDROLASE
20.	1VJ5	2.856	3	1	1	Epoxide hydrolase 2	HYDROLASE
21.	13GS	2.843	3	2	0	Glutathione S-transferase P	COMPLEX (TRANSFERASE/SULFASALAZINE)
22.	1Z6E	2.826	3	1	1	Coagulation factor X	HYDROLASE
23.	1Y2C	2.816	4	1	0	cAMP-specific 3,5-cyclic phosphodiesterase 4D	HYDROLASE
24.	1ISG	2.803	0	5	1	ADP-ribosyl cyclase 2	HYDROLASE
25.	1B3O	2.799	0	3	1	Inosine-5-monophosphate dehydrogenase 2	DEHYDROGENASE
26.	1RKP	2.792	1	2	0	cGMP-specific 3,5-cyclic phosphodiesterase	HYDROLASE
27.	1LD7	2.79	2	1	0	Protein farnesyltransferase/geranylgeranyl transferase type-1 subunit alpha	TRANSFERASE
28.	1R0P	2.786	4	2	0	Hepatocyte growth factor receptor	TRANSFERASE
29.	1YRS	2.772	3	0	2	Kinesin-like protein KIF11	CELL CYCLE
30.	1D3H	2.765	3	3	0	Dihydroorotate dehydrogenase, mitochondrial	OXIDOREDUCTASE
31.	1P0I	2.76	1	2	0	Cholinesterase	HYDROLASE

32.	1WLJ	2.732	0	4	1	Interferon-stimulated gene 20 kDa protein	HYDROLASE
33.	1PWM	2.696	2	2	0	Aldose reductase	OXIDOREDUCTASE
34.	1YXU	2.694	0	4	0	Proto-oncogene serine/threonine-protein kinase Pim-1	TRANSFERASE
35.	3CQU	2.678	2	1	1	RAC-alpha serine/threonine-protein kinase	TRANSFERASE
36.	2OCF	2.677	2	1	0	Estrogen receptor	HORMONE/GROWTH FACTOR
37.	1C5O	2.64	1	2	0	Prothrombin	BLOOD CLOTTING
38.	1C86	2.64	1	2	0	Tyrosine-protein phosphatase non-receptor type 1	HYDROLASE
39.	1V45	2.636	0	3	1	Purine nucleoside phosphorylase	TRANSFERASE
40.	1HKC	2.628	0	3	2	Hexokinase-1	PHOSPHOTRANSFERASE
41.	1F92	2.55	1	2	1	Urokinase-type plasminogen activator	HYDROLASE
42.	1M6W	2.547	3	0	1	Alcohol dehydrogenase class-3	OXIDOREDUCTASE
43.	1E5A	2.53	3	1	0	Transthyretin	TRANSPORT(THYROXINE)
44.	1U4D	2.528	0	2	3	Activated CDC42 kinase 1	TRANSFERASE
45.	3CHO	2.484	2	1	0	Leukotriene A-4 hydrolase	HYDROLASE
46.	2JNP	2.457	2	2	1	Stromelysin-1	HYDROLASE
47.	1M9J	2.443	2	1	1	Nitric oxide synthase, endothelial	OXIDOREDUCTASE
48.	2BKZ	2.424	2	2	0	Cyclin-A2	TRANSFERASE/COMPLEX
49.	1MMQ	2.398	1	2	2	Matrilysin	METALLOPROTEASE
50.	1OJA	2.37	1	1	1	Amine oxidase [flavin-containing]	OXIDOREDUCTASE

						B	
51.	1Q41	2.363	2	2	1	Glycogen synthase kinase-3 beta	TRANSFERASE
52.	1SOJ	2.326	1	2	0	cGMP-inhibited 3,5-cyclic phosphodiesterase B	HYDROLASE
53.	1JJ9	2.284	2	2	0	Neutrophil collagenase	HYDROLASE
54.	2OVH	2.282	3	1	0	Progesterone receptor	TRANSCRIPTION
55.	1AGW	2.278	2	1	1	Basic fibroblast growth factor receptor 1	PROTEIN KINASE
56.	2H96	2.27	3	1	0	Mitogen-activated protein kinase 8	TRANSCRIPTION
57.	1XLZ	2.26	3	1	0	cAMP-specific 3,5-cyclic phosphodiesterase 4B	HYDROLASE
58.	1HAK	2.189	3	1	0	Annexin A5	CALCIUM/PHOSPHOLIPID-BINDING
59.	2OI0	2.179	3	1	0	ADAM 17	HYDROLASE
60.	1CSB	2.091	1	3	0	Cathepsin B	HYDROLASE (THIOL PROTEASE)
61.	2CGW	2.055	1	1	1	Serine/threonine-protein kinase Chk1	TRANSFERASE
PINOSTROBIN							
1.	1L9N	3.818	3	4	1	Protein-glutamine gamma-glutamyltransferase E	TRANSFERASE
2.	1XO2	3.787	2	3	0	Cell division protein kinase 6	CELL CYCLE/TRANSFERASE
3.	2P2I	3.348	4	1	1	Vascular endothelial growth factor receptor 2	TRANSFERASE
4.	1S2A	3.215	4	3	0	Aldo-keto reductase family 1	OXIDOREDUCTASE

						member C3	
5.	3BM9	3.152	2	2	1	Heat shock protein HSP 90-alpha	CHAPERONE
6.	1QCF	3.142	3	3	1	Tyrosine-protein kinase HCK	TYROSINE KINASE
7.	1WMA	3.084	2	2	1	Carbonyl reductase [NADPH] 1	OXIDOREDUCTASE
8.	1UPV	2.98	5	1	0	Oxysterols receptor LXR-beta	RECEPTOR
9.	1K59	2.975	0	4	0	Angiogenin	HYDROLASE
10.	1OG5	2.945	3	3	0	Cytochrome P450 2C9	ELECTRON TRANSPORT
11.	1LHN	2.898	4	1	1	Sex hormone-binding globulin	TRANSPORT PROTEIN
12.	2AMB	2.897	3	1	1	Androgen receptor	HORMONE/GROWTH FACTOR RECEPTOR
13.	1XBB	2.877	5	0	1	Tyrosine-protein kinase SYK	TRANSFERASE
14.	1VJ5	2.874	3	1	1	Epoxide hydrolase 2	HYDROLASE
15.	1A7A	2.868	0	3	2	Adenosylhomocysteinase	HYDROLASE
16.	3BLR	2.86	2	2	0	Cyclin-T1	TRANSCRIPTION
17.	13GS	2.841	3	2	0	Glutathione S-transferase P	COMPLEX (TRANSFERASE/SULFASALAZINE)
18.	1R0P	2.812	4	2	0	Hepatocyte growth factor receptor	TRANSFERASE
19.	1LD7	2.811	2	1	0	Protein farnesyltransferase/geranylgeranyl transferase type-1 subunit alpha	TRANSFERASE
20.	1Z6E	2.802	3	1	1	Coagulation factor X	HYDROLASE
21.	1RKP	2.787	1	2	0	cGMP-specific 3,5-cyclic phosphodiesterase	HYDROLASE
22.	1P0I	2.786	1	2	0	Cholinesterase	HYDROLASE
23.	1Y2C	2.781	4	1	0	cAMP-specific 3,5-cyclic	HYDROLASE

						phosphodiesterase 4D	
24.	1B3O	2.779	0	3	1	Inosine-5-monophosphate dehydrogenase 2	DEHYDROGENASE
25.	1YXU	2.728	0	4	0	Proto-oncogene serine/threonine-protein kinase Pim-1	TRANSFERASE
26.	1RW8	2.723	5	1	0	TGF-beta receptor type-1	TRANSFERASE
27.	1WLJ	2.721	0	4	1	Interferon-stimulated gene 20 kDa protein	HYDROLASE
28.	1PWM	2.695	2	2	0	Aldose reductase	OXIDOREDUCTASE
29.	3CQU	2.679	2	1	1	RAC-alpha serine/threonine-protein kinase	TRANSFERASE
30.	1JAK	2.663	0	2	3	Calcium-activated potassium channel subunit beta-2	HYDROLASE
31.	1C5O	2.657	1	2	0	Prothrombin	BLOOD CLOTTING
32.	1V45	2.652	0	3	1	Purine nucleoside phosphorylase	TRANSFERASE
33.	1HKC	2.63	0	3	2	Hexokinase-1	PHOSPHOTRANSFERASE
34.	1C86	2.624	1	2	0	Tyrosine-protein phosphatase non-receptor type 1	HYDROLASE
35.	1YRS	2.62	3	0	2	Kinesin-like protein KIF11	CELL CYCLE
36.	1HLC	2.62	0	3	3	Galectin-2	LECTIN
37.	1FLS	2.619	4	1	1	Collagenase 3	HYDROLASE
38.	1F92	2.597	1	2	1	Urokinase-type plasminogen activator	HYDROLASE
39.	2OCF	2.574	2	1	0	Estrogen receptor	HORMONE/GROWTH FACTOR
40.	3BBT	2.552	5	1	0	Receptor tyrosine-protein kinase erbB-4	TRANSFERASE

41.	1KBO	2.518	3	0	1	NAD(P)H dehydrogenase [quinone] 1	OXIDOREDUCTASE
42.	1E5A	2.5	3	1	0	Transthyretin	TRANSPORT(THYROXINE)
43.	1M9J	2.479	2	1	1	Nitric oxide synthase, endothelial	OXIDOREDUCTASE
44.	2JNP	2.462	2	2	1	Stromelysin-1	HYDROLASE
45.	2BKZ	2.432	2	2	0	Cyclin-A2	TRANSFERASE/COMPLEX
46.	1OJA	2.422	1	1	1	Amine oxidase [flavin-containing] B	OXIDOREDUCTASE
47.	3CHO	2.42	2	1	0	Leukotriene A-4 hydrolase	HYDROLASE
48.	1MMQ	2.408	1	2	2	Matrilysin	METALLOPROTEASE
49.	1Q41	2.397	2	2	1	Glycogen synthase kinase-3 beta	TRANSFERASE
50.	2H96	2.349	3	1	0	Mitogen-activated protein kinase 8	TRANSCRIPTION
51.	1AGW	2.332	2	1	1	Basic fibroblast growth factor receptor 1	PROTEIN KINASE
52.	1SOJ	2.326	1	2	0	cGMP-inhibited 3,5-cyclic phosphodiesterase B	HYDROLASE
53.	1XLZ	2.295	3	1	0	cAMP-specific 3,5-cyclic phosphodiesterase 4B	HYDROLASE
54.	1JJ9	2.29	2	2	0	Neutrophil collagenase	HYDROLASE
55.	1HAK	2.278	3	1	0	Annexin A5	CALCIUM/PHOSPHOLIPID-BINDING
56.	1M6W	2.266	3	0	1	Alcohol dehydrogenase class-3	OXIDOREDUCTASE
57.	2OVH	2.242	3	1	0	Progesterone receptor	TRANSCRIPTION
58.	1CSB	2.126	1	3	0	Cathepsin B	HYDROLASE (THIOL PROTEASE)
59.	2OI0	2.092	3	1	0	ADAM 17	HYDROLASE
60.	2CGW	2.047	1	1	1	Serine/threonine-protein kinase	TRANSFERASE

						Chk1	
ALPINETIN							
1.	1XO2	3.798	2	3	0	Cell division protein kinase 6	CELL CYCLE/TRANSFERASE
2.	1S2A	3.256	4	3	0	Aldo-keto reductase family 1 member C3	OXIDOREDUCTASE
3.	1WMA	3.241	2	2	1	Carbonyl reductase [NADPH] 1	OXIDOREDUCTASE
4.	1QCF	3.16	3	3	1	Tyrosine-protein kinase HCK	TYROSINE KINASE
5.	1K59	2.98	0	4	0	Angiogenin	HYDROLASE
6.	2B7A	2.969	3	2	2	Tyrosine-protein kinase JAK2	TRANSFERASE
7.	1UPV	2.959	5	1	0	Oxysterols receptor LXR-beta	RECEPTOR
8.	1P5Z	2.914	1	1	3	Deoxycytidine kinase	TRANSFERASE
9.	1D3H	2.914	3	3	0	Dihydroorotate dehydrogenase, mitochondrial	OXIDOREDUCTASE
10.	1OG5	2.911	3	3	0	Cytochrome P450 2C9	ELECTRON TRANSPORT
11.	1KBO	2.898	3	0	1	NAD(P)H dehydrogenase [quinone] 1	OXIDOREDUCTASE
12.	1LHO	2.892	4	1	1	Sex hormone-binding globulin	TRANSPORT PROTEIN
13.	1XBB	2.883	5	0	1	Tyrosine-protein kinase SYK	TRANSFERASE
14.	1RTK	2.875	1	1	2	Complement factor B	HORMONE/GROWTH FACTOR
15.	13GS	2.849	3	2	0	Glutathione S-transferase P	COMPLEX (TRANSFERASE/SULFASALAZINE)
16.	3BLR	2.842	2	2	0	Cyclin-T1	TRANSCRIPTION
17.	1P0I	2.833	1	2	0	Cholinesterase	HYDROLASE
18.	2AMB	2.824	3	1	1	Androgen receptor	HORMONE/GROWTH

							FACTOR RECEPTOR
19.	1R0P	2.784	4	2	0	Hepatocyte growth factor receptor	TRANSFERASE
20.	1RKP	2.78	1	2	0	cGMP-specific 3,5-cyclic phosphodiesterase	HYDROLASE
21.	1Z6E	2.776	3	1	1	Coagulation factor X	HYDROLASE
22.	1LD7	2.77	2	1	0	Protein farnesyltransferase/geranylgeranyl transferase type-1 subunit alpha	TRANSFERASE
23.	1YRS	2.769	3	0	2	Kinesin-like protein KIF11	CELL CYCLE
24.	1B3O	2.759	0	3	1	Inosine-5-monophosphate dehydrogenase 2	DEHYDROGENASE
25.	1YXU	2.753	0	4	0	Proto-oncogene serine/threonine-protein kinase Pim-1	TRANSFERASE
26.	1Y2C	2.747	4	1	0	cAMP-specific 3,5-cyclic phosphodiesterase 4D	HYDROLASE
27.	1PWM	2.745	2	2	0	Aldose reductase	OXIDOREDUCTASE
28.	3BM9	2.733	2	2	1	Heat shock protein HSP 90-alpha	CHAPERONE
29.	1QKU	2.713	2	0	1	Estrogen receptor	NUCLEAR RECEPTOR
30.	1WLJ	2.698	0	4	1	Interferon-stimulated gene 20 kDa protein	HYDROLASE
31.	1C5O	2.689	1	2	0	Prothrombin	BLOOD CLOTTING
32.	1RW8	2.672	5	1	0	TGF-beta receptor type-1	TRANSFERASE
33.	1ISG	2.66	0	5	1	ADP-ribosyl cyclase 2	HYDROLASE
34.	1V45	2.618	0	3	1	Purine nucleoside phosphorylase	TRANSFERASE
35.	1C86	2.615	1	2	0	Tyrosine-protein phosphatase non-receptor type 1	HYDROLASE

36.	1JAK	2.599	0	2	3	Calcium-activated potassium channel subunit beta-2	HYDROLASE
37.	1A7A	2.587	0	3	2	Adenosylhomocysteinase	HYDROLASE
38.	1M6W	2.571	3	0	1	Alcohol dehydrogenase class-3	OXIDOREDUCTASE
39.	1HLC	2.558	0	3	3	Galectin-2	LECTIN
40.	1HA2	2.539	4	2	0	Serum albumin	SERUM PROTEIN
41.	1HKC	2.534	0	3	2	Hexokinase-1	PHOSPHOTRANSFERASE
42.	1U4D	2.534	0	2	3	Activated CDC42 kinase 1	TRANSFERASE
43.	2BKZ	2.513	2	2	0	Cyclin-A2	TRANSFERASE/COMPLEX
44.	2H96	2.497	3	1	0	Mitogen-activated protein kinase 8	TRANSCRIPTION
45.	2JNP	2.475	2	2	1	Stromelysin-1	HYDROLASE
46.	3CHO	2.468	2	1	0	Leukotriene A-4 hydrolase	HYDROLASE
47.	1E5A	2.46	3	1	0	Transthyretin	TRANSPORT(THYROXINE)
48.	1MMQ	2.441	1	2	2	Matrilysin	METALLOPROTEASE
49.	1HAK	2.44	3	1	0	Annexin A5	CALCIUM/PHOSPHOLIPID-BINDING
50.	1CSB	2.386	1	3	0	Cathepsin B	HYDROLASE (THIOL PROTEASE)
51.	2OVH	2.357	3	1	0	Progesterone receptor	TRANSCRIPTION
52.	1JJ9	2.326	2	2	0	Neutrophil collagenase	HYDROLASE
53.	1SOJ	2.295	1	2	0	cGMP-inhibited 3,5-cyclic phosphodiesterase B	HYDROLASE
54.	1XLZ	2.288	3	1	0	cAMP-specific 3,5-cyclic phosphodiesterase 4B	HYDROLASE
55.	2AYP	2.176	3	2	0	Serine/threonine-protein kinase Chk1	TRANSFERASE

From the list of protein targets suggested by PharmMapper the members with fitscores 3.000 and above were selected for detailed docking studied using Autodock Vina [21]. For pinocembrin, there were five proteins namely human cyclin-dependent kinase 6 (PDB ID: 1XO2), Transglutaminase 3 (PDB ID: 1L9N), VEGFR2 Kinase (PDB ID: 2P2I), prostaglandin D2 11-ketoreductase (PDB ID: 1S2A) and carbonyl reductase 1(PDB ID: 1WMA). For pinostrobin, the proteins were Transglutaminase 3 (PDB ID: 1L9N), human cyclin-dependent kinase 6 (PDB ID: 1XO2), VEGFR2 Kinase (PDB ID: 2P2I), prostaglandin D2 11-ketoreductase (PDB ID: 1S2A) and Chaperon Hsp90 (PDB ID: 3BM9), Human Tyrosine kinase (PDB ID: 1QCF) and carbonyl reductase 1(PDB ID: 1WMA). For alpinetin, only four proteins had fitscore of 3.000 and above, they were human cyclin-dependent kinase 6 (PDB ID: 1XO2), prostaglandin D2 11-ketoreductase (PDB ID: 1S2A), carbonyl reductase 1(PDB ID: 1WMA) and Human Tyrosine kinase (PDB ID: 1QCF). These proteins are subjected to detailed docking analysis using conventional docking protocol using Autodock Vina.

8.3.2. Conventional docking

Human cyclin dependent kinase 6 (CDK6) is a vital protein which along with CDK4 controls the entrance of cells to cell cycle [22]. The progression of cells through G1 phase and G1/S transition is regulated by these proteins. Appropriate cell cycle regulation is required for controlled cell proliferation. Alterations and mutations in the expression of CDKs are frequently associated with cancer. Thus, design of potent inhibitors to control the expression of CDKs is important in cell cycle research. PDB ID: 1XO2 describes a complex

of CDK6 with a flavanol molecule fisetin with a resolution of 2.9 Å [22]. Inhibitor fisetin was redocked into the protein cavity and showed a binding affinity of -9.4 kcal/mol. Redocking shows superposition with the actual inhibitor with great accuracy thereby confirming the docking parameters used (Fig. 8.1). All the ligand molecules studied here namely pinocembrin, pinostrobin and alpinetin showed good binding affinities to CDK6 with values -10.5 kcal/ mol, -9.2 kcal/ mol and -9.6 kcal/ mol respectively. We can infer from these values that pinocembrin and alpinetin are better inhibitors to CDK6 than fisetin. Redocked fisetin forms two hydrogen bonds in the immediate vicinity; one with Lys43 and another with Val101.

Table 8.2. Binding affinities and inhibition constant for native ligand (fisetin) and title molecules with CDK6.

Ligand	Binding affinity (kcal/mol)	Inhibition constant (μM)
Fisetin	-9.4	0.1265
Pinocembrin	-10.5	0.0197
Pinostrobin	-9.2	0.1774
Alpinetin	-9.6	0.0902

Pinocembrin molecule formed three hydrogen bonds when docked into the same cavity with Val101, Gln149 and Asp104 and a π-π interaction with His100. Alpinetin formed one hydrogen bond with Gln 149 and a π-π interaction with His100. Pinostrobin assumes a slightly rotated location and do not form any hydrogen bonds with immediate neighbours but engages in π-π interaction with His100. The studied molecules inhibit the protein CDK6 quite efficiently and could be helpful in regulating altered cell cycle which may lead to cancers.

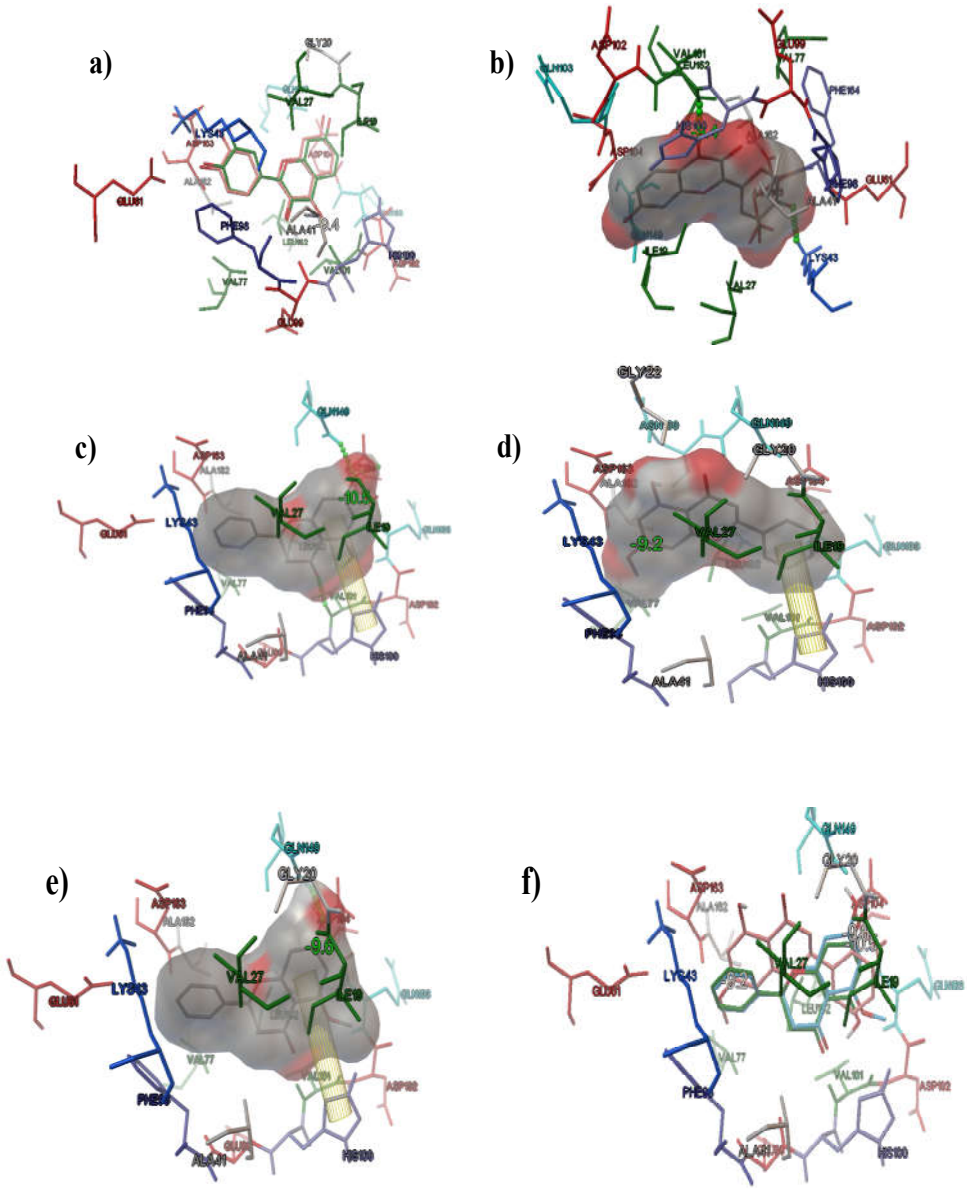

Fig 8.1. Figure depicting a) redocking of native ligand showing appreciable overlap; interactions of b) fisetin with CDK6 c) Pinocembrin with CDK6 d) Pinostrobin with CDK6 e) Alpinetin with CDK6 and f) docked poses of all ligands.

Transglutaminases are a class of enzymes capable of forming crosslinks between protein bound glutamines and lysines [23]. Among this, transglutaminase 3 (TGase 3) is involved in epithelial barrier formation by crosslinking structural proteins in the epidermis in a calcium dependent manner. TGase 3 is a cytosolic enzyme which is widely expressed in various tissues including brain and muscles. Guanosine triphosphate (GTP) is found to inhibit the activities of TGase 3 to some extent [24]. Designing inhibitors for TGase 3 may help to suppress inappropriate activation in early stages of keratinocytes [24]. The protein structure did not have any docked native ligands so active site was selected from literature. Title molecules were docked into the active site of TGase 3 (PDB ID:1L9N), comprising of residues Trp236, Trp273, Phe275, Trp327, Val331, Phe329, Trp332, Leu352, Thr355, Phe387, and Tyr525 [23][25]. Pinocembrin formed a stable complex with binding affinity of -7.2 kcal/mol and engages itself in forming two hydrogen bonds, one with His300 and another with Trp327. Pinostrobin forms three hydrogen bonds, one with His 300, another with Ser325 and the last with Trp327. The binding affinity of the complex formed is -7.3 kcal/mol. The docked images are shown in Fig.8.2.

Table 8.3. Binding affinities and inhibition constant for the title molecules with TGase 3.

Ligand	Binding affinity (kcal/mol)	Inhibition constant (μM)
Pinocembrin	-7.2	5.204
Pinostrobin	-7.3	4.397

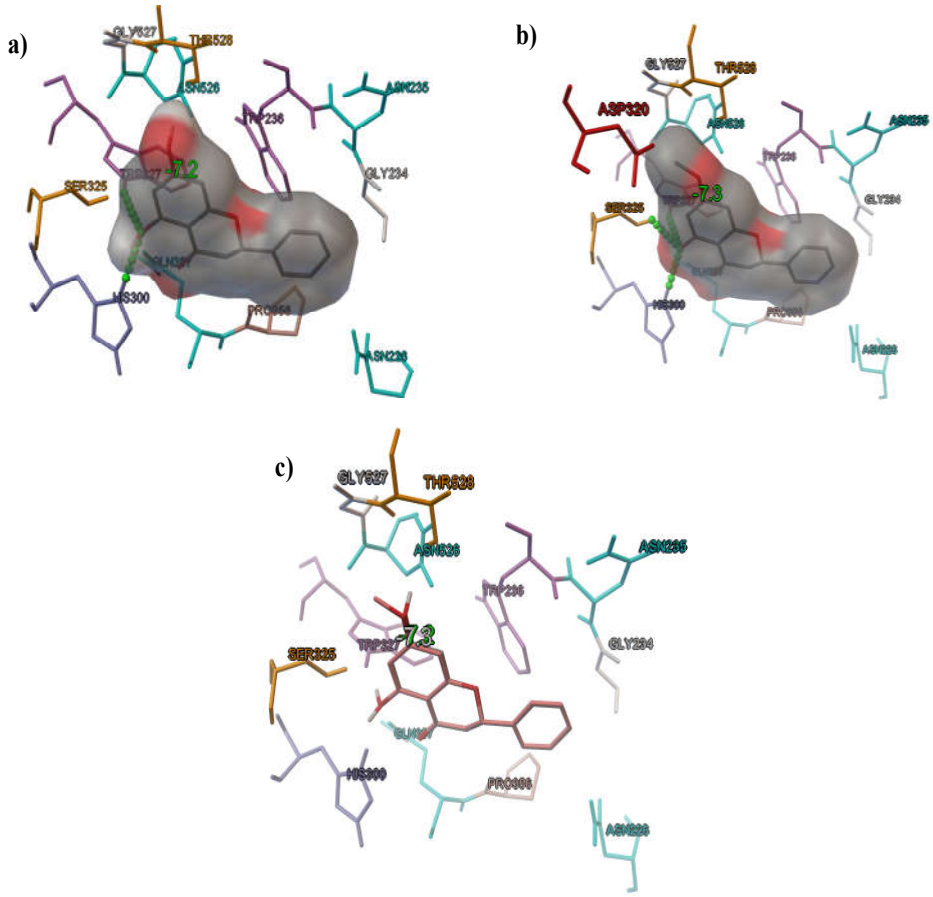

Fig 8.2. Figure depicting interactions of a) Pinocembrin with TGase 3 b) Pinostrobin with TGase 3 c) docked poses of all ligands.

Receptor tyrosine kinases (RTK) represent a large family of enzymes which are responsible for a diverse range of biological processes including angiogenesis. RTKs which are involved in tumor angiogenesis is vascular endothelial growth factor receptor (VEGFR) [26]. Among different VEGFRs, VEGFR2 (kinase domain-containing receptor, KDR) is especially important in cell proliferation and

migration. VEGFR inhibition provides an attractive path to prevent tumor growth and metastasis without affecting the surrounding tissues. Several small molecular inhibitors are designed to inhibit VEGFRs in particular VEGFR2. PDB ID: 2P2I describes a complex of VEGFR2 with an inhibitor nicotinamide. Redocking of nicotinamide into the active site provided satisfactory superposition. The binding energy value was -11.8 kcal/mol and forms a hydrogen bond with Asp1046. Proceeding along the same lines all the molecules under study was docked into the active site of VEGFR2. Pinostrobin produced the highest binding affinities among the studied molecules which was -8.7 kcal/mol. Pinocembrin had a closer value of -8.5 kcal/mol. Both pinostrobin and pinocembrin engages in π-π interaction with Phe1047. This molecular framework could be beneficial in designing VEGRF2 inhibitors.

Table 8.4. Binding affinities and inhibition constant for native ligand (nicotinamide), pinocembrin and pinostrobin with VEGFR2.

Ligand	Binding affinity (kcal/mol)	Inhibition constant (μM)
Nicotinamide	-11.8	0.0022
Pinocembrin	-8.5	0.5789
Pinostrobin	-8.7	0.4128

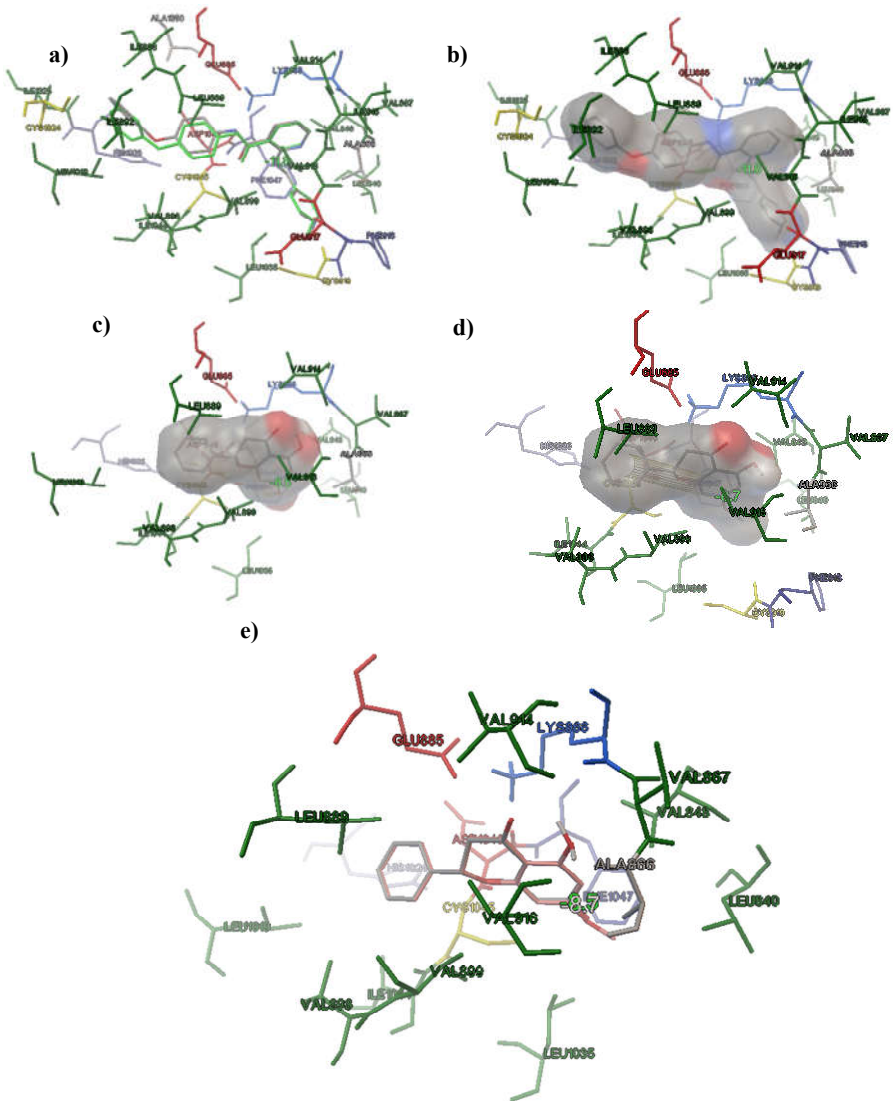

Fig 8.3. Figure depicting a) redocking of native ligand showing good overlap; interactions of b) nicotinamide with VEGFR2 c) Pinocembrin with VEGFR2 d) Pinostrobin with VEGFR2 and e) docked poses of both ligands together.

Aldo-keto reductase family (AKR1C3) are proteins which have broad tissue differentiation and converts prostaglandins PGD2 to PGF2α [27,28]. AKR1C3 provides a plausible target for the non-COX

dependent anti-neoplastic activities of non-steroidal anti-inflammatory drug (NSAID). Chemoprotective activities of NSAIDs against cancer are also mediated through non-COX mechanisms. Thus AKR1C3 inhibitors provide new clinical roads for the treatment of tumor and cancer. PDB ID: 1S2A describes the protein AKRIC3 complexed with NSAID indomethacin at 1.8 Å resolution [27]. Native ligand namely indomethacin was redocked to the protein structure to confirm the docking parameters. Dimethyl sulphoxide molecule and unknown atom or ion present in PDB structure was removed prior to docking. Redocked structure provided a binding affinity of -11.1 kcal/mol. The redocked ligand engaged in π-π interaction with His117.

Table 8.5. Binding affinities and inhibition constant for native ligand (indomethacin) and title compounds with AKR1C3.

Ligand	Binding affinity (kcal/mol)	Inhibition constant (μM)
Indomethacin	-11.1	0.0071
Pinocembrin	-9.9	0.5435
Pinostrobin	-10.2	0.0327
Alpinetin	-10.2	0.0327

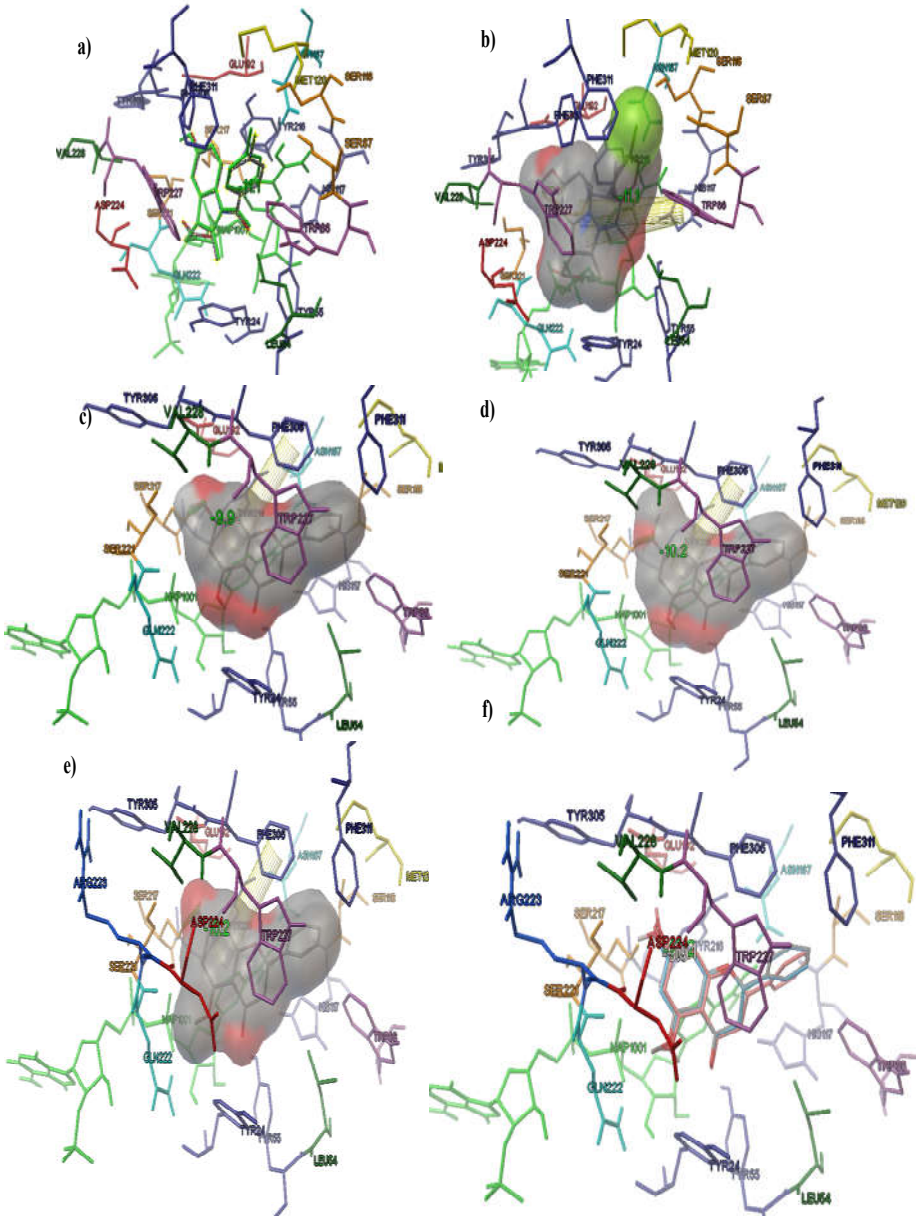

Fig 8.4. Figure depicting a) redocking of native ligand; interactions of b) indomethacin with AKR1C3 c) Pinocembrin with AKR1C3 d) Pinostrobin with AKR1C3 e) Alpinetin with AKR1C3 and f) docked poses of all ligands together.

The molecules studied here were then docked using the same grid parameters and the binding energies obtained were comparable. Pinocembrin had a binding energy of -9.9 kcal/mol, and both pinostrobin and alpinetin had a binding energy of -10.2 kcal/mol. These molecules forms hydrogen bond with Ser217 and showed the existence of π-π interaction with Phe306. Unlike that predicted by PharmMapper, binding energy of pinocembrin is slightly less compared to other ligands. Thus the flavanone molecules studied shows potentiality towards inhibition of the protein of interest AKR1C3.

Carbonyl reductase 1 (CBR1) is an oxidoreductases protein which is mainly associated with two cellular functions 1) detoxification of xenobiotics 2) metabolism of ketone-containing cellular messengers [29]. Cardiotoxicity associated with the treatment using daunorubicin is due to the conversion of daunorubicin to daunorubicinol in presence of CBR1 which is anti-proliferative and cardiotoxic [30]. Effective inhibition of CBR1 will potentiate cancer therapy. In the PDB ID: 1WMA authors have reported an X-crystal data of CBR1 complexed with the inhibitor 3-(1-tert-butyl-4-amino-1H-pyrazolo [3,4-d]pyrimidin-3-yl)phenol (hydroxy-PP) at a resolution of 1.24 Å [31]. The native ligand was initially redocked into the structure. Effective redocking was only possible by reducing the NADP to NADPH as suggested by D. Pirolli et.al [30]. Upon satisfactory docking the same parameters were followed for docking the title compounds. Binding energies of all the molecules were almost in the same range. Hydroxy PP formed a hydrogen bond with SER139 and π-π interactions with Trp229 and NADPH. Pinostrobin and

Alpinetin had a binding energy of -6.6 kcal/mol. Pinostrobin engages in π-π interactions with neighbouring amino acid residues like Trp229, Phe94 and forms a hydrogen bond with Tyr193. Alpinetin has π-π interactions with Tyr 193 and Trp229. Pinocembrin has a slightly lower binding energy of -6.5 kcal/mol and form π-π interaction with Trp229 and Tyr193. These molecules are hence likely to be potent CBR1 inhibitors.

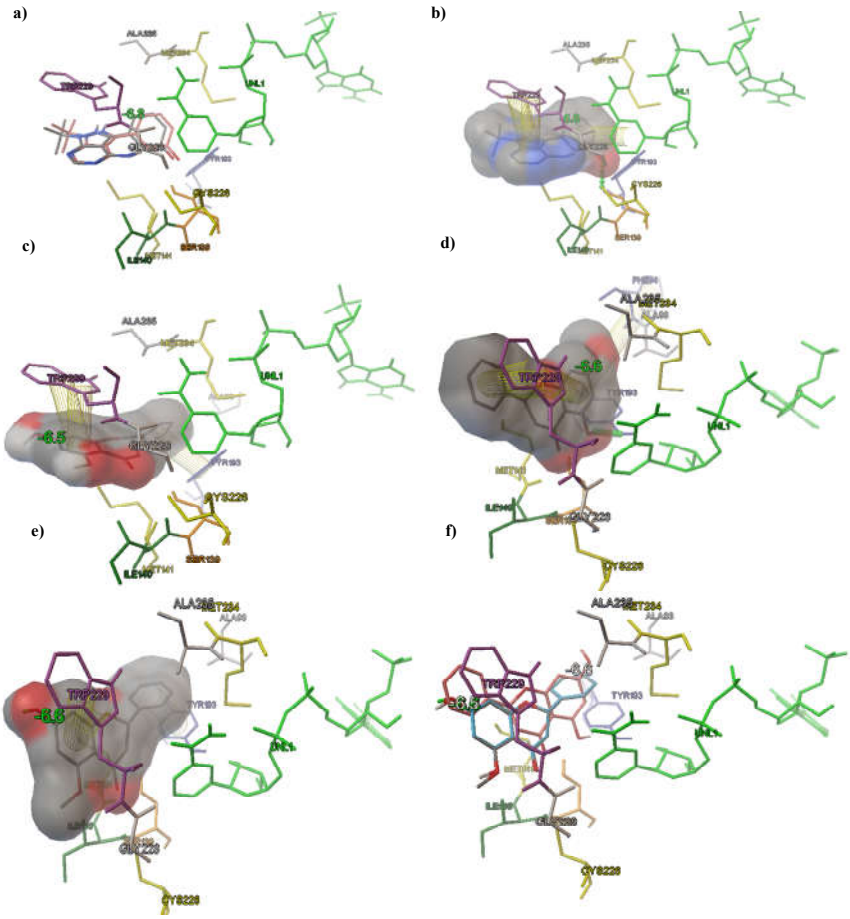

Fig 8.5. Figure depicting a) redocking of native ligand; interactions of b) hydroxyPP with CBR1 c) Pinocembrin with CBR1 d) Pinostrobin with CBR1 e) Alpinetin with CBR1 and f) docked poses of all ligands together.

Table 8.6. Binding affinities and inhibition constant for native ligand (hydroxyl PP) and title compounds with CBR1.

Ligand	Binding affinity (kcal/mol)	Inhibition constant (μM)
Hydroxy PP	-6.8	10.234
Pinocembrin	-6.5	16.990
Pinostrobin	-6.6	14.349
Alpinetin	-6.6	14.349

Multiple signal transduction pathways contribute to the origin and spread of cancer in human body. A global inhibition will therefore be effective only when these multiple activated pathways are inhibited. One such way of global inhibition is via inhibiting molecular chaperone complexes. Chaperons regulate the folding, stabilization and activation of proteins. Of this, one of the extensively studied chaperon is Heat shock protein 90 (Hsp90). It regulates the functioning of many different proteins like telomerase, nitric oxide synthase, nuclear hormone receptors and protein kinases. Several small molecular inhibitors of Hsp90 have been discovered.

Table 8.7. Binding affinities and inhibition constant for native ligand (benzioxazole derivative) and title compounds with Hsp90.

Ligand	Binding affinity (kcal/mol)	Inhibition constant (μM)
Benzioxazole derivative	-8.1	1.138
Pinocembrin	-7.2	5.204
Pinostrobin	-7.3	4.397

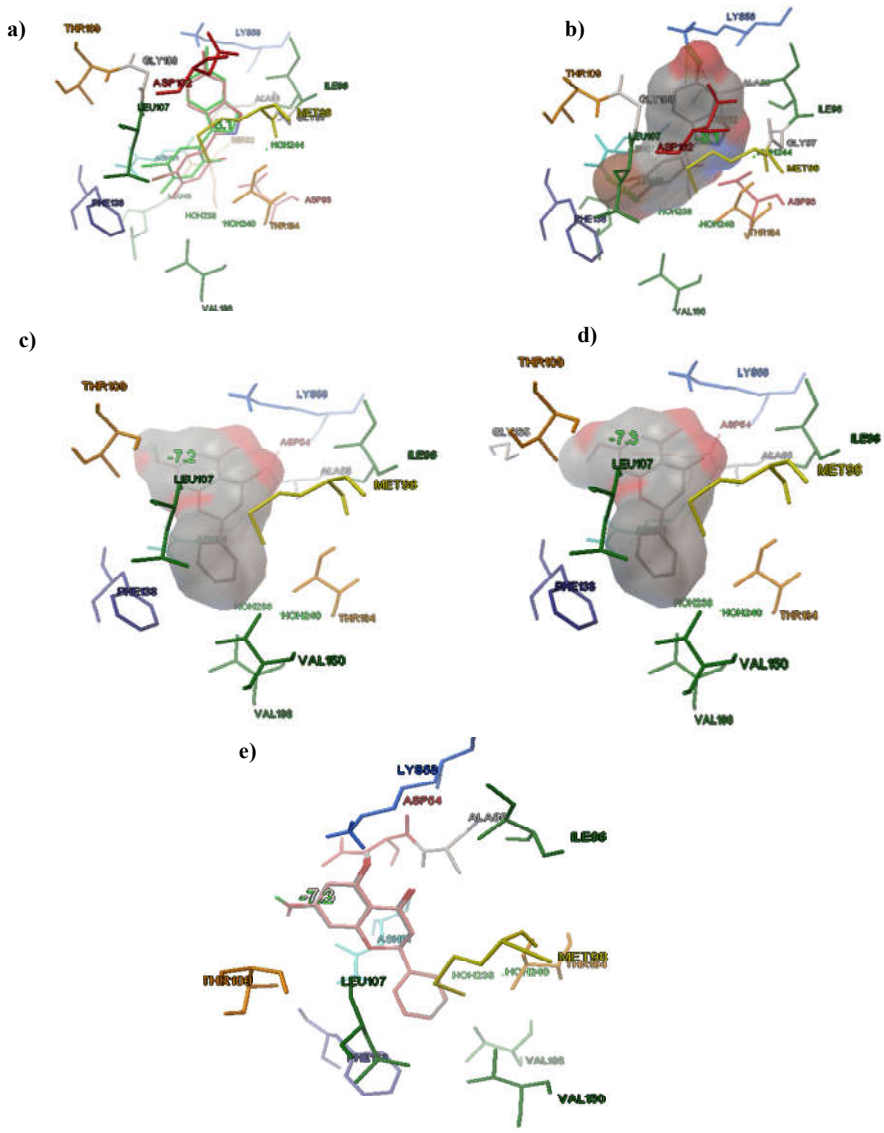

Fig 8.8. Figure depicting a) redocking of native ligand, interactions of b) benzioxazole derivative with Hsp90 c) Pinocembrin with Hsp90 d) Pinostrobin with Hsp90 and e) docked poses of all ligands together.

The current PDB entry 3BM9 reports the structure of Hsp 90 complexed with benzioxazole derivative at 1.6 Å resolution [32]. Redocking was quite effective and produced a binding energy of -8.1 kcal/mol and the redocked ligand formed two hydrogen bonds with Asn51 and Lys58. Lys58 also engages in π-cation interaction with the ligand. Following the same grid parameters, target ligands were also docked and gave very close values of binding energy. Pinocembrin had a binding energy -7.2 kcal/mol, pinostrobin had an energy value of -7.3 kcal/mol. Pinocembrin has a comparable binding energy to that of pinostrobin and hence is considered though the fit score predicted by Pharm Mapper is less than the cut off we selected for this study (Fit score = 3.000). Thus flavonone moiety can be another scaffold for design of Hsp90 inhibitors.

Src family of tyrosine kinases is a family of signaling proteins which are signaling proteins. The current protein named 1QCF is a variant of human Hck with modified tail region. It has an inhibitor 4-amino-5-(4-methylphenyl)-7-(t-butyl) pyrazolo pyrimidine known as PP1 which shows specificity in binding to Src family tyrosine kinase Hck at a resolution of 2.0 Å [33]. Using the redocking protocol, docking of the title compounds showed very close binding energies as can be seen from the table. All the molecules including the native ligand form a hydrogen bond with Met 341 and π-π interaction with benzene ring of Phe340. These inhibitors could thus be subjected to further research as Src family tyrosine kinase Hck inhibitors.

Table 8.8. Binding affinities and inhibition constant for native ligand (PP1) and title compounds with Src kinase.

Ligand	Binding affinity (kcal/mol)	Inhibition constant (μM)
PP1	-9.0	0.249
Pinocembrin	-8.5	0.579
Pinostrobin	-8.4	0.685
Alpinetin	-8.3	0.812

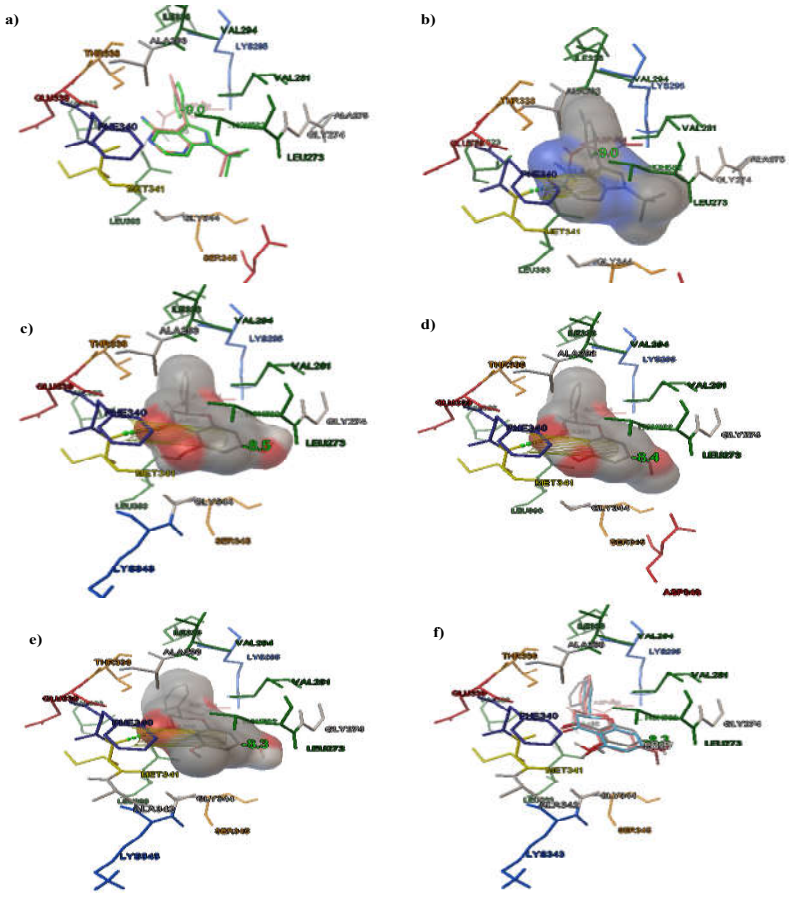

Fig 8.9. Figure depicting a) redocking of native ligand, interactions of b) PP1 derivative with Src kinase c) Pinocembrin with Src kinase d) Pinostrobin with Src kinase and e) docked poses of all ligands together.

Here Pharm Mapper has not predicted 1QCF as a probable target for pinocembrin but all the ligands show almost same binding affinity to the protein unlike that predicted by pharmmapper. Except for very few missing links inverse docking almost guides us to sensible protein targets for further study.

8.4. Conclusions

Multi-targeted drugs becoming the focus of the century, we have analyzed the most probable protein targets of the title molecules pinocembrin, pinostrobin and alpinetin using PharmMapper. On subjecting them to conventional docking, some turns out to be better or atleast comparable to existing ligands whereas some are not as good as existing ligands but could form stable complexes. It could be also seen that all the highest scored ligands are mainly associated directly or indirectly with cancer therapy. Some prevent alterations and mutations in cell cycle while others prevent cardiotoxicity associated with existing chemotherapeutic agents and the like. It is beneficial to modulate multi-target drugs than single target drugs in terms of overall efficacy, possible side effects and resistance or compensatory mechanisms of action. This increases and ascertains the therapeutic potential of the studied flavanone molecules.

References

[1] C. Ezerzer, M. Dolgin, J. Skovorodnikova, N. Harris, Pept. 30 1296–1305. 30 (2009) 1296–1305.

[2] C. Hart, Drug Discov. Today 10 (2005) 513–9.

[3] A. Cavalli, M.L. Bolognesi, A. Minarini, M. Rosini, V. Tumiatti, M. Recanatini, C. Melchiorre, J. Med. Chem. 51 (2008) 347–372.

[4] Y. Chen, D. Zhi, Proteins 43 (2001) 217–226.

[5] Q. Do, I. Renimel, P. Andre, C. Lugnier, C. Muller, P. Bernard, Curr. Drug Discov. Technol. 2 (2005) 161–167.

[6] P. P, Muller, G. Lena, E. Boilard, S. Bezzine, G. Lambeau, G. Guichard, D. Rognan, J. Med. Chem. 49 (2006) 6768–6778.

[7] S.Z. Grinter, Y. Liang, S.-Y. Huang, S.M. Hyder, X. Zou, J Mol Graph Model 29 (2011) 795–799.

[8] X. Liu, S. Ouyang, B. Yu, Y. Liu, K. Huang, J. Gong, S. Zheng, Z. Li, H. Li, H. Jiang, Nucleic Acids Res 38 (2010) 5–7.

[9] X. Wang, C. Pan, J. Gong, X. Liu, H. Li, J. Chem. Inf. Model. 56 (2016) 1175–1183.

[10] X. Wang, Y. Shen, S. Wang, S. Li, W. Zhang, X. Liu, L. Lai, J. Pei, H. Li, Nucleic Acids Res. 45 (2017) W356–W360.

[11] G. Wolber, T. Langer, J. Chem. Inf. Model. 45 (2005) 160–169.

[12] R. Vasseur, S. Baud, L. Angelo, X. Vigouroux, L. Martiny, M. Krajecki, M. Dauchez, Parallel Comput. (2014) 1–12.

[13] A. Rasul, F.M. Millimouno, W.A. Eltayb, M. Ali, J. Li, X. Li, BioMed Res. Int. 2013 (2013).

[14] W.A. Roman Junior, D.B. Gomes, B. Zanchet, A.P. Schönell, K.A.P. Diel, T.P. Banzato, A.L.T.G. Ruiz, J.E. Carvalho, A. Neppel, A. Barison, C.A.M. Santos, Brazilian J. Pharmacogn. 27 (2017) 592–598.

[15] J.-C. Le Bail, L. Aubourg, G. Habrioux, Cancer Lett. 156 (2000) 37–44.

[16] W. He, Y. Li, C. Xue, Z. Hu, X. Chen, F. Sheng, Bioorg. Med. Chem. 13 (2005) 1837–1845.

[17] M. Huo, N. Chen, G. Chi, X. Yuan, S. Guan, H. Li, W. Zhong, X. Deng, H. Feng, Int. Immunopharmacol. 12 (2012) 241–248.

[18] http://lilab.ecust.edu.cn/pharmmapper/index.php.

[19] N. Guex, M.C. Peitsch, Electrophoresis 18 (1997) 2714–2723.

[20] http://www.expasy.org/spdbv/.

[21] O. Trott, A.J. Olson, J. Comput. Chem. 31 (2010) 455–461.

[22] H. Lu, D.J. Chang, B. Baratte, L. Meijer, U. Schulze-gahmen, J. Med. Chem. 48 (2005) 737–743.

[23] B. Ahvazi, H.C. Kim, S. Kee, Z. Nemes, P.M. Steinert, EMBO J. 21 (2002) 2055–2067.

[24] K. Hitomi, K. Ikura, M. Maki, Biosci. Biotechnol. Biochem. 8451 (2014) 1347–6947.

[25] B. Ahvazi, P.M. Steinert, Exp. Mol. Med. 35 (2003) 228–242.

[26] B.L. Hodous, S.D. Geuns-meyer, P.E. Hughes, B.K. Albrecht, S. Bellon, J. Bready, S. Caenepeel, V.J. Cee, S.C. Chaffee, A. Coxon, M. Emery, J. Fretland, P. Gallant, Y. Gu, D. Hoffman, R.E. Johnson, R. Kendall, J.L. Kim, A.M. Long, M. Morrison, P.R. Olivieri, V.F. Patel, A. Polverino, P. Rose, P. Tempest, L. Wang, D.A. Whittington, H. Zhao, J. Med. Chem. 50 (2007) 611–626.

[27] A.L. Lovering, J.P. Ride, C.M. Bunce, J.C. Desmond, S.M. Cummings, S.A. White, Cancer Res 3 (2004) 1802–1810.

[28] J.U. Flanagan, Y. Yosaatmadja, R.M. Teague, M.Z.L. Chai, A.P. Turnbull, C.J. Squire, PLoS One 7 (2012).

[29] M. Tanaka, R. Bateman, D. Rauh, E. Vaisberg, S. Ramachandani, C. Zhang, K.C. Hansen, A.L. Burlingame, J.K. Trautman, K.M. Shokat, C.L. Adams, 3 (2005).

[30] D. Pirolli, B. Giardina, A. Mordente, S. Ficarra, M. Cristina, D. Rosa, Eur. J. Med. Chem. 56 (2012) 145–154.

[31] D. Ghosh, M. Sawicki, V. Pletnev, M. Erman, S. Ohno, S.

Nakajin, W. Duax, J Biol Chem 276 (2001) 18457–18463.

[32] A. Gopalsamy, M. Shi, J. Golas, E. Vogan, J. Jacob, M. Johnson, F. Lee, R. Nilakantan, R. Petersen, K. Svenson, R. Chopra, M.S. Tam, Y. Wen, J. Ellingboe, K. Arndt, J. Med. Chem. 51 (2008) 373–375.

[33] T. Schindler, F. Sicheri, A. Pico, A. Gazit, A. Levitzki, J. Kuriyan, Mol. Cell 3 (1999) 639–648.

Chapter 9

Conclusions and future outlook

Flavonoids are plant polyphenols of great therapeutic importance. Flavonoids are classified into many subgroups based on their basic structure. Of the different flavonoid families, the current work focuses on flavanones. These are flavonoid molecules devoid of C2-C3 double bond and C3-OH. This subgroup was one of the less focused subgroups but during the last 15 years, importance of this group has tremendously increased making this one of the major flavonoid subgroups.

Among the various flavanone molecules known, the current study focused on three flavanone aglycones namely pinocembrin, pinostrobin and alpinetin. These are well known in ancient medicine. These molecules have grabbed attention as anti-oxidant, anti-bacterial, anti-viral, anti-inflammatory and even anti-cancer agents.

With the advancements in density functional theory, it finds large applications in explaining experimental research at molecular

level and also in some cases predicted possible applications and mechanisms. In this scenario, we have attempted a density functional theory based study on the flavanone molecules, pinocembrin, pinostrobin and alpinetin.

To begin with, the structure of these molecules was carefully optimized and NMR spectral characterization was carried out. Frontier molecular orbital analysis and molecular electrostatic potential mapping provided an indication towards reactivity of the molecule and different groups in the molecule. Antioxidant potential of these molecules was then explored by calculating quantum chemical descriptors and then various mechanisms of antioxidant action were studied from thermodynamic point of view. It was concluded that the mechanism operative in gaseous phase was hydrogen atom transfer mechanism whereas in polar aqueous solvents the mechanism was changed to sequential proton loss electron transfer mechanism. Having elucidated this, druggability and toxicity of the molecules were also checked using online softwares.

Next, we aimed at improving the antioxidant potentialities of these molecules via derivatizing them with electron releasing and electron withdrawing groups. It was concluded that the molecules act as good electron donors and electron releasing groups increase the donating capacity of the molecules. But this derivatization should be carefully dealt without triggering pro-oxidant nature.

Various applications of the molecules were subsequently studied. UV absorption characteristics of the molecules were studied

using TDDFT and NLMO formalisms which showed that these molecules could be potential UV filters. With the photoprotection activity and UV absorption ability, these molecules could find potential application in sunscreen industry.

An insight into the interaction of the flavanone molecules with heavy metals was provided. The molecules could form stable complexes with zinc, cadmium, mercury, palladium and lead. The complexes showed characteristic optical signatures as well. These could find potential application in chelation therapy against heavy metal poisoning.

Currently, Multi-targeted drugs find great application in pharmaceutical industry. To identify the potential targets of the molecules, inverse docking was carried out against pharmacophore database maintained by PharmMapper. Highly ranked targets were then studied using conventional docking strategy. The studies revealed that most of the top ranked targets were directly or indirectly related to cancer therapy. This gives an indication that these molecules could be beneficial for cancer treatment.

Thus the molecules selected for the present study finds application in various fields. The molecular framework with modifications could be of great importance in the industry. Several extensions of the current work may be possible in the future.

- Kinetics of antioxidant mechanism with several radicals could be carried out.

- ❖ Metal complexes of higher coordination like 1:2, 1:3 complexes could be studied.
- ❖ The molecular targets which are highly ranked could be experimentally studied.
- ❖ Prooxidant activity of the molecules can be studied.

Research Papers Published

1. Basila Hassan, Ajmala Shireen, K. Muraleedharan, V.M. Abdul Mujeeb, Virtual screening of molecular properties of chitosan and derivativesin search for druggable molecules, Int. J. Biol. Macromol., 74 (2015) 392–396.

2. P. Ajmala Shireen, V.M. Abdul Mujeeb, K. Muraleedharan, Theoretical insights on flavanones as antioxidants and UV filters: A TDDFT and NLMO study, J. Photoch. Photobio B, 170(2017) 286-294.

3. P. Ajmala Shireen, K. Muraleedharan, V.M. Abdul Mujeeb, Identification of flavanones from Boesenbergia rotunda as potential antioxidants and monoamine oxidase B inhibitors, Chem. Papers, 71(2017) 2473-2483.

Conference proceedings

1. Ajmala Shireen P., V. M. Abdul Mujeeb Virtual screening of molecular properties of Flavanones in search of druggable molecules 3(2016) 97-105

2. P. Ajmala Shireen, V.M. Abdul Mujeeb Theoretical studies on anti-oxidant potential of alpinetin, Materials Today: Proceedings 5 (2018) 8908–8915.

DEPARTMENT OF CHEMISTRY
UNIVERSITY OF CALICUT
KERALA 673635
2018